UNIVERSIDADE FEDERAL DO RIO GRANDE DO SUL
INSTITUTO DE CIÊNCIAS BÁSICAS DA SAÚDE
PROGRAMA DE PÓS-GRADUAÇÃO EM CIÊNCIAS BIOLÓGICAS:
FISIOLOGIA

Karina Pires Reis

ASSOCIAÇÃO ENTRE O ÁCIDO VALPRÓICO E O FATOR DE CRESCIMENTO DE FIBROBLASTOS EM MATRIZES PRODUZIDAS POR ELETROFIAÇÃO COAXIAL NO TRATAMENTO DA LESÃO DA MEDULA ESPINAL EM RATOS

Porto Alegre
2018

Karina Pires Reis

ASSOCIAÇÃO ENTRE O ÁCIDO VALPRÓICO E O FATOR DE CRESCIMENTO DE FIBROBLASTOS EM MATRIZES PRODUZIDAS POR ELETROFIAÇÃO COAXIAL NO TRATAMENTO DA LESÃO DA MEDULA ESPINAL EM RATOS

Tese apresentada ao Programa de Pós- Graduação em Ciências Biológicas: Fisiologia do Instituto de Ciências Básicas da Saúde da Universidade Federal do Rio Grande do Sul como requisito parcial para a obtenção do título de doutora em Fisiologia.

Orientadora: Professora Dra. Patricia Pranke
Coorientadora: Professora Dra. Laura Elena Sperling

Porto Alegre
2018

Dedico

À minha mãe que tanto fez e faz pelo meu crescimento pessoal e profissional

Agradecimentos

À minha mãe, Suzana, pelo esforço incansável em querer me ver bem, por ter me dado o sopro da vida, não apenas quando nasci, mas em vários momentos ao longo da vida.

À toda minha família, em especial, meu irmão (Ederson) e minha avó (Sônia) por todo o amor, carinho e apoio durante todos os anos. Também ao meu pai (*in memorian*) que infelizmente não está mais presente, mas deixou seu apoio incondicional à minha educação.

A todos os meus amigos pelos maravilhosos momentos juntos, pelas risadas, pelos momentos de descontração, pelos desabafos e reflexões. Em especial, Gisele, Juliane, Pamela, Ane, Bruna, Nithiane, Rosângela, Cláudia, Márcio, Vanessa, Carolina, Rafael, Filipe.

Ao Marcelo, por ser o melhor amigo que eu poderia desejar ter na vida e que me faz morrer de saudade pela distância.

À Helenita por toda a amizade, compreensão e ajuda com o inglês.

Ao Felipe pelos momentos leves em meio à turbulência do final da tese.

À minha psicóloga, Roberta, por ser uma excelente profissional e tanto me auxiliar nessa trajetória.

À minha co-orientadora, Laura, por tudo que me ensinou, pela paciência, pela compreensão em diversos momentos, pela presença, por não me deixar desistir, por ser uma inspiração em vários aspectos e pela amizade que construímos nesse período.

Aos ex-colegas de laboratório, em especial, Laura P., Andréa e Isabele que estarão sempre no meu coração.

Aos atuais colegas com quem divido momentos de aprendizado e descontração: Maurício, Carolina, Fernanda, Gabriele, Luís, Oranian, Marcelo, Brenda, Daikelly.

Ao aluno de iniciação científica, Cristian, por toda a ajuda nos experimentos e já se mostrar um excelente profissional. Pela dedicação e competência que fizeram toda a diferença nos experimentos *in vivo*.

À minha orientadora Patricia Pranke que me recebeu de braços abertos no laboratório. Por todos os ensinamentos e oportunidades, que tanto contribuíram para a minha formação. Por ter confiado em mim e no meu trabalho. Por lutar incansavelmente pelo bom andamento do laboratório.

À Mariana pelas análises no HPLC.

A todos os funcionários do Instituto de Ciências Básicas da Saúde. Em especial o "Toninho" por estar ao nosso lado e nos ajudar em absolutamente tudo que solicitamos a ele, uma inspiração como pessoa e como profissional. Também, à bioterista Catiele e ao veterinário Andre.

Ao PPG Fisiologia pelo ensino de qualidade, pela disciplina de Fisiologia e, também, pela disciplina de estágio didático que tanto nos auxilia a sermos professores além de pesquisadores. A professora Maria Flávia que ministra essa disciplina com grande motivação.

À professora Márcia que me orientou durante o estágio didático, um dos momentos mais gratificantes do doutorado. Por todo o apoio e carinho. Por me permitir participar da elaboração da aula prática sobre lipídeos e, assim, conhecer outras formas de ensino e participar do Salão de Ensino da UFRGS.

À CAPES pela bolsa de doutorado.

Ao Instituto de Pesquisa com Células-tronco pelo apoio financeiro, contribuindo com a aprendizagem e formação de profissionais mais capacitados.

E a todos aqueles que de alguma forma contribuíram para o desenvolvimento desse trabalho,

Muito obrigada!

Sumário

Resumo

Diversos estudos têm sido realizados em busca de tratamentos para a lesão da medula espinal (LME) e o uso de estratégias da medicina regenerativa mostra-se promissor para promover o reparo no local da lesão. Os *scaffolds* de microfibras, produzidos por eletrofiação coaxial podem fornecer uma ponte para conectar as áreas de tecidos lesados na LME e desempenhar papéis ativos quando associados a moléculas bioativas. O fator de crescimento de fibroblastos 2 (FGF-2) e o ácido valpróico (VPA) têm sido descritos na literatura como importantes agentes que promovem neuroproteção e neuroregeneração. No presente trabalho, dois tipos de *scaffolds* foram produzidos pela técnica de eletrofiação coaxial, um deles contendo FGF-2 e o outro contendo VPA, no interior das microfibras. O potencial biológico desses biomaterias foi analisado em testes *in vivo* e *in vitro*. As fibras foram caracterizadas por microscopia eletrônica de varredura, de transmissão e confocal, bem como pela medida do ângulo de contato e das propriedades mecânicas. Além disso, estudos *in vitro* foram realizados para avaliar a liberação dessas substâncias dos *scaffolds*. A bioatividade do FGF-2 e do VPA foi analisada através de testes com células PC12, uma linhagem celular derivada de feocromocitomas de ratos geralmente utilizadas para estudos de *scaffolds* que visam a regeneração neural. As microfibras foram implantadas em um modelo de LME por hemisecção em ratos e, posteriormente, foram realizadas análises da recuperação motora, histologia e a quantificação da expressão de marcadores neurais. Os *scaffolds* produzidos por eletrofiação coaxial apresentaram microfibras uniformes com estrutura núcleo-casca e características morfológicas e mecânicas compatíveis para aplicação na LME. Os testes de liberação indicaram uma liberação rápida das duas substâncias nas primeiras oito horas de incubação e o FGF-2 foi detectado no meio por pelo menos 30 dias. As fibras coaxiais contendo tanto FGF como VPA suportaram a adesão, viabilidade e proliferação das células PC12. Além disso, o FGF-2 liberado induziu a diferenciação desse tipo celular. Enquanto o VPA provocou a redução da viabilidade dessas células como já descrito na literatura. A análise histológica do tecido da medula demonstrou que os *scaffolds* implantados *in vivo* foram integrados ao local da lesão. Os *scaffolds* com FGF-2 promoveram melhora locomotora dos animais aos 28 dias após a lesão e também reduziram a expressão de GFAP no local da lesão, indicando diminuição da cicatriz glial. Esses resultados indicam o excelente potencial dos *scaffolds* produzidos para o tratamento da LME.

Palavras-chave: lesão da medula espinal**,** FGF-2, VPA, eletrofiação coaxial

Abstract

Several studies have been performed in search of treatments for spinal cord injury (SCI) and the use of regenerative medicine strategies is promising for promoting repair at the site of injury. Microfiber scaffolds, producing by coaxial electrospinning, can provide a bridge to connect the injured tissue areas in the SCI and play active roles when associated with bioactive molecules. The basic fibroblast growth factor (FGF-2) and valproic acid (VPA) have been described in the literature as important agents that promote neuroprotection and neuroregeneration. In this work, two types of biomaterials were produced by the coaxial electrospinning technique, one of them containing FGF-2 and the other containing VPA inside the microfibers. The biological potential of these scaffolds was analyzed using *in vitro* and *in vivo* tests. The fibers were characterized by scanning electron microscopy, transmission electron microscopy, laser confocal scanning microscopy, water contact angle and mechanical properties. In vitro studies were conducted to evaluate the release of these substances from the scaffolds . The bioactivity of FGF-2 and VPA was analyzed by tests with PC12 cells, a cell line derived from pheochromocytomas of rats commonly used for studies of scaffolds when the aim is neural regeneration. The microfibers were implanted in a hemisection SCI rat model and after 6 weeks the behavioral and histological analyses were performed; the expression of neural markers was quantified. The scaffolds produced by coaxial electrospinning presented uniform microfibers with core-shell structure and compatible morphological and mechanical characteristics for application in the SCI. Release tests indicated a rapid release of the two substances within the first hours of incubation and the FGF-2 was detected in the medium for at least 30 days. Coaxial fibers containing both FGF and VPA supported adhesion, viability and proliferation of PC12 cells. In addition, FGF-2 released by the fibers showed that its bioactivity was inducing the differentiation of this cell type, while VPA caused the reduction of PC12 cell viability, as already described in the literature. Histological analysis of the spinal cord tissue demonstrated that scaffolds implanted *in vivo* were integrated at the lesion site. PLGA and FGF-2/PLGA scaffolds promoted locomotor improvement at 28 days post-injury and also reduced GFAP expression at the site of the lesion, indicating a decrease in glial scarring. These results indicate the excellent potential of the scaffolds produced for the treatment of SCI.

Key-words: spinal cord injury**,** FGF-2, VPA, coaxial electrospinning

Lista de abreviaturas e siglas

BDNF	Fator neutrófico derivado do cérebro
BHE	Barreira hematoencefálica
DAPI	4',6-diamidino-2-fenilindol
DMSO	Dimetilsulfóxido
FGF-2	Fator de crescimento de fibroblastlos 2
GABA	Ácido gama-aminobutírico
GDNF	Fator neurotrófico derivado da glia
HDAC	Enzimas histonas deacetilases
HDACi	Inibidor das enzimas histonas deacetilases
kV	Quilovolt
LME	Lesão da medula espinal
MEV	Microscopia Eletrônica de Varredura
MET	Microscopia Eletrônica de Transmissão
mL	Mililitros
MPa	Megapascal
MTT	{brometo de [3-(4,5-dimetiltiazol-2yl)-2,5-difenil tetrazolium]}
PLGA	Poli(ácido lático-co-ácido glicólico)
PEG	Polietilenoglicol
RE	Retículo endoplasmático
ROS	Espécies reativas de oxigênio
VPA	Ácido valpróico
WST-8	(4-[3-(2-metoxi-4-nitrofenil)-2-(4-nitrofenil)-2H-5-tetrazolio]-1,3-benzeno disulfonato)

Lista de figuras

Lista de tabelas

1. Revisão bibliográfica

1.1. Lesão da medula espinal (LME)

A lesão na medula espinal (LME) resulta em perda generalizada de conexões axonais e também em uma limitada regeneração neuronal que normalmente leva à incapacidade funcional abaixo do local da lesão (Liu *et al.*, 2012). Essa incapacidade é de longa duração e apresenta respostas limitadas à administração de drogas e tentativas de reabilitação (Furuya *et al.*, 2013). Estima-se que ocorram cerca de 768 mil novos casos de LME ao redor do mundo anualmente (Kumar *et al.*, 2018). No Brasil, são cerca de 40 casos novos por ano por milhão de habitantes, ou seja, cerca de 6 a 8 mil casos novos por ano (Ministério da Saúde, Brasil). Aproximadamente, 80% dos casos de LME traumática são causados por acidentes de trânsito, violência urbana, quedas e acidentes relacionados à prática de esportes (Thomaty *et al.*, 2017).

A fisiopatologia da LME pode ser dividida em fase primária e secundária e, também, pode ser classificada temporalmente em fases aguda (até 48h depois da lesão), subaguda (48 horas à 14 dias após a lesão), intermediária (14 dias à 6 meses após a lesão) e fase crônica (acima de 6 meses após a lesão) (Ahuja *et al.*, 2017).

- *Fase aguda*:

A lesão primária é imediata e irreversível (Rabchevsky *et al.*, 2000). O trauma mecânico inicial provoca ruptura e deslocamento da coluna vertebral, que causa compressão ou transecção da medula espinal (Ahuja *et al.*, 2017). O trauma resulta na lesão direta dos elementos neurais, ruptura dos axônios e dos vasos sanguíneos, comprometimento da barreira hematoencefálica (BHE), além de provocar hemorragia aguda e isquemia. A lesão primária na medula espinal desencadeia uma cascata de danos secundários que envolvem eventos bioquímicos e neurológicos que podem continuar a progredir desde alguns minutos até meses (Zhou *et al.*, 2018).

As alterações celulares presentes durante a fase aguda da injúria, como a disfunção e a morte celular são causadas pela permeabilização das membranas celulares, sinalização pró-apoptótica e lesão isquêmica devido à destruição do suprimento microvascular da medula espinal (Choo *et al.*, 2007; Laplaca *et al.*, 2007). Além disso, a lesão dos vasos sanguíneos pode

expor a medula espinal ao influxo de células inflamatórias, citocinas e peptídeos vasoativos. Esse aumento no nível de citocinas pró-inflamatórias, como o fator de necrose tumoral (TNF) e a interleucina-1 beta (IL-1β), é evidente na medula espinal minutos após a lesão e é associado à chegada das células inflamatórias como macrófagos, neutrófilos e linfócitos na medula espinal que permanecem presentes além da fase subaguda. Essa resposta inflamatória combinada com a ruptura da BHE, leva progressivamente ao edema no local da lesão. Ao longo do tempo, esse edema pode levar à compressão mecânica da medula espinal que pode se estender por múltiplos segmentos e agravar a lesão (Figura 1a) (Ahuja *et al.*, 2017).

- *Fase subaguda*:

Entre a fase aguda e a fase subaguda, a isquemia e a excitotoxicidade contribuem para a perda da homeostasia iônica intracelular e extracelular, contribuindo para o aumento do edema e da morte celular de neurônios e oligodendrócitos. Dados de modelos animais indicam que altos níveis de cálcio intracelular ativa calpaínas, que causam disfunção mitocondrial e morte celular. Além disso, a necrose de neurônios e glia devido a isquemia, inflamação e excitotoxicidade libera ATP, DNA e potássio que podem ativar as células da micróglia. A micróglia e as outras células inflamatórias ativadas (macrófagos, células polimorfonucleadas e linfócitos) infiltram o local da lesão onde propagam a resposta inflamatória e contribuem para a progressão da apoptose dos neurônios e dos oligodendrócitos e, também, a formação de microcavidades císticas. As células inflamatórias fagocíticas limpam os debris de mielina no local da injúria, mas podem também induzir danos futuros na medula espinal através da liberação de produtos citotóxicos como as espécies reativas de oxigênio ROS (O_2^-, peróxido de hidrogênio e peróxido de nitrito). Essas ROS podem causar peroxidação lipídica, dano oxidativo ao DNA e oxidação de proteínas, que são uma causa adicional para a necrose e apoptose celular, contribuindo ainda mais para a formação de um microambiente hostil à regeneração tecidual. Além disso, os astrócitos proliferam e depositam moléculas da matriz extracelular na área ao redor da lesão (Figura 1b) (Ahuja *et al.*, 2017).

- *Fase intermediária-crônica*:

À medida que a resposta inflamatória diminui, a lesão evolui através de uma dinâmica fase intermediária-crônica. Essa fase é caracterizada por tentativas de remielinização, reorganização vascular, alterações na composição da matriz extracelular e remodelamento dos circuitos neurais (Kwon *et al.*, 2004). A morte e degeneração celular na fase aguda levam a formação de cavidades císticas no local da lesão que contém fluido extracelular, finas bandas

de tecido conectivo e macrófagos (Norenberg *et al.*, 2004) sendo um pobre substrato para a migração celular (Figura 1C) (Ahuja *et al.*, 2017).

Estudos utilizando modelos animais têm demonstrado a existência de uma zona perilesional ao redor da cavidade cística, em que astrócitos reativos proliferam e se interlaçam fortemente, criando uma matriz de malha inibitória. Na fase aguda, a sinalização da microglia ativada, astrócitos e macrófagos causam a secreção de proteínas da matriz extracelular que são inibitórias ao crescimento axonal, como proteoglicanos de sulfato de condroitina (CSPGs), tenascina e NG2 proteoglicano (também conhecido como sulfato de condroitina proteoglicano 4), que se condensam com os astrócitos para formar a cicatriz glial. A cicatriz glial destaca-se por ser uma das principais barreiras para regeneração axonal (Zhou *et al.*, 2018) (figura 1c). Os danos secundários podem ser prevenidos e são considerados o alvo para agentes neuroprotetores que visam preservar a função dos tecidos neuronais (Beattie, 2004; Jia *et al.*, 2018).

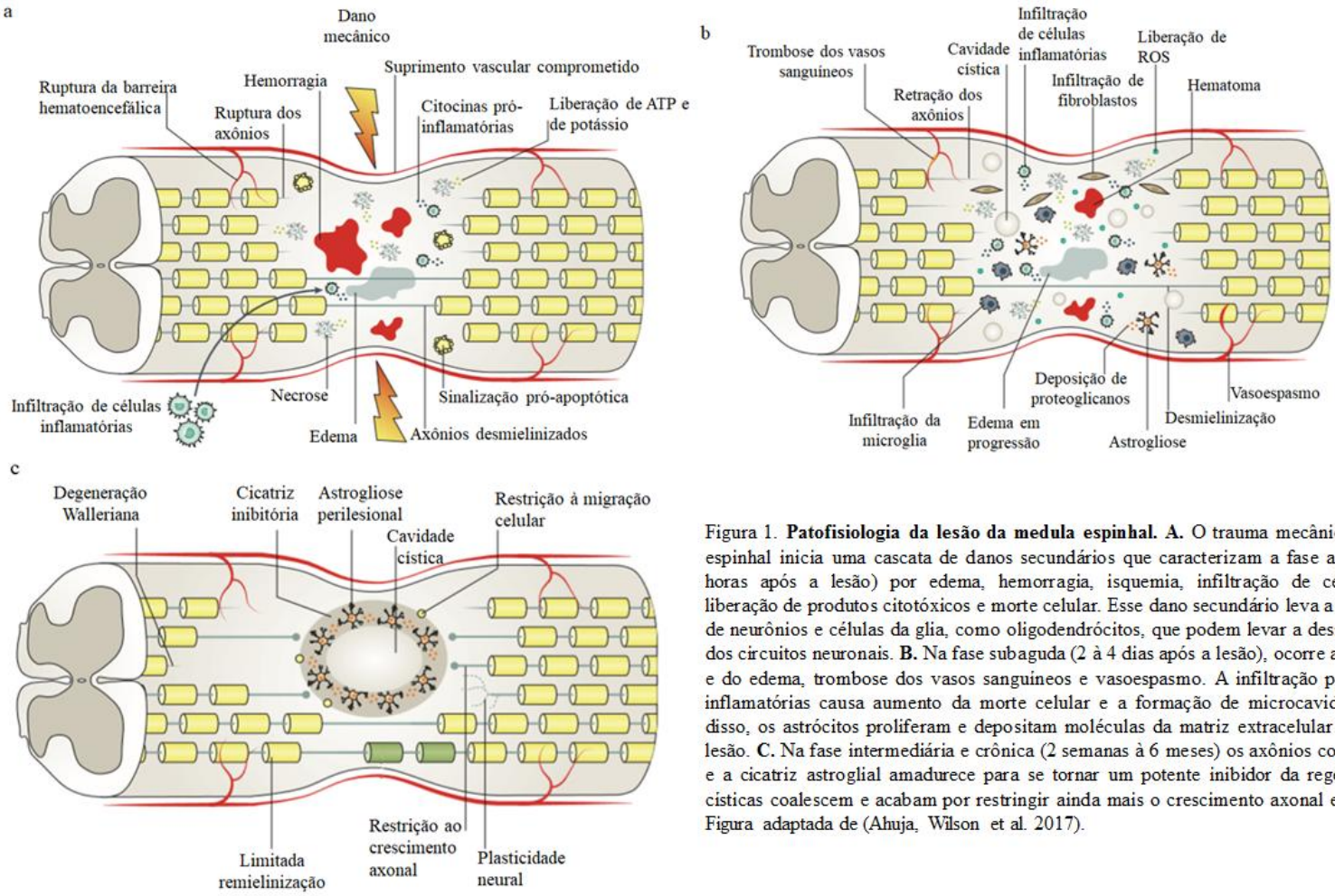

Figura 1. **Patofisiologia da lesão da medula espinhal. A.** O trauma mecânico inicial na medula espinhal inicia uma cascata de danos secundários que caracterizam a fase aguda (isto é, 0 à 48 horas após a lesão) por edema, hemorragia, isquemia, infiltração de células inflamatórias, liberação de produtos citotóxicos e morte celular. Esse dano secundário leva a necrose ou apoptose de neurônios e células da glia, como oligodendrócitos, que podem levar a desmielinização e perda dos circuitos neuronais. **B.** Na fase subaguda (2 à 4 dias após a lesão), ocorre aumento da isquemia e do edema, trombose dos vasos sanguíneos e vasoespasmo. A infiltração persistente de células inflamatórias causa aumento da morte celular e a formação de microcavidades císticas. Além disso, os astrócitos proliferam e depositam moléculas da matriz extracelular na área ao redor da lesão. **C.** Na fase intermediária e crônica (2 semanas à 6 meses) os axônios continuam a degenerar e a cicatriz astroglial amadurece para se tornar um potente inibidor da regeneração. Cavidades císticas coalescem e acabam por restringir ainda mais o crescimento axonal e a migração celular. Figura adaptada de (Ahuja, Wilson et al. 2017).

Segundo o mecanismo da lesão, os modelos de LME podem ser classificados como contusão, compressão, distração (o contrário de compressão), lesão química e transecção completa ou incompleta (parcial, unilateral e hemisecção). A contusão se caracteriza por uma força transitória aplicada sobre a medula espinal seja por um queda de um peso, eletromagnetismo ou dispositivos de pressão de ar. Os modelos de compressão incluem a compressão da medula espinal por um longo período de tempo. A distração consiste na aplicação de forças opostas para alongar a medula espinal. O mecanismo químico é útil para investigar aspectos específicos dos danos secundários. E por fim, a transecção envolve o corte parcial ou incompleto da medula (Cheriyan *et al.*, 2014).

O modelo de transecção completa ou parcial são apropiados e extensivamente utilizados, em especial, para o estudo de novos *scaffolds* (biomateriais que atuam como arcabouços) na área de engenharia de tecidos para investigar os processos e mecanismos envolvidos no reparo da LME (Kubinová *et al.*, 2015). Além de ser um modelo de lesão menos invasivo e devastador também permite analisar a infiltração de células endógenas no local do implante (Kubinová *et al.*, 2011; Kubinová *et al.*, 2015; Tukmachev *et al.*, 2016). Um quadro clínico decorrente da hemisecção da medula espinal é a Síndrome de Brown-Séquard. Essa síndrome geralmente é observada em indivíduos com LME traumática penetrante, secundária a ferimentos de bala e faca. Os déficits encontrados em pacientes com essa síndrome incluem perda de função motora, propriocepção e sensação de vibração ipsilateral à lesão e perda de dor e sensação de temperatura contralateral à lesão (Ahuja *et al.*, 2017).

Entre os modelos animais empregados nos estudos preliminares para o tratamento da LME, os ratos são mais comumente utilizados por serem relativamente baratos, prontamente disponíveis e demonstrarem resultados funcionais, eletrofisiológicos e morfológicos similares aos dos humanos (Metz *et al.*, 2000; Cheriyan *et al.*, 2014). Em adição às vantagens inerentes aos modelos animais de avaliação do efeitos terapêuticos das potenciais estratégias de tratamento, esses modelos são altamente úteis na avaliação do grau de comprometimento motor após lesão (Kim *et al.*, 2017).

Atualmente, não há tratamento efetivo para a LME. Os tratamentos clínicos, em geral, envolvem a administração intravenosa de uma alta dose de metilprednisolona (Ahuja *et al.*, 2017). A metilprednisolona é um costicosteróide capaz de diminuir a ativação de várias vias inflamatórias (Hsu e Dimitrijevic, 1990; Ziemba e Gilbert, 2017) e é aprovado pelo FDA para uso em pacientes com LME aguda (Ziemba e Gilbert, 2017). No entanto, a eficácia dessa

abordagem tem sido amplamente contestada (Fehlings, 2001; Chen *et al.*, 2015). Benefícios clínicos nem sempre superam os efeitos colaterais dessa substância, como aumento do risco de infecções e hiperglicemia (Bydon *et al.*, 2014). A administração deste esteróide não é mais um tratamento padrão, nem mesmo uma diretriz para o tratamento da LME no Canadá e em muitos outros países que adotaram políticas semelhantes (Ramer *et al.*, 2005). Outra alternativa clínica é a cirurgia de descompressão que visa realinhar a coluna vertebral, restabelecer a estabilidade da medula espinal e provocar a descompressão (alívio da compressão óssea ou ligamentar no canal medular) (Ahuja *et al.*, 2017).

Cerca de 942 ensaios clínicos são encontrados no site *clinicaltrials.gov* utilizando o temos de busca *spinal cord injuries*. Diversos ensaios clínicos estão recrutando voluntários ou estão sendo realizados visando o tratamento da LME. Entre esses tratamentos, encontra-se, por exemplo, o transplante de células-tronco mesenquimais derivadas do cordão umbilical, transplante de células mononucleares autólogas derivadas de medula óssea por injeção lombar e transplante de células-tronco mesenquimais autólogas, entre outros. O potencial da aplicação de biomateriais no tratamento da LME tem sido explorado em numerosos estudos pré-clínicos, bem como em testes clínicos (Xiao *et al.*, 2016).Também, atualmente, está em andamento um estudo clínico da empresa InVivotherapeutics (NCT02138110) utilizando *scaffolds* de co-polímero de ácido lático e ácido glicólico (PLGA) em casos de LME (Estudo Piloto da Segurança Clínica do PLGA para o Tratamento da LME Aguda Completa visando verificar a segurança e viabilidade desses *scaffolds)*.

1.2. Medicina regenerativa

A medicina regenerativa abrange o espectro de tecnologias e abordagens que visam regenerar, reparar ou substituir células, tecidos ou órgãos danificados. Inclui a geração e uso de substâncias bioativas, biomateriais e células-tronco (Corona *et al.*, 2010; Advancing regenerative medicine, 2014; Steffens *et al.*, 2018). Essa é, portanto, uma abordagem multidisciplinar que envolve conhecimentos de diversas áreas: biologia celular, nanotecnologia, bioquímica, fisiologia, farmacologia, genética, biologia molecular, engenharia de tecidos entre outros (Corona *et al.*, 2010; Sampogna *et al.*, 2015).

O objetivo da engenharia de tecidos é criar um microambiente que imite a matriz extracelular nativa, capaz de promover interações célula-matriz específicas, influenciando o comportamento celular e promovendo a regeneração tecidual do hospedeiro. A esse respeito,

os *scaffolds* são atualmente os substratos avançados mais promissores capazes de suportar o crescimento celular e a liberação substâncias bioativas (Raspa *et al.*, 2016).

Os biomateriais ideais para uso no tratamento da LME devem ter uma estrutura tridimensional específica, apresentar biocompatibilidade, promover a liberação de moléculas bioativas prover suporte mecânico e topografia favorável para a adesão, proliferação e diferenciação celular (Colello *et al.*, 2016; Liu *et al.*, 2017). Além disso, esse tipo de biomaterial deve se degradar lentamente no ambiente fisiológico, permitindo que o tecido em crescimento possa substituir o local preenchido como *scaffold*. Esses biomateriais podem ser produzidos utilizando-se polímeros naturais ou sintéticos e são subdivididos em três principais formas; *scaffolds* sólidos, hidrogéis e micro/nanopartículas (Liu *et al.*, 2017). Uma importante vantagem dos *scaffolds* sólidos de microfibras em relação aos outros materiais é que ele imita a arquitetura da matriz extracellular, imitando sinais biológicos e resultando em atração fisiológica de células permitindo sua adesão, proliferação e diferenciação (Kubinová e Syková, 2012; Liu *et al.*, 2012), além de fornecer suporte mecânico para a regeneração tecidual.

Os *scaffolds* de microfibras podem fornecer uma ponte para conectar as áreas de tecidos lesados na LME. Além desse papel, como uma plataforma estrutural, os *scaffolds* podem desempenhar papéis ativos quando associados a células ou a moléculas bioativas, inibindo a apoptose das células, a inflamação e a formação da cicatriz, também induzindo a neurogênese, o crescimento axonal e a angiogênese (Kim *et al.*, 2014). Assim, os *scaffolds* ideais para a engenharia de tecidos devem ser integrados com agentes bioativos de modo a modular finamente a migração, a proliferação e a diferenciação celular (Yao et al., 2009). A liberação local de drogas com o uso dessas matrizes pode diminuir a dose mínima necessária de uma determinada droga, levando a menor absorção sistêmica e redução dos indesejados efeitos colaterais (Zamani *et al.*, 2014).

Portanto, diversos estudos têm sido realizados na tentativa de encontrar formas de reduzir os danos posteriores à lesão. A utilização de substâncias neuroprotetoras como o fator de crescimento de fibroblastos (FGF) (Kang *et al.*, 2013; Goldshmit *et al.*, 2014) e o ácido valpróico (VPA) têm se mostrado promissora nos casos de LME (Lv *et al.*, 2011; Abdanipour *et al.*, 2012; Chen *et al.*, 2018). Além disso, para a criação de um ambiente desejável para a regeneração dos axônios, os estudos também têm focado em orientar o crescimento axonal na direção correta com *scaffolds* naturais ou sintéticos visando reduzir a formação da cicatriz glial e as outras lesões secundárias (Shi *et al.*, 2014). A combinação de estratégias, substâncias

bioativas e biomateriais, são úteis para o tratamento da LME devido a sua capacidade de atuar como suporte para o crescimento celular e na liberação de agente terapêuticos no local da lesão recriando a conexão neural.

1.3.Fator de crescimento de fibroblastos 2 (FGF-2)

O fator de crescimento de fibroblastos (FGF) recebeu esse nome porque foi originalmente isolado do cérebro e hipófise como mitógeno para cultura de fibroblastos (Itoh, 2007; Itoh e Ornitz, 2011). Contudo, atualmente, o FGF é reconhecido como um fator de crescimento polipeptídeo com diversas atividades biológicas incluindo angiogênese, diferenciação, proliferação e migração celular (Thisse e Thisse, 2005) em diferentes tecidos. A família FGF em mamíferos é composta por 22 membros (Itoh, 2007; Yun *et al.*, 2010; Itoh e Ornitz, 2011), dentre os quais inclui o fator de crescimento de fibroblastos 2 (FGF-2 ou bFGF).

O FGF-2 é altamente expresso nos tecidos neuronais (Shi *et al.*, 2014; Zhou *et al.*, 2018) sendo crucial para o desenvolvimento do SNC e durante toda a vida (Zhou *et al.*, 2018), incluindo a neurogênese nos adultos (Woodbury e Ikezu, 2014). Expresso tanto em astrócitos quanto em neurônios, é envolvido na neurogênese, no crescimento axonal, na neuroproteção e na neuroregeneração (Li *et al.*, 2010). *In vitro*, o FGF-2 promove a diferenciação de neurônios, da glia e de células endoteliais de várias regiões do SNC (Morrison *et al.*, 1988; Chan *et al.*, 2013), além de ter efeitos neuroprotetores (Noda *et al.*, 2014) (figura 2). Após a LME, há um rápido aumento de FGF- 2 no local da injúria (Mocchetti *et al.*, 1996; Rabchevsky *et al.*, 2000; Zai *et al.*, 2005) o que pode ser um dos fatores que contribui para a recuperação espontânea observada após a lesão que ocorre tanto em ratos quanto em humanos (Zai *et al.*, 2005).

Em 1999, Teng e colaboradores verificaram que a injeção de FGF-2 diretamente no local da lesão medular, 5 minutos após a LME, promoveu a sobrevivência neuronal (Teng *et al.*, 1999). Desde então, diversos estudos têm sido publicados demonstrando que o FGF-2 provoca melhora locomomotora, neuroproteção e regeneração dos axônios na LME em modelo animal de ratos. Nos parágrafos a seguir, na tabela 1 e na figura 2 será realizada uma breve descrição desses resultados.

Zhang e colaboradores, em 2012, estudaram alguns mecanismos que podem ser relacionados aos efeitos benéficos do FGF-2 na LME, em especial, na melhora locomotora dos animais estudados (figura 2). O estudo mostrou que esse fator de crescimento causa a redução

da apoptose de neurônios e astrócitos. O efeito protetor doFGF-2 foi relacionado à inibição das proteínas CHOP, GRP78 e caspase-12, proteínas que respondem ao estresse do retículo endoplasmático e induzem a apoptose celular. Também, nesse mesmo estudo, o tratamento com FGF-2 levou a ativação da rota de sinalização PI3K/Akt/GSK-3b e ERK1/2. Essa via de sinalização intracelular é importante na regulação do ciclo celular e está relacionada com a sobrevivência, diferenciação e migração celular (Zhang, Zhang*, et al.*, 2013).

Acrescenta-se também que o efeito do FGF-2 é relacionado à prevenção da ativação excessiva da autofagia intracelular e aumenta a remoção de proteínas ubiquitinadas pela ativação da rota de sinalização PI3K/Akt/mTOR. Essa via da autofagia intracelular é um mecanismo celular proteolítico que envolve o sequestro de componentes citoplasmáticos para serem degradados e pode preceder a apoptose celular (Zhang, Wang*, et al.*, 2013).

Além disso, o tratamento com FGF-2 provoca o aumento na expressão dos progenitores neurais (nestina e SOX-2) e redução da inflamação pela diminuição da infiltração de monócitos e macrófagos e da expressão de TNF-α (Goldshmit *et al.*, 2014). A resposta inflamatória e a perda da homeostase no local da lesão é diretamente relacionada a desintegração da BHE que leva à infiltração de células sanguíneas no local da lesão e está envolvida com os danos secundários que ocorrem após a lesão. O tratamento com FGF-2, mantém a integridade da BHE por provocar o aumento na expressão das proteínas das junções oclusivas (*junction proteins*): ocludina, claudina, β-catenina e, também, reduz a expressão e ativação da metaloproteinase de matriz 9 e, dessa forma, contribui para redução da inflamação e, consequentemente, provoca a melhora locomotora dos animais (Ye *et al.*, 2016).

Em um modelo de transecção, após o tratamento com FGF-2, houve diminuição do tamanho da cavidade cística presente no local da lesão. A cavidade foi preenchida por células intrínsecas que proliferaram e/ou se acumularam no local da lesão em resposta ao fator de crescimento, o que pode ter auxiliado na regeneração nervosa. Essas observações demonstram que as células positivas para marcação com fibronectina induzidas pelo FGF-2 preencheram a cavidade do local da lesão e podem ter contribuído para a regeneração axonal após a lesão medular (Kasai *et al.*, 2014).

Utilizando outra via de administração do FGF-2, Rabchevsky e colaboradores (1999 e 2000), implantaram uma minibomba osmótica no ventrículo lateral e no saco tecal lombar, dessa forma, liberando FGF-2 no fluido cerebroespinal durante uma semana. O estudo mostrou que, com esse tipo de administração, houve melhora locomotora dos animais, após lesão

medular moderada ou grave (Rabchevsky *et al.*, 1999; Rabchevsky *et al.*, 2000). Embora esse método seja bem sucedido para liberação gradual e local do FGF-2, apresenta duas principais limitações: formação de cicatriz no local onde foi implantado a minibomba que pode levar à falha na infusão e danos na medula causados pela presença do cateter (Jones e Tuszynski, 2001).

Estudos anteriores já demonstraram os efeitos benéficos da utilização do FGF-2 associado a biomateriais no tratamento LME, tais como o uso de como hidrogéis (Chen *et al.*, 2015; Xu *et al.*, 2018), membranas (Shi *et al.*, 2014), nanoesferas (Shin *et al.*, 2018) e microesferas (Lan *et al.*, 2017), demonstrando melhora lomotora em animais. Além disso, a utilização de *scaffolds* de colágeno com FGF-2 promoveu o crescimento das fibras axonais através dos implantes (Shi *et al.*, 2014). No entanto, até o momento, não há estudos em que o FGF-2 tenha sido encapsulado dentro de microfibras que forneçam suporte estrutural para o crescimento celular.

As limitações da administração sistêmica relacionada com a exposição do fator à degradação de enzimas, dificuldade de ultrapassar a barreira hematoencefálica e o potencial mitogênico do FGF-2 pode levar a formação de tumores nos tecidos saudáveis na aplicação sistêmica (Lan *et al.*, 2017). Para superar as deficiências da terapêutica baseada em proteínas, sistemas de administração de medicamentos “in situ” oferecem uma alternativa eficaz e segura para a administração local desse fator de crescimento.

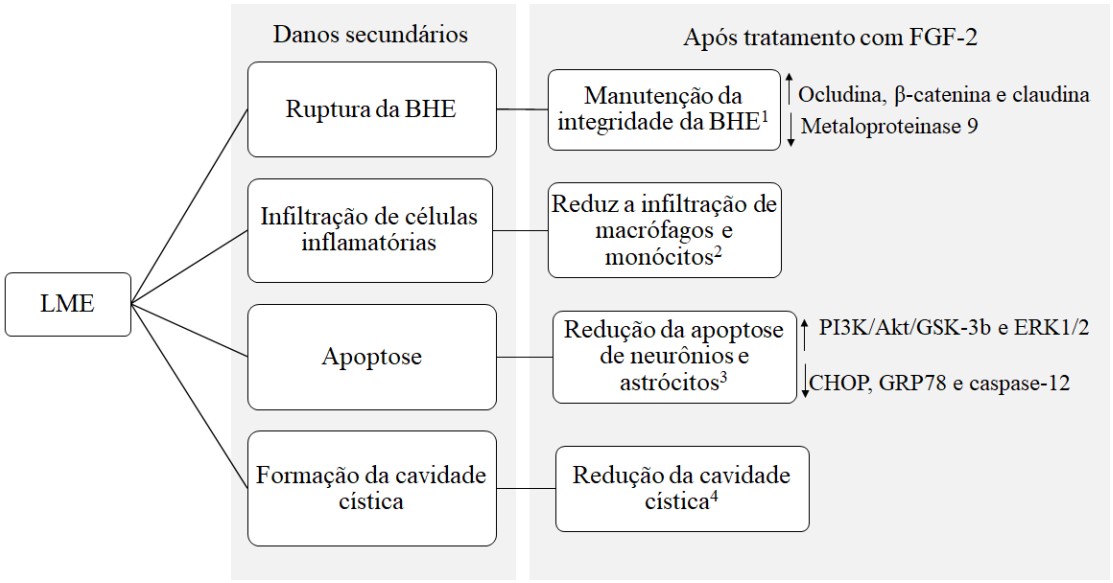

Figura 2. Mecanismos de ação do FGF-2 na LME. Figura de autoria própria. 1- (Ye *et al.*, 2016); 2 - (Goldshmit *et al.*, 2014); 3 - (Zhang, Zhang, *et al.*, 2013); 4 - (Kasai *et al.*, 2014). BHE: barreira hematoencefálica / FGF-2: Fator de crescimento de fibroblastos 2 / LME: lesão da medula espinal.

Tabela 1. Resumo dos estudos publicados em que o FGF-2 foi utilizado no tratamento da LME.

Estudo	Tipo de lesão	Via de administração	Dose e frequência	Resultados
(Teng *et al.*, 1999)	Contusão	Injeção diretamente no local da lesão, 5 minutos após a lesão	3μg de FGF-2, 5 minutos após a LME	Sobrevivência de neurônios motores e melhora da função respiratória
(Rabchevsky *et al.*, 1999)	Contusão moderada	Minibomba intratecal	3 ou 6 μg/dia durante 7 dias	Melhora locomotora
(Rabchevsky *et al.*, 2000)	Contusão severa	Minibomba intratecal	3 ou 6 μg/dia durante 7 dias	Melhora locomotora
(Kang *et al.*, 2013)	Compressão	Nanopartículas diretamente no local da lesão	Dados não demonstrados	Aumento na densidade dos vasos sanguíneos
(Zhang, Zhang, *et al.*, 2013)	Compressão	Subcutâneo	80 μg/kg/dia durante 7 dias	Melhora locomotora e a inibição da ativação de vias de sinalização que levam à apoptose celular
(Zhang, Wang, *et al.*, 2013)	Compressão	Subcutâneo	80μg/kg/dia durante 7 dias	Regulação da autofagia, remoção das proteínas ubiquitinadas, melhora locomotora

(Goldshmit *et al.*, 2014)	Hemisecção	Subcutâneo	135µg/kg, 30 minutos após a lesão e, posteriormente, a cada dois dias	Melhora locomotora, diminuição da gliose e aumento progenitores neurais
(Kasai *et al.*, 2014)	Transecção	Injeção diretamente no local da LME	1µg/µL	Melhora locomotora e redução da cavidade cística
(Shi *et al.*, 2014)	Hemisecção	*Scaffold* de colágeno contendo FGF-2 no local da lesão	Dados não demonstrados	Melhora locomotora e regeneração neural
(Chen *et al.*, 2015)	Transecção	Hidrogel contendo FGF-2 no local da lesão	Dados não demonstrados	Melhora locomotora e regeneração do tecido neural
(Ye *et al.*, 2016)	Contusão	Subcutâneo	80µg/kg 30 minutos após a lesão e, posteriormente, a cada dois dias	Melhora locomotora e manutenção da integridade da BHE
(Lan *et al.*, 2017)	Hemisecção	Microesferas no local da lesão	Dados não demonstrados	Melhora locomotora, redução da apoptose e da necrose celular
(Xu *et al.*, 2018)	Hemisecção	Hidrogel contendo FGF-2	Dados não demonstrados	Melhora locomotora, aumento de fibras neurofilamento positivas e da densidade dos axônios

1.4.Ácido Valpróico (VPA)

O ácido valpróico (VPA) é uma droga bem estabelecida para o tratamento à longo prazo da epilepsia (Blaheta e Cinatl, 2002; Zhu *et al.*, 2017). Uma de suas principais ações é o aumento no nível do ácido gama-aminobutírico (GABA) no cérebro. O GABA é um importante inibidor de convulsões e a redução nos níveis desse neurotransmissor pode potencializar as crises convulsivas (Ornoy, 2009). Além disso, esse medicamento é amplamente prescrito para tratar distúrbios neurológicos e psiquiátricos, incluindo a dor neuropática e o transtorno de humor bipolar (Lv *et al.*, 2011; Zhu *et al.*, 2017). Estudos, tanto *in vitro* como *in vivo*, demonstraram o papel neuroprotetor e anti-inflamatório do VPA (Lv *et al.*, 2011; Ximenes *et al.*, 2013; Lee *et al.*, 2014)

O VPA também é um conhecido inibidor das enzimas histonas deacetilases (HDACi) (Phiel *et al.*, 2001; Chuang *et al.*, 2009; Goey *et al.*, 2016). Essas enzimas histonas deacetilases (HDAC) pertencem a uma família de enzimas que removem grupos acetil dos resíduos de lisina localizados na cauda amino-terminal das proteínas histonas e levam a compactação da cromatina associada com a repressão da transcrição e expressão genética (Zhang *et al.*, 2018). Os inibidores dessas enzimas, HDACi, regulam a acetilação das histonas, o remodelamento da cromatina e a expressão genética (Lv *et al.*, 2011; Yu *et al.*, 2012). A hipoacetilação das histonas ocorre em um grande número de doenças do SNC e o uso dos HDACi são uma intervenção terapêutica promissora para esses casos (Lv *et al.*, 2011). Os HDACis podem reduzir os danos secundários da LME e contribuir para novas abordagens que, dessa forma, estimulem o reparo endógeno (York *et al.*, 2013).

Além disso, esses eventos epigenéticos têm sido recentemente reportados por desempenhar papéis importantes na regulação da regeneração de axônios (Ganai *et al.*, 2016). Após a LME, há uma redução na acetilação de histonas no local da lesão medular (Lv *et al.*, 2011). Já foi demonstrado que o tratamento com injeção intraperitoneal de VPA foi capaz de restaurar a acetilação das histonas nas medulas lesionadas e provocou melhoras locomotoras significativas nos ratos (Lv *et al.*, 2011; Lee *et al.*, 2012; Yu *et al.*, 2012). Esse efeito foi relacionado à prevenção da redução das histonas acetiladas H3 (Lv *et al.*, 2011; Lee *et al.*, 2012; Yu *et al.*, 2012) e H4 (Lv *et al.*, 2011) e à redução da HDAC3 (Chen *et al.*, 2018). Os estudos de Lv e colaboradores e de Yu e colaboradores falharam em identificar os genes regulados pela terapia com VPA na LME. Porém, acredita-se que esse efeito seja porque os HDACi promove

a transcrição e expressão de genes neuroprotetores, como a HSP70 e Bcl-2, já observado em estudos isquemia (Kim, H. J. *et al.*, 2007; Sinn *et al.*, 2007).

Ademais, o tratamento com VPA causa a redução da cavidade cística no local da lesão (Yu *et al.*, 2012; Darvishi *et al.*, 2014) com uma área de tecido preservado significativamente maior quando comparada aos grupos controle. Essa regeneração tecidual pode ser explicada por uma série de diferentes efeitos do VPA. Primeiramente, pela redução da apoptose celular (Lv *et al.*, 2011; Lee *et al.*, 2012) e da autofagia intracelular (Hao *et al.*, 2013), além de aumentar o número relativo de oligodendrócitos no local da lesão (Penas *et al.*, 2011). Também, o VPA o estimula da expressão da proteína associada aos microtúbulos 2 (MAP-2), um indicativo de crescimento de neuritos no local da lesão. Por fim, essa substância provoca o aumento na expressão dos progenitores neuronais (nestina e SOX2) (Bang *et al.*, 2013) e de fatores neurotróficos BDNF e GDNF (Lv *et al.*, 2012) no local da injúria.

Também, em outros experimentos realizados em modelos *in vivo*, demonstrou-se que o VPA reduz a morte celular dos neurônios motores por inibir o estresse oxidativo e o estresse do RE mediado pela liberação de citocromo C (Lee *et al.*, 2014). O VPA também inibe a liberação de citocromo C pela inibição da ativação da JNK dependende de ROS em condições de estresse oxidativo. Além disso, sob condições de estresse do RE há a ativação da caspase-12 que leva a apoptose celular, o VPA reduz a ativação dessa caspase e a expressão de CHOP.

Além disso, o VPA provoca a diminuição das reações inflamatórias por reduzir o número de macrófagos e a mudança de fenótipo desse tipo celular (Yu *et al.*, 2012; Chen *et al.*, 2018), por inibir a ativação da microglia (Lu *et al.*, 2013; Chen *et al.*, 2018) e a produção de mediadores inflamatório (TNF-α, IL-1β, IL-6, iNOS e COX-2). Além disso, a infusão intraespinal contínua de VPA, por três dias após a LME, reduziu a gliose, a porcentagem da migroglia ativada e causou melhora locomotora em ratos (Lu *et al.*, 2013). Também envolvida com as reações inflamatórias, a redução na ruptura da BHE foi reportada como um dos efeitos do VPA por diminuir a proteína matriz metaloproteinase 9 (enzima conhecida por induzir a ruptura da BHE e por degradar a matriz extracelular) (Lee *et al.*, 2012) (figura 3 e tabela 2).

Por outro lado, há uma série de efeitos indesejados relacionados ao uso sistêmico do VPA como efeitos gastrointestinais, ganho de peso, tremores, perda de cabelo, hepatopatia, pancreatite, ovário policístico (Gerstner *et al.*, 2008). Em vista de reduzir os efeitos sistêmicos dessa droga e garantir a aplicação local e liberação gradual desse fármaco, uma excelente ferramenta é encapsular o VPA em microfibras que possam ser aplicadas diretamente no local da lesão. Com essa estratégia, é possível reduzir o aparecimento de doses tóxicas ou

subterapêuticas e, também, utilizar uma menor quantidade do princípio ativo, resultando em menor custo. Até o momento, não há estudos em que essa substância tenha sido associada a biomateriais, para uso na medicina regenerativa.

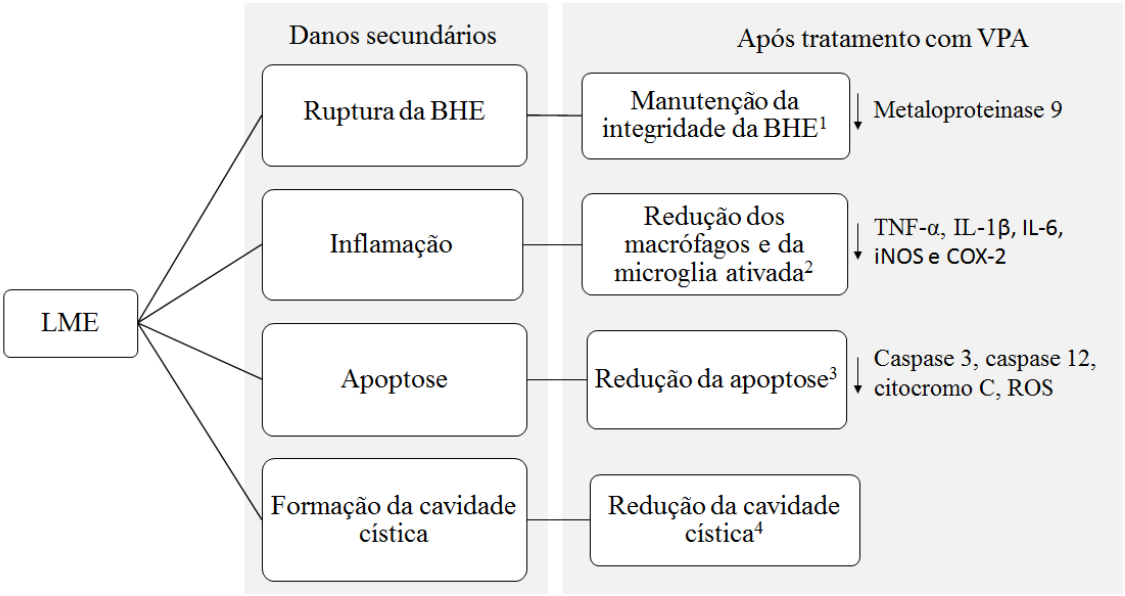

Figura 3. Mecanismos de ação do VPA na LME. Figura de autoria própria. 1 - (Lee *et al.*, 2012); 2 - (Chen *et al.*, 2018) ; 3 - (Lv *et al.*, 2012); 4 - (Darvishi *et al.*, 2014). BHE: barreira hematoencefálica / iNOS: óxido nítrico sintase induzível / LME: lesão da medula espinal / ROS: espécies reativas de oxigênio / VPA: ácido valpróico

Tabela 2. Resumo dos estudos publicados em que o VPA foi utilizado no tratamento da LME.

Estudo	Tipo de lesão	Via de administração	Dose e frequência	Resultados
(Lv *et al.*, 2011)	Contusão	Intraperitoneal	300mg/kg, duas vezes ao dia durante 7 dias	Previne a redução das histonas acetiladas H3 e H4, redução da apoptose e melhora locomotora
(Penas *et al.*, 2011)	Contusão	Intraperitoneal	150 mg/kg 3horas após a LME seguido de doses de 300mg/kg duas vezes ao dia durante a primeira semana e uma vez ao dia nas duas semanas seguintes	Aumento no número relativo de oligodendrócitos no local da lesão e melhora locomotora
(Abdanipour *et al.*, 2012)	Contusão	Intraperitoneal	100, 200 e 400 mg/dia uma vez ao dia durante 7 dias	Melhora locomotora (400 mg/kg)
(Lee *et al.*, 2012)	Contusão	Subcutâneo	150 ou 300 mg/kg, duas vezes ao dia por 5 dias	Redução da ruptura da BHE e melhora locomotora
(Lv *et al.*, 2012)	Contusão	Intraperitoneal	300 mg/kg duas vezes ao dia durante uma semana	Redução da apoptose e do tamanho da lesão, aumento de fatores neurotróficos BDNF e GDNF, melhora locomotora
(Yu *et al.*, 2012)	Compressão	Intraperitoneal	200 mg/kg duas vezes ao dia durante 7 dias	Redução de macrófagos no local da lesão, redução da cavidade cística e melhora locomotora

(Bang *et al.*, 2013)	Compressão	Intraperitoneal	200 mg/kg duas vezes ao dia durante 7 dias	Aumento na expressão de progenitores neurais no local da lesão
(Hao *et al.*, 2013)	Contusão	Intraperitoneal	300 mg/kg duas vezes ao dia durante duas semanas	Redução da autofagia intracelular e melhora locomotora
(Lu *et al.*, 2013)	Contusão	Minibomba osmótica	1µL/h de u durante 3 dias, a minibomba foi preenchida com 1,5µg de VPA	Redução da micróglia e macrófagos, aumento de fibras neuronais e melhora locomotora
(Darvishi *et al.*, 2014)	Contusão	Intraperitoneal	150, 200, 300, 400 e 500mg/kg 2, 6, 12 e 24 horas após a lesão	Redução na expressão de GFAP, redução da cavidade cística e melhora locomotora (300 mg/kg 12 horas após a lesão)
(Lee *et al.*, 2014)	Contusão	Subcutâneo	300 mg/kg duas vezes ao dia durante	Redução da morte celular de neurônios motores
(Chen *et al.*, 2018Chen *et al.*, 2018)	Contusão	Intraperitoneal	300 mg/kg uma vez ao dia durante 3 dias	Redução da inflamação no local da lesão

1.5.Eletrofiação

Antonin Formhalds, um pesquisador alemão, patenteou a técnica de eletrofiação ou *electrospinning* em 1934. No entanto, até 1993 havia poucas publicações utilizando essa técnica, inicialmente chamada de *electrostatic spinning*. Apenas no início de 1990, diversos grupos de pesquisadores retomaram o interesse por essa técnica, devido a sua capacidade de produção de fibras muito pequenas a partir de polímeros orgânicos. Então, o termo eletrofiação (*electrospinning)* passou a ser utilizado. Porém, até o ano de 2000, o número de publicações utilizando essa técnica ainda era insignificante. A partir de 2003, no entanto, esse número começou a aumentar significativamente e o interesse pela técnica cresce cada vez mais (Li e Xia, 2004). Atualmente, o número de artigos publicados mostrando a utilização da eletrofiação é muito grande, e vem aumentado exponencialmente.

A eletrofiação é o método mais comumente utilizado para criar nanofibras (Hromadka *et al.*, 2008). O mesmo é considerado um processo econômico e é conhecido como o único procedimento capaz de formar fibras contínuas (Gelain, 2008), ultrafinas e bastante longas (Venugopal *et al.*, 2008). Esse método funciona pelo princípio eletrostático, no qual são processadas soluções poliméricas produzidas a partir de diversos solventes. Por este método, a solução é provida ao equipamento por uma seringa que é submetida a uma diferença de voltagem elétrica. Nesse processo, a solução forma um jato de material fluído que é acelerado e estirado através de um campo elétrico produzindo fibras de diâmetro reduzido (Ziabari *et al.*, 2009).

Os principais componentes para a realização da eletrofiação são: fonte de alta tensão, agulha, placa coletora, seringa e a bomba propulsora (figura 4). A agulha é conectada à seringa que contém a solução polimérica através de um tubo de silicone. Com o auxílio da bomba propulsora, a solução polimérica presente dentro da seringa é fornecida à agulha em uma taxa constante e controlável. Quando a solução polimérica chega à pontada agulha, é submetida a um potencial elétrico aplicado entre a gota da solução polimérica na ponta dessa agulha e uma placa coletora aterrada. A agulha é carregada eletricamente a uma tensão elevada, induzindo cargas no interior do polímero, resultando na repulsão de cargas dentro da solução. As forças elétricas superam a tensão superficial e o jato líquido carregado é lançado a partir do ápice da gota pendurada na agulha. Quando o jato se afasta poucos centímetros da gota, a interação entre as superfícies e as forças moleculares se torna instável, o jato começa a chicotear flexionando

e estirando o jato polimérico, que reduz de tamanho enquanto o solvente evapora, diminuindo a velocidade do jato e dando origem a uma fibra sólida (Ziabari *et al.*, 2009; Chase *et al.*, 2011; Okutan *et al.*, 2014).

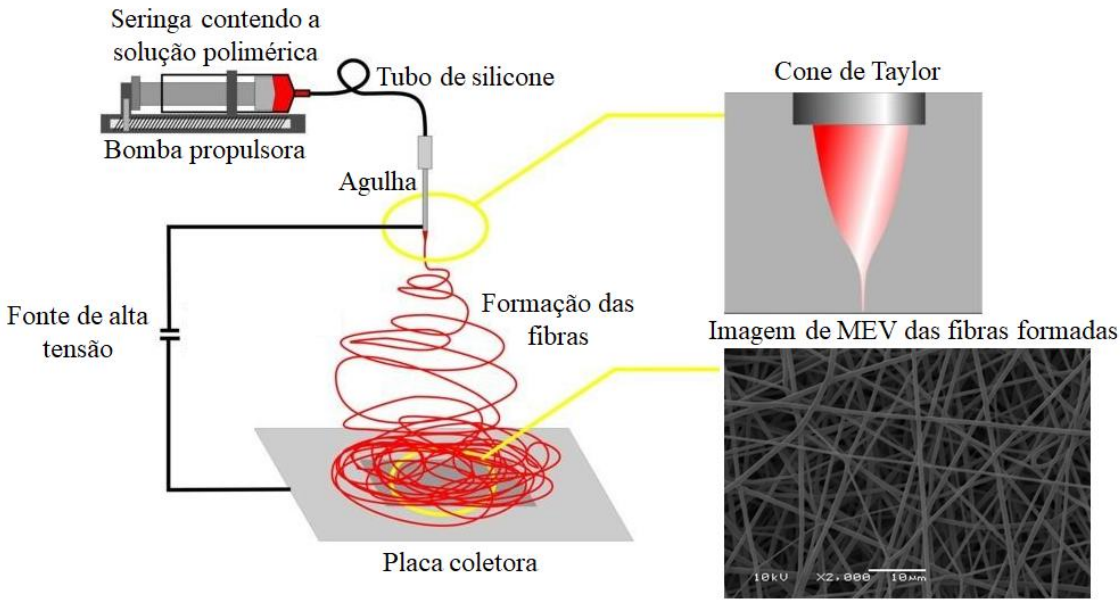

Figura 4. Ilustração esquemática da configuração básica do equipamento utilizado para eletrofiação. Figura adaptada de http://www.oxolutia.com/technology/electrospinning/. A imagem de MEV mostrando a morfologia das fibras é de autoria própria.

Embora a configuração da eletrofiação seja extremamente simples, atingir a estabilidade e a repetibilidade do processo é um grande desafio. Dentre os parâmetros que influenciam a estabilidade do processo e a morfologia das fibras destacam-se: distância da agulha até a placa coletora, voltagem aplicada, o fluxo na bomba propulsora (Neo *et al.*, 2012), concentração do polímero, temperatura e umidade.

As microfibras podem ser produzidas utilizando-se polímeros naturais ou sintéticos. Um dos polímeros do grupo dos poliésteres comumente utilizados para a realização dessa técnica é o copolímero de ácido lático e ácido glicólico (PLGA) (Xie *et al.*, 2006). Esse é o polímero de escolha por ser altamente biocompatível, biodegradável, de baixa toxicidade e imunogenicidade além de ser aprovado pela "Food and Drug Administration" (FDA) e pela Agência Europeia de Medicamentos (Jaworek e Sobczyk, 2008; Danhier *et al.*, 2012). Além disso, outra vantagem desse polímero é que a sua hidrólise leva à formação de monômeros de ácido lático e glicólico que são facilmente metabolizados pelo ciclo de Krebs apresentando, portanto, mínima

toxicidade sistêmica (Kumari *et al.*, 2010; Danhier *et al.*, 2012). O PLGA tem sido extensivamente utilizado na área biomédica e na engenharia de tecidos, com excelentes aplicações *in vivo* (Xie *et al.*, 2006; Yao *et al.*, 2016).

1.6.Eletrofiação coaxial

Atualmente, existem diversas estratégias para a incorporação de agentes bioativos nas matrizes produzidas por eletrofiação. Essas incluem a incorporação direta do agente bioativo na solução polimérica; o encapsulamento do agente bioativo através de uma emulsão posteriormente submetida ao processo de eletrofiação e, por fim, o encapsulamento por eletrofiação coaxial, uma variação da técnica principal (Lu *et al.*, 2009) porém, com vantagens superiores às demais técnicas de incorporação de moléculas bioativas relacionadas à técnica de eletrofiação.

A eletrofiação coaxial, portanto, é uma forma inovadora da eletrofiação tradicional e foi demonstrado pela primeira vez em 2002 (Loscertales *et al.*, 2002). A técnica utiliza dois tubos capilares alinhados concentricamente para forçar a formação de fibras com uma estrutura núcleo-casca (*core-shell*) (figura 5) (Moghe e Gupta, 2008). Uma das vantagens da eletrofiação coaxial é a possibilidade de encapsular frágeis agentes bioativos solúveis em água e, também, a liberação mais controlada dos agentes encapsulados e até a coencapsulação de vários fármacos com diferentes características de solubilidade (Jiang *et al.*, 2014). Além disso, as fibras são fabricadas a partir de duas soluções separadas, minimizando a interação entre moléculas biológicas solúveis em água e os solvente orgânicos em que o polímero é dissolvido, preservando a estabilidade das moléculas biológicas (Jiang *et al.*, 2014). Assim, as nanofibras ou microfibras geradas por eletrofiação coaxial podem ser fabricadas tendo um núcleo com a droga de escolha e na parte exterior – casca – uma camada de polímero biodegradável.

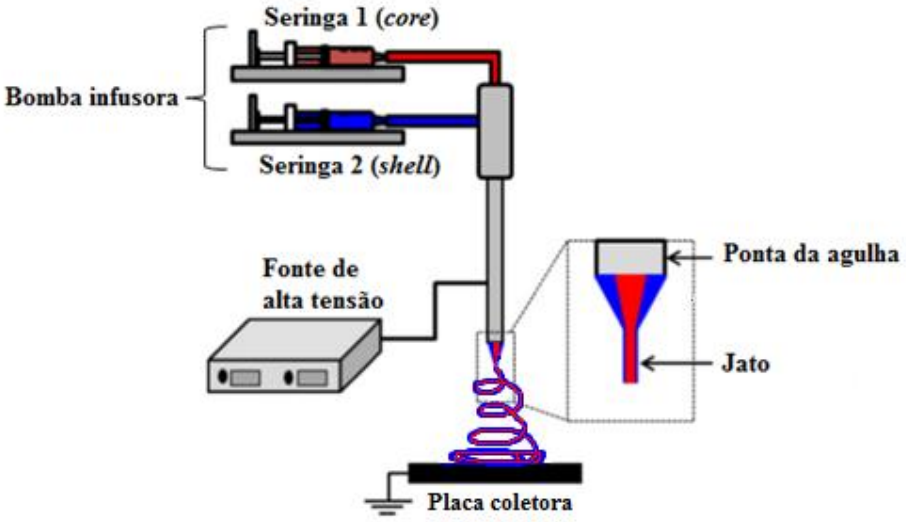

Figura 5. Configuração da eletrofiação coaxial. Figura adaptada de Davoodi e colaboradores, 2015 (Davoodi *et al.*, 2015).

As células PC12 (linhagem celular derivada de Feocromocitomas de ratos) têm sido utilizadas em diversos estudos para testar a biocompatibilidade e a bioatividade de *scaffolds* de microfibras para futuro uso na regeneração neural (Genchi *et al.*, 2015; Zhang *et al.*, 2016; Heidari *et al.*, 2017). Isso se deve ao fato desse tipo celular assemelhar-se às células cromafins das suprarrenais, que compartilham muitas propriedades fisiológicas dos neurônios (Young e Hung, 2003).

2. Hipóteses

A partir dos dados encontrados na literatura as hipóteses testadas neste estudo foram: a) que seja possível encapsular fator de crescimento de fibroblastos 2 e o ácido valpróico em microfibras da técnica de eletrofiação coaxial; b) que esse biomaterial seja adequado para proporcionar a adesão e a proliferação de células PC12 nos testes *in vitro*; c) que o implante dos *scaffolds* de microfibras, *in vivo*, em modelo animal de lesão da medula espinal por hemisecção promova melhora locomotora, regeneração tecidual e redução da cicatriz glial no local da lesão.

3. Justificativa

A lesão da medula espinal é um grave problema de saúde pública que ainda não conta com um tratamento clínico efetivo. No Brasil, são cerca de 6 a 8 mil casos novos por ano, sendo uma importante causa de morbidade e mortalidade com altos custos relacionados ao manejo dessa condição. As fibras produzidas por eletrofiação podem ser ferramentas promissoras para o tratamento da lesão da medula espinal. Esse tipo de biomaterial promove suporte estrutural ao tecido lesionado e agentes terapêuticos podem ser incluídos em sua estrutura para serem liberados diretamente no local da lesão. Até o momento, não há estudos em que microfibras contendo substâncias bioativas produzidos através da técnica de eletrofiação coaxial tenham sido aplicados em modelo animal de lesão de medula espinal.

4. Objetivos

- Incorporar as substâncias fator de crescimento de fibroblastos 2 (FGF-2) e ácido valpróico (VPA) em *scaffolds* de microfibras através da técnica de eletrofiação coaxial;

- Analisar a morfologia e as propriedades físico-químicas dos *scaffolds* produzidos.

- Avaliar a cinética de liberação do FGF-2 e do VPA dos *scaffolds*;

- Testar a biocompatibilidade e a bioatividade dos *scaffolds* contento FGF-2 e o VPA *in vitro* com células PC12;

- Implantar os *scaffolds* contendo FGF-2 e VPA em modelo animal de LME por hemisecção e avaliar a atividade locomotora, a morfologia do tecido da medula espinal e, também, a expressão de marcadores neurais.

5. Resultados

Capítulo I.

Application of PLGA/FGF-2 coaxial microfibers in spinal cord tissue engineering: an *in vitro* and *in vivo* investigation

Karina P. Reis[1,2,3], Laura E. Sperling[1,2], Cristian Teixeira[1,2], Ágata Paim[1,2], Bruno Alcântara[1,2], Gema Vizcay-Barrena [5], Roland A. Fleck [5], Patricia Pranke[1,2,3,4]

[1] Hematology and Stem Cell Laboratory, Faculty of Pharmacy, [2] Stem Cell Laboratory, Fundamental Health Science Institute, [3] Post Graduate Program in Physiology, Universidade Federal do Rio Grande do Sul, [4] Stem Cell Research Institute, Porto Alegre, RS, Brazil, [5] Centre for Ultrastructural Imaging, King's College London, UK

Artigo publicado no periódico *Regenerative Medicine* (fator de impacto 2,992)

A carta de aceite encontra-se no anexo I desse trabalho

Research Article

For reprint orders, please contact: reprints@futuremedicine.com

Regenerative Medicine

Application of PLGA/FGF-2 coaxial microfibers in spinal cord tissue engineering: an *in vitro* and *in vivo* investigation

Karina P Reis*[1,2,3], Laura E Sperling[1,2], Cristian Teixeira[1,2], Ágata Paim[1,2], Bruno Alcântara[1,2], Gema Vizcay-Barrena[4], Roland A Fleck[4] & Patricia Pranke[1,2,3,5]

[1]Hematology & Stem Cell Laboratory, Faculty of Pharmacy, Universidade Federale do Rio Grande do Sul, Porto Alegre, RS, 90610-000, Brazil

[2]Stem Cell Laboratory, Fundamental Health Science Institute, Universidade Federal do Rio Grande do Sul, Porto Alegre, RS, 90050-170, Brazil

[3]Post Graduate Program in Physiology, Universidade Federal do Rio Grande do Sul, Porto Alegre, RS, 90050-170, Brazil

[4]Centre for Ultrastructural Imaging, King's College London, London, WC2R 2LS, UK

[5]Stem Cell Research Institute, Porto Alegre, RS, 90020-10, Brazil

*Author for correspondence: kapire@yahoo.com.br

Aim: Scaffolds are a promising approach for spinal cord injury (SCI) treatment. FGF-2 is involved in tissue repair but is easily degradable and presents collateral effects in systemic administration. In order to address the stability issue and avoid the systemic effects, FGF-2 was encapsulated into core–shell microfibers by coaxial electrospinning and its *in vitro* and *in vivo* potential were studied. **Materials & methods:** The fibers were characterized by physicochemical and biological parameters. The scaffolds were implanted in a hemisection SCI rat model. Locomotor test was performed weekly for 6 weeks. After this time, histological analyses were performed and expression of nestin and GFAP was quantified by flow cytometry. **Results:** Electrospinning resulted in uniform microfibers with a core–shell structure, with a sustained liberation of FGF-2 from the fibers. The fibers supported PC12 cells adhesion and proliferation. Implanted scaffolds into SCI promoted locomotor recovery at 28 days after injury and reduced GFAP expression. **Conclusion:** These results indicate the potential of these microfibers in SCI tissue engineering.

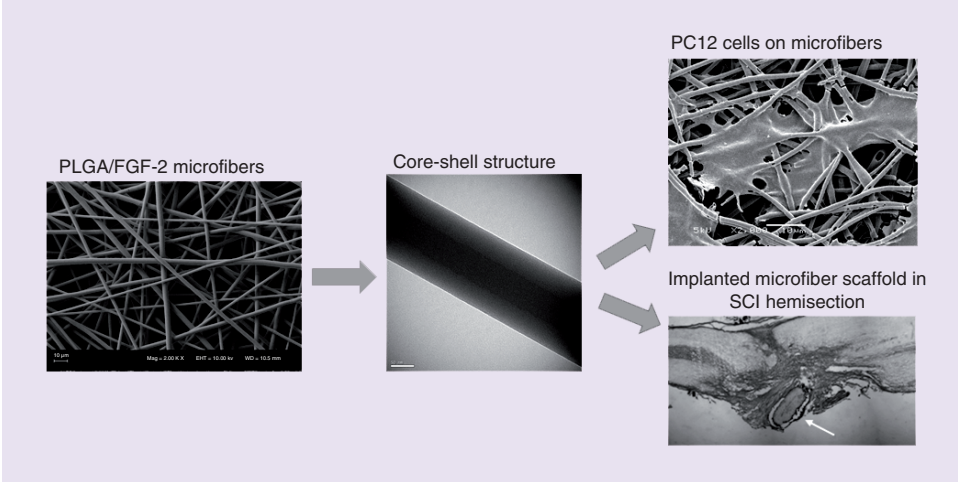

First draft submitted: 12 May 2018; Accepted for publication: 4 September 2018; Published online: 5 October 2018

Keywords: coaxial electrospinning • FGF-2 • hemisection • PC12 cells • spinal cord injury

Spinal cord injury (SCI) is a devastating neurological condition that results in severe sensory and motor deficits [1]. It is a major public health issue that affects approximately 2.5 million patients worldwide [2]. To date, there is no

Future Medicine

effective treatment available for SCI patients [3,4]. Therefore, it is necessary to study novel effective treatments for this condition. The difficulty in finding an effective treatment lies in the limited CNS regeneration. After injury, there is a cascade of pathophysiological events, including loss of blood supply, inflammation and demyelination, glial scar formation and cystic cavitation, among others [5] that contribute to a nonpermissive microenvironment at the injury site, impairing neural regeneration and restoration [6,7]. The application of functionalized biomaterials to modify this growth-inhibitory environment in the injured spinal cord is potentially helpful in promoting axonal regeneration and functional restoration. Biomaterials can provide a structural support that can bridge the lesion gap and act as contact guidance for axonal growth and glia migrating into the injury site [4,8,9]. Moreover, these biomaterials can also act as a vehicle to deliver bioactive substances in order to modify the microenvironment [10].

One technique that has the capacity to generate such an ideal biomaterial for use in the treatment of SCI is coaxial electrospinning. Fibers produced by electrospinning have shown great potential as a scaffold platform for the repair and regeneration of various types of tissue [11]. Coaxial electrospinning is an advanced variation of conventional electrospinning [12]. Through this technique, it is possible to obtain fibers with a core–shell structure that allows for safe encapsulation of drugs or biologically active compounds [12].

The FGF-2 is a representative growth factor (GF) that controls general processes, such as cell proliferation, migration, differentiation and angiogenesis [13]. Previous studies that evaluated the effect of FGF2 in a rat SCI model indicated that the effect of this GF is related to inhibited inflammation, decreasing gliosis and increasing radial glia and neural progenitor cells [14] and that improves functional recovery [14–19]. However, the systemic administration of this GF results in vasodilatation and hypotension [20] in addition to its mitogenic effect that may result in malignant tumors [21,22]. Additionally, the blood–spinal cord barrier has a very limited permeability to FGF-2 [23]. Besides, free GFs are readily degradable *in vivo*, which leads to the rapid loss of biological activity [13,24]. To avoid these unwanted effects and to protect FGF-2 from *in vivo* degradation, this GF was encapsulated in core–shell fibers and implanted in the injury local.

Previous studies demonstrated the beneficial effect of the use of FGF-2 containing biomaterials in the treatment of SCI in form of hydrogel [25], membranes [26], nanoparticle–hydrogel [27], microspheres [23]. However, up until now, no studies using microfibers encapsulating FGF-2 for SCI treatment were published. An important advantage of electrospun fibers over the above-mentioned biomaterial processing methods is that they mimic the architecture of the extracellular matrix, biomimicking signals and resulting in the attraction of more physiologically relevant cellular phenotypes allowing the adhesion, proliferation and differentiation of various cells [28,29]. In view of the aforementioned, the aim of this study has been to generate scaffolds of poly(lactic-*co*-glycolic acid) (PLGA) microfibers that release FGF-2 via coaxial electrospinning and tested *in vitr*o and *in vivo* experiments. The morphological and mechanical properties of the coaxial electrospun fibers were analyzed and the FGF-2 release profile was examined. The proliferation and spreading of PC12 cells on scaffolds was investigated to determine the biocompatibility and bioactivity of the microfibers. The scaffold was implanted into a hemisected thoracic spinal cord andhe motor functional recovery and immunohistochemical analyses were performed.

Materials & methods

Biomaterial production

Production of core–shell PLGA microfibers

The microfibers were prepared by coaxial electrospinning. The core of the fibers consisted of 100 μg/ml FGF-2 (FGF-2; Peprotech, London, England), 10% polyethylene glycol (PEG; Mn ≈ 20,000; Sigma-Aldrich, MO, USA) and 2% bovine serum albumin (BSA; Sigma-Aldrich) diluted in water; the shell solution consisted of 18% (PLGA; Mw ≈ 50–75 kg/mol; 75:25 lactide/glicolide; PURAC Biochem BV) in 1,1,1,3,3,3-hexafluoro-2-propanol (Sigma-Aldrich) and chloroform (Dinâmica; 3:1). The core solution was injected at a controlled flow rate of 0.2 ml/h and the shell solution at 2 ml/h. The applied voltage was in the range of 16–25 kV and the spinneret tip/collector distance was 15 cm. The fibers were collected on cover slips of 15-mm diameter placed on an aluminum-collecting plate. The coaxial electrospinning procedure was performed at 22°C and 45% controlled air humidity within the electrospinning apparatus (IME Technologies, Waalre, iThe Netherlands). The control samples were produced by the same procedure cited above, but without the GF.

For the cell culture studies, an additional control was used; a film of PLGA 6% in acetonitrile (Êxodo Científica, Brazil) on cover slips of 15-mm diameter was prepared.

Morphological characterization of electrospun scaffolds & contact angle measurement

Scanning electron microscopy

The collected fibers were dried overnight and gold-coated using a sputter coater (Bal-Tec SCD 050) prior to observation by a scanning electron microscope (SEM; Carl Zeiss EVO50) operating at an accelerating voltage of 10 kV. The average diameter of the fibers was determined using the software ImageJ 1.383 by measuring 30 fibers from each of the images obtained by SEM (n = 30).

Transmission electron microscopy

Verification of the core–shell structure was performed by transmission electron microscopy (TEM). The samples for TEM were prepared by direct deposition of the electrospun fibers (n = 2) onto copper grids for 15 s. The brightfield TEM images of coaxial microfibers were obtained using a FEI Tecnai G^2 transmission electron microscope, operated at 200 kV, fitted with a Gatan Ultrascan camera US1000 (2k × 2k).

Laser confocal scanning microscopy

To visualize the core of the microfibers, fluorescein for fluorescence free acid (Sigma-Aldrich) was added to the core solution and the resulting fibers were analyzed with a laser confocal scanning microscope (LCSM; Olympus Fluoview FV1000 and the corresponding software).

Static water surface contact angle measurement

The contact angle was measured using a Drop Shape Analyzer (Krüss). Approximately 5 µl of deionized water was carefully placed on to the surface of the electrospun scaffolds and contact angle values were calculated. Both scaffolds with core–shell structure and scaffolds fabricated using the traditional electrospinning method were analyzed (n = 3).

Mechanical properties tests

Young's modulus, maximum load (tensile stress) and maximum elongation (ultimate strain %) were determined by dynamic mechanical analysis (DMA) in a Q800AT DMA instrument equipped with a tension film clamp in the DMA-controlled force mode as described in the literature [30]. Briefly, scaffolds were cut into rectangular shapes (25 × 7 mm). The assays were carried out at a constant temperature (37°C) with a ramp force of 0.5 N/min until 18 N maximum load, under 0.005 N static load. Data from the stress–strain curves were recorded and the tensile stress at maximal load was obtained from this data for each sample. The diagrams and analyses were made using the *TA Universal* Analysis software. Young's modulus of the samples was determined as the slope of the straight-line stress–strain relationship (n = 3).

FGF-2 release kinetics

The electrospun scaffolds were placed in 7 ml of phosphate-buffered saline (PBS) with 1% penicillin/streptomycin (Sigma) and 0.1% amphotericin (Sigma). The test was performed in an incubator at 37°C in the presence of 5% CO_2. At appropriate intervals of 1, 8, 24 h, and 5, 10, 15, 20, 25 and 30 days, 1 ml of the supernatant was removed and replenished with an identical volume of fresh buffer. The FGF-2 concentrations were determined by an FGF-Basic Human ELISA Kit (Thermo Fisher Scientific) using the manufacturer's protocol. Each sample was assayed in triplicate. The results are presented as mean ± standard deviation (n = 3).

In vitro studies: cell culture

PC12 cell culture

The scaffolds were cut to fit into the wells of a 24-well plate and fixed with silicon o-rings. The material was sterilized by UV light for 1 h before cell seeding. PC12 cells at 10,000 cells per well were seeded on the scaffolds at 37°C with 5% CO_2. The culture medium was DMEM high glucose (Sigma) supplemented with 15% fetal bovine serum (Gibco) and 5% horse serum (Laborclin), 1% penicillin/streptomycin (Sigma) and 0.1% amphotericin (Sigma).

After 3 and 7 days, the cells were washed with PBS and treated with 3-(4,5-dimethylthiazol-2-yl)-2,5-diphenyltetrazolium bromide (MTT) for 2 h. This test is based on the principle that the mitochondrial dehydrogenases of viable cells cleave the yellow MTT tetrazolium salt to give purple formazan crystals. The formazan complex formed was dissolved in dimethyl sulfoxide and the absorption was measured at 570 nm with a reference wavelength of 630 nm in a microplate reader. The percentage of viability was calculated using the optical density of the control and treated cells.

10.2217/rme-2018-0060

Three experimental groups were used: control – cells cultivated on a PLGA film, PLGA scaffold – cells cultivated on electrospun PLGA core–shell fibers and PLGA/FGF-2 scaffold – cells cultivated on electrospun PLGA core–shell fibers with FGF-2 on the core.

SEM analysis of cell growth on scaffolds

The cells were fixed for 20 min with 4% paraformaldehyde and dehydrated in graded series of alcohol (25, 40, 60, 75, 85, 100%), each for 1 h. After drying, the scaffolds were coated with gold (Bal-Tec SCD 050) and analyzed. An SEM (Carl Zeiss EVO50) was used to observe the morphology of the cells on the microfibers at an accelerating voltage of 7 kV.

Immunocytochemistry & confocal microscopy

PC12 cells were fixed for 20 min with 4% paraformaldehyde and permeabilized with 0.1% Triton X-100. Then, cells were then stained with 20 μg/ml rhodamine-phalloidin and 0.5 μg/ml 4′,6-diamidino-2-phenylindole (Life Technologies, CA, USA) and washed three-times with PBS. Following this, images were taken by Z-stack scanning and 3D reconstruction of Olympus Fluoview FV1000 confocal microscope.

FGF-2 bioactivity

PC12 cells, which differentiate from a neuronal phenotype in the presence of bioactive FGF-2 [31,32], were used to test for the bioactivity of the FGF-2 released from the PLGA/FGF-2 microfibers. PC12 cells were cultivated in 24-well plates at a density of 10,000 cells per well. A volume of 1 ml of the FGF-2 supernatant from the PLGA/FGF-2 fibers was added to each well of PC12 cells. For obtaining the conditioned medium, the scaffolds (PLGA only and FGF-2/PLGA) were placed in 7 ml of culture medium in an incubator at 37°C in the presence of 5% CO_2.

Three experimental groups were used: cell medium – cells cultivated with conventional cell culture medium; PLGA scaffold conditioned medium; and PLGA/FGF-2 scaffold-conditioned medium.

Expression of βIII-tubulin was determined by flow cytometry. The cells were fixed for 20 min with 4% paraformaldehyde, washed twice with PBS, blocked with 3% BSA in PBST (PBS plus Triton 0.1%) and stained with an antibody anti-βIII-tubulin (1:200; Millipore, MA, USA) for 1 h at room temperature. They were then washed once with PBS, followed by incubation with a goat antimouse Alexa-Fluor-488 secondary antibody (Thermo, 10 μg/ml) for a further hour at 37°C. 20,000 events were analyzed using a FACSAria III cytometer (Becton Dickinson Biosciences, CA, USA) and the FACSDiva 6.0 software. Cell viability was measured using MTT assay.

In vivo studies: hemisection SCI model

Experimental design

40 male Wistar rats aged 2 months (200–250 g body weight) were obtained from the Animal House of the Instituto de Ciências Básicas da Saúde da Universidade Federal do Rio Grande do Sul. They were maintained in a temperature-controlled room (21 ± 2°C) on a 12/12 h light/dark cycle, with food and water available *ad libitum*. All procedures were in accordance with the Guide for the Care and Use of Laboratory Animals adopted by the NIH (USA) and with the Federation of Brazilian Societies for Experimental Biology. The study was approved by the Research Ethics Committee of the University (#28079). The animals were randomly divided into four experimental groups: SCI (laminectomy followed by SCI); FGF-2 injection (SCI treated with one injection of FGF-2 in the local of the lesion); PLGA scaffold (SCI with implanted PLGA scaffold); and FGF-2/PLGA scaffold (SCI with implanted FGF-2/PLGA scaffold).

Spinal cord injury

Spinal cord injury by right-side hemisection was performed as described previously [33], with some modifications. Under general anesthesia with a mixture of xylasine (5–10 mg/kg) and ketamine (75–100 mg/kg), a longitudinal incision was made and a laminectomy was performed at two vertebral segments, T9–T10. The spinal cord was then hemisected at T10 on the right side by placing a 28-gauge needle dorsiventrally at the midline of the cord and pulling it laterally to ensure the completeness of the hemisection. The scaffolds, with a diameter of 2 mm and a thickness of approximately 300 μm, were carefully placed over the hemisected gap immediately after the SCI. The FGF-2 injection group received an injection of 5 μl of FGF-2 (1 μg/ml) dissolved in PBS in the hemisected lesion

immediately after the SCI. Subsequently, the fascia, musculature and skin were sutured. Antibiotic (Enrofloxacino, Bayer, Brazil; 10 mg/kg) was administered IP for 5 days after the procedure to prevent infection and analgesic (Tramal, Pfizer; 10 mg/kg) to prevent pain, followed by two drops of baby tylenol twice a day for 5 days.

Locomotor activity assessment

Behavior was recorded in an open field and following this, the motor function of the hind limbs was evaluated using the Basso, Beattie and Bresnahan scale (BBB), which assesses hind limb motor function with scores ranging from 0 (complete paralysis) to 21 (normal locomotion) [34]. Evaluation began 2 days after injury and was repeated weekly until the sixth week after SCI.

Histological procedures

Animals were euthanized with a lethal dose of chloral hydrate followed by transcardiac perfusion with 0.9% saline followed by 4% paraformaldehyde (Reagen, Brazil) in 0.1 M PBS (pH 7.4). The spinal cord was removed from C5 to L5 in the thoracic region, postfixed in the same fixative solution and cryoprotected with 15 and 30% sucrose diluted in PBS. After cryoprotection, the samples were maintained at -80°C until cryosectioning. For histological analysis, the thoracic region of the spinal cord was transversally cut into 30-µm sections in cryostat (Leica, Wetzlar, Germany). The sections were stained with hematoxylin and eosin and the images were captured using a Nikon Eclipse E-600 microscope (Japan) coupled with a digital camera [35].

For immunofluorescence analysis, the slices were dried, permeabilized with 0.1% Triton X-100 in PBS and treated with 3% BSA in PBST. The following primary antibodies were used: mouse anti-β-tubulin class III clone 2G10 (1:200, Milipore, 05-559) and rabbit antiglial fibrillary acidic protein (GFAP; 1:200, DAKO, Z0334). To reveal primary antibodies, the following secondary antibodies were used: goat antirabbit Alexa 488 (1:500, Thermo Scientific) or goat antimouse Alexa 488 (1:500, Thermo Scientific). The sections were counterstained with 4′,6-diamidino-2-phenylindole.

Flow cytometry analysis

6 weeks after the implantation, the animal spinal cords were isolated. A fragment of 1 cm, including the epicenter of the lesion and equal rostral end caudal portions, was washed with PBS; the membranes were removed and the tissue was mechanically and enzymatically dissociated with trypsin (Sigma-Aldrich). The single cell suspension was fixed for 20 min with 4% paraformaldehyde and subsequently blocked for 30 min with 3% BSA in PBST. After blocking, the cells were incubated with primary antibodies against astrocyte GFAP (DAKO; 14.5 µg/ml) and against neural stem cells nestin (Santa Cruz, 1 µg/ml) overnight at 4°C. The cells were washed twice with PBS1 X and incubated for 1 h at 37°C with the secondary antibody Alexa-fluor 488 antimouse (Thermo Scientific, 10 µg/ml). Negative controls (samples incubated only with the secondary antibody) were included for setting up the machine voltages and to determine the negative region of dot plot. The events were analyzed using an FACSAria III cytometer (Becton Dickinson, Biosciences) and the FACSDiva 6.0 software. Data from 50,000 events (intact cells) were acquired and the number of cells was determined after exclusion of debris events from the dataset. The number of cells in each quadrant was computed, and the cells which were stained separately were expressed as the percentage of positive immune-labeled cells.

Statistical analysis

The experiments were repeated three-times and the results were expressed as mean ± standard deviation of the three replicates. Statistical analysis was performed using one-way ANOVA, followed by the Bonferroni post-hoc test. A p-value of less than 0.05 was considered statistically significant.

Results

Characterization of electrospun microfibers

PLGA microfibers were successfully produced by both traditional and coaxial electrospinning. SEM images of the fibers demonstrated a uniform morphology without any beads in both groups with an average diameter of 2.06 µm ± 0.68 of the PLGA fibers produced by traditional electrospinning and 2.18 µm ± 0.74 of the PLGA core–shell fibers produced by coaxial electrospinning (Figure 1).

As the SEM images cannot provide evidence that the fibers have a core–shell structure, several methods were employed to demonstrate this structure. Figure 2A shows the TEM images of the core–shell structure of the

10.2217/rme-2018-0060

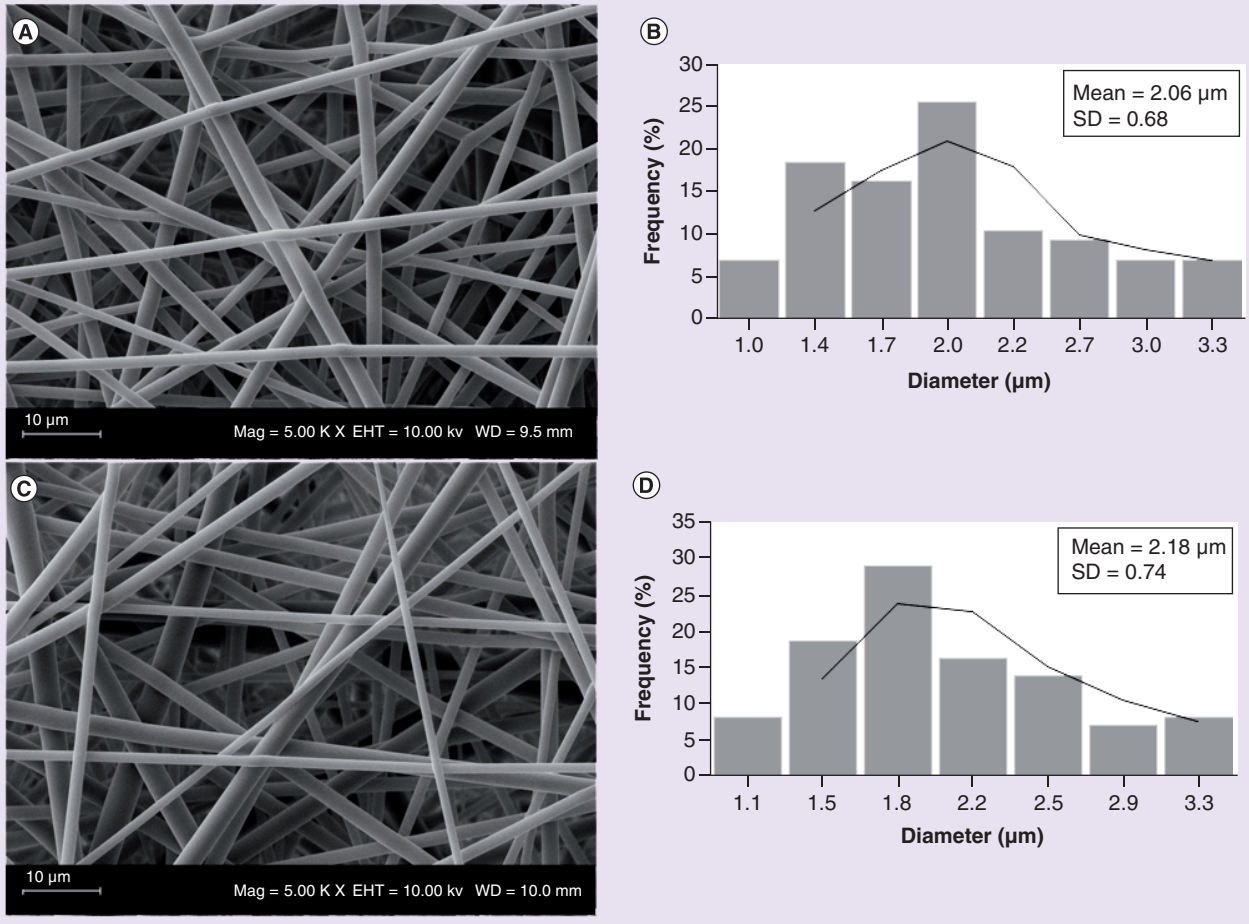

Figure 1. Scanning electron microscopy images showing the morphology of microfibers. (A) Traditional electrospinning uniaxial fibers of an average diameter of 2.06 µm and **(C)** coaxial microfibers of an average diameter of 2.18 µm. **(B)** and **(D)** show the corresponding histograms of the fiber diameter distribution.
SD: Standard deviation.

microfibers, indicated by the differences in electron density between the inner core and outer shell of the fibers. Fibers that contained fluorescein in the core were analyzed with a confocal microscope. LSCM analysis showed the presence of green fluorescence (Figure 2B), suggesting the incorporation of the fluorescein in the core. The control group (fibers where the core solution did not include fluorescein) did not show green fluorescence, as can be seen in Figure 2C.

The water contact angle was measured in order to analyze the hydrophilicity of the scaffolds. For PLGA-only microfibers, the contact angle was 127.6° ± 6.2, which is similar to the value of 127° ± 1.8 obtained for the PLGA core–shell microfibers. The PLGA film presented less hydrophobicity among the tested groups, 117.9° ± 6.

Mechanical properties tests

The mechanical properties of the traditional and coaxial microfibers were measured and evaluated according to the following categories: Young's modulus (MPa), tensile stress at yield (MPa) and tensile strain at maximum (%). The values of the measured mechanical properties for the core–shell microfiber scaffolds were higher than for the traditional electrospinning microfiber scaffolds (Table 1).

In vitro GF release

The FGF-2 release from scaffolds in pH 7.4 PBS at 37°C was measured by the ELISA assay, as shown in Figure 3.

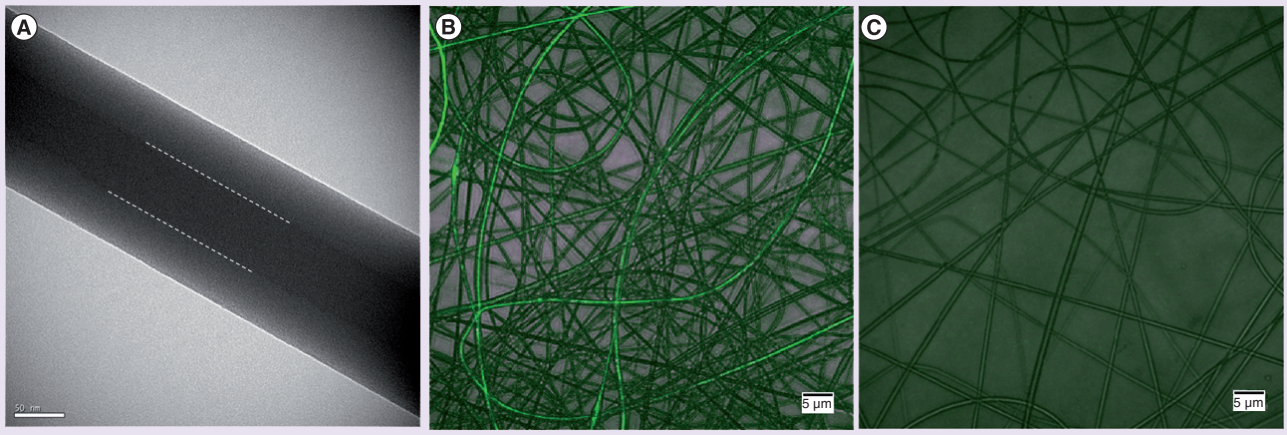

Figure 2. Core–shell structure of coaxial electrospun microfibers. (A) Transmission electron microscopy image of a segment of coaxial microfiber showing the core–shell structure, scale bar: 50 nm. **(B)** Confocal microscopy image of coaxial electrospun microfibers using fluorescein in the core and **(C)** a negative control without the fluorescein, scale bar: 5 µm.

Table 1. Values for Young's Modulus (MPa), the maximal elongation (%) under the applied force and the maximal load (MPa).

Sample	Young's modulus (MPa)	Max elongation (%)	Max load (MPa)
Traditional scaffold	0.859 ± 0.81	173.25 ± 8.07	0.432 ± 0.18
Coaxial scaffold	1.437 ± 1.11	177.83 ± 13.97	0.538 ± 0.06

All results are shown as mean ± standard deviation of the mean. n = 3.

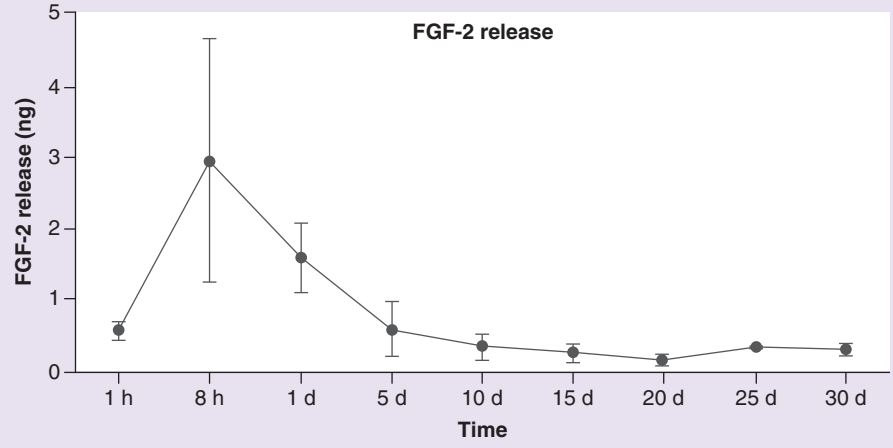

Figure 3. Release profile of FGF-2 from core–shell fibers determined by the ELISA assay. Results are average plus standard deviation. n = 3.

An initial burst release was observed within 8 h followed by a decelerating release and a subsequent relatively steady release phase for at least 30 days.

10.2217/rme-2018-0060

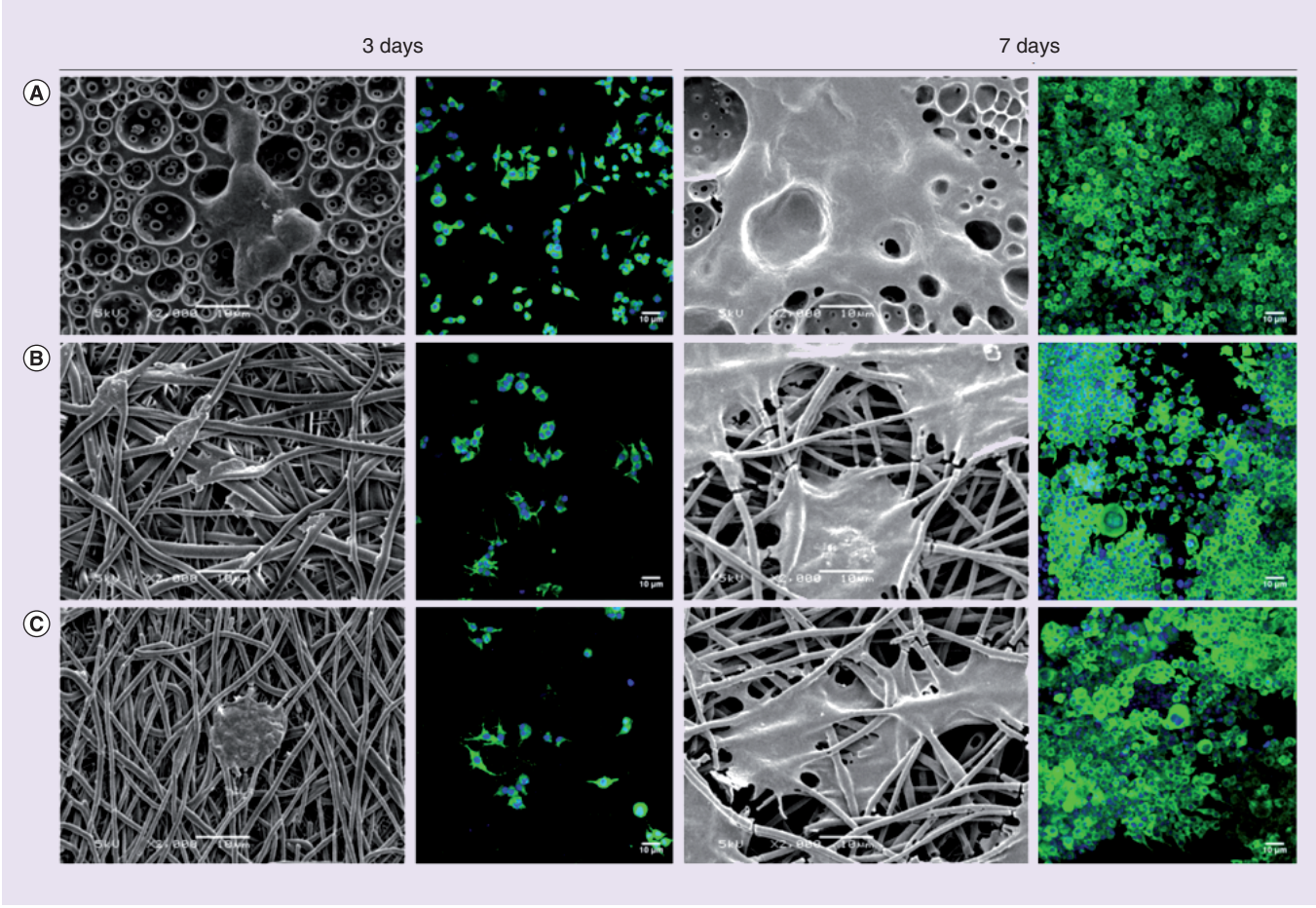

Figure 4. PC12 cells attachment and growth on the biomaterials. Scanning electron microscopy and fluorescence microscopy images of PC12 cells cultivated on the PLGA film **(A)**; PLGA scaffold **(B)**; and PLGA/FGF-2 scaffold **(C)** after 3 and 7 days in culture. Green βIII-tubulin antibody staining, Blue – cell nuclei, DAPI staining. The cells attached and spread on the biomaterials. Scale bar: 10 μm, n = 2.
DAPI: 4′,6-Diamidino-2-phenylindole; PLGA: Poly(lactic-*co*-glycolic acid).

In vitro results

Cell–scaffold interaction

In order to study the biocompatibility of the FGF-2/PLGA core–shell scaffolds for neuronal tissue engineering applications, PC12 cells were cultivated on the scaffolds. After 3 and 7 days of cultivation, the cells/scaffolds were analyzed by SEM and stained with an antibody against βIII-tubulin and visualized by LCSM (Figure 4). Figure 4 shows that the scaffolds were able to support cell attachment and growth.

The MTT assay was used to assess the effects of microfibers/FGF-2 on cell viability on the third and seventh day of cultivation. Cell viability on core–shell scaffolds increased with the culture time period. However, at day 7, a significant decrease of the cell viability for the microfiber scaffolds compared with the PLGA film was observed (Figure 5).

FGF-2 bioactivity

When treated with FGF-2, PC12 cells differentiate into a neuronal phenotype [32]. In order to investigate the bioactivity of the FGF-2 released from the core–shell fibers, the PC12 cells were incubated with scaffold-conditioned media and the expression of βIII-tubulin, a neuronal marker, was analyzed by flow cytometry. Figure 6 shows that after 7 days in culture, there is a tendency for an increase in β-III tubulin expression on cells treated with conditioned medium containing FGF-2 compared with the another groups. However, these differences between the groups were not significant.

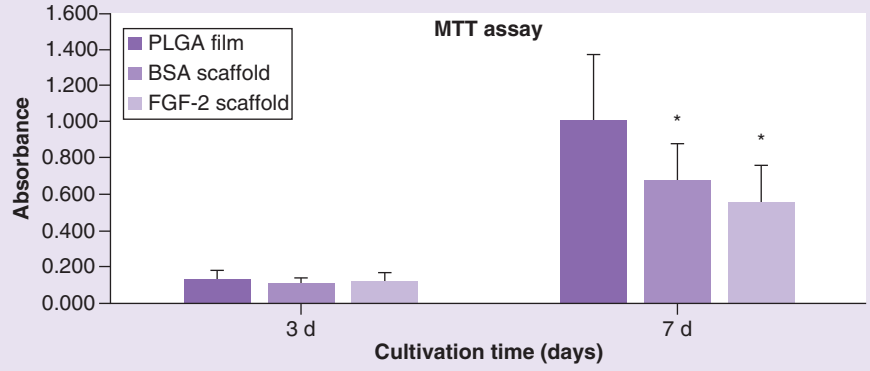

Figure 5. Analysis of cell viability on scaffolds by the 3-(4,5-dimethylthiazol-2-yl)-2,5-diphenyltetrazolium bromide assay. The optical density value was measured at 3 and 7 days in culture.
*$p < 0.05$.
BSA: Bovine serum albumin; MTT: 3-(4,5-dimethylthiazol-2-yl)-2,5-diphenyltetrazolium bromide; PLGA: Poly(lactic-*co*-glycolic acid).

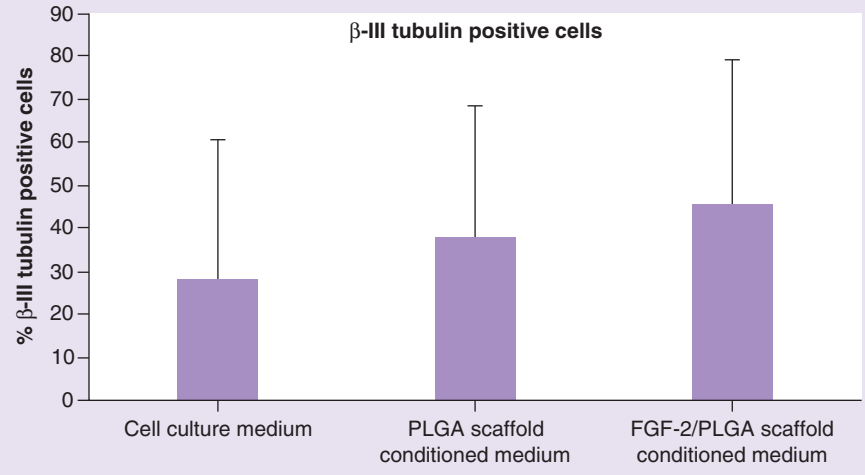

Figure 6. Analysis of expression of βIII-tubulin of PC12 cells by flow cytometry. n = 3.
PLGA: Poly(lactic-*co*-glycolic acid).

The PC12 cells were incubated either with culture medium or with conditioned culture medium (PLGA scaffold or FGF-2/PLGA scaffold) for 7 days. The cell proliferation and viability was analyzed by the MTT assay. Following treatment with a PLGA/FGF-2 scaffold-conditioned medium for 7 days, the PC12 cell cultures presented a reduction in cell viability compared with the cells that were cultivated with cell culture medium (Figure 7).

In vivo results

Functional evaluation

The BBB locomotor rating scale [34] was used to assess the motor recovery at 2 days and 1–6 weeks post-hemisection SCI. The function of hindlimb ipsilateral to the injury was impaired severely after the surgery. Typically, the animals show spontaneous recovery. The treated groups showed the tendency to have higher scores than the control. However, the only significant difference was observed 28 days after SCI in PLGA scaffold and PLGA/FGF-2 scaffold groups when compared with SCI control (Figure 8).

10.2217/rme-2018-0060

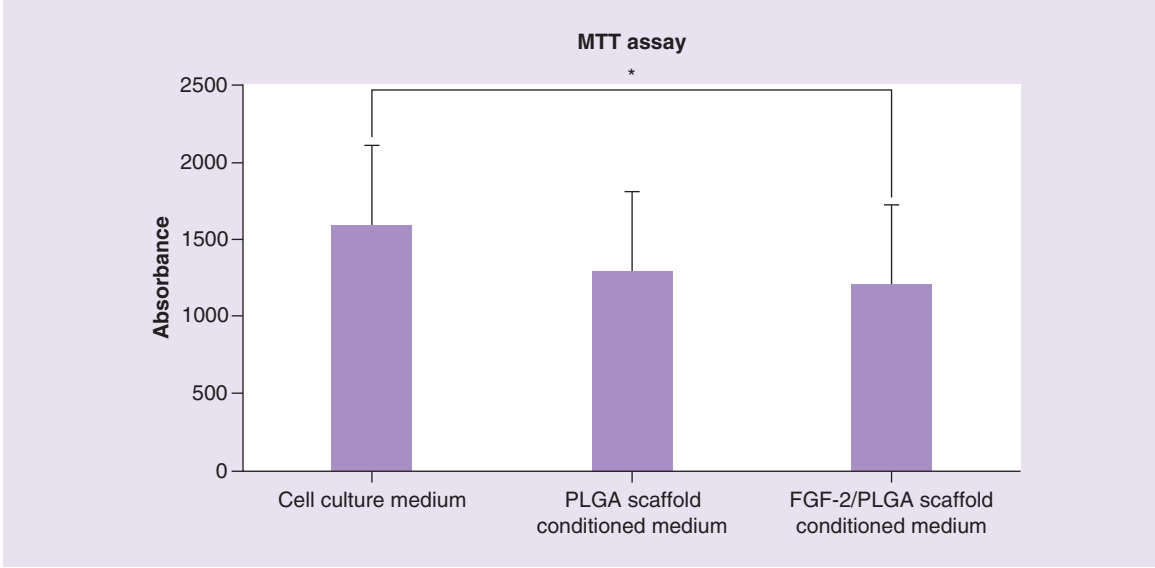

Figure 7. Analysis of cell viability on scaffolds with the 3-(4,5-dimethylthiazol-2-yl)-2,5-diphenyltetrazolium bromide assay. The optical density value was measured at 7 days in culture.
*$p < 0.05$. $n = 3$.
MTT: 3-(4,5-dimethylthiazol-2-yl)-2,5-diphenyltetrazolium bromide; PLGA: Poly(lactic-co-glycolic acid).

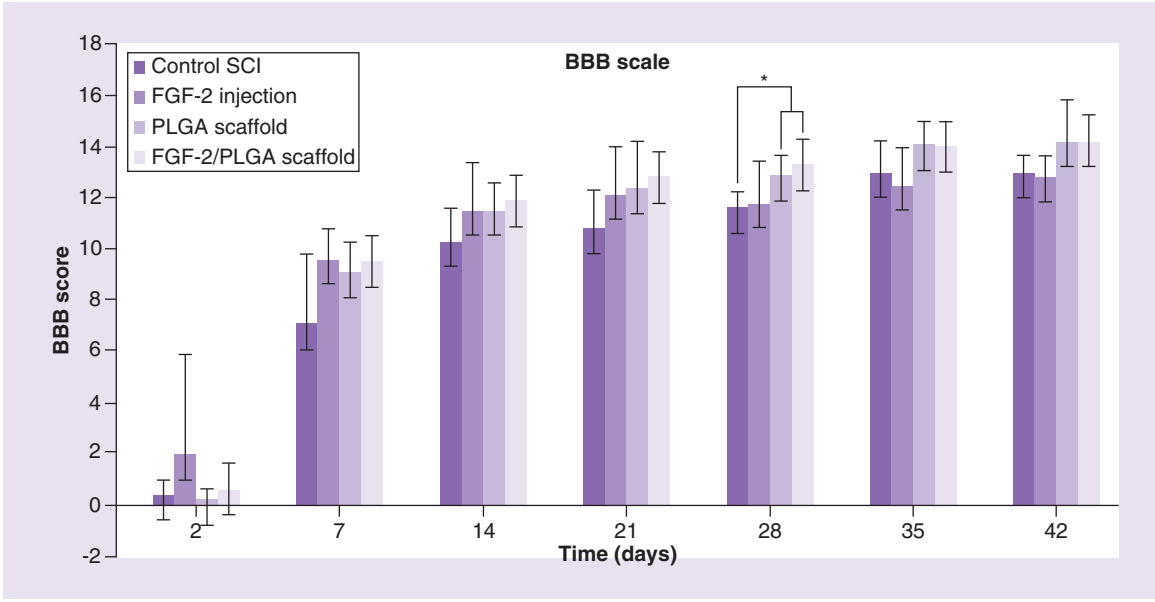

Figure 8. Basso, Beattie and Bresnahan open-field walking scores for the four groups on the ipsilateral, lesioned side. 28 days after implantation, the mean BBB score in the PLGA scaffold and the FGF-2/PLGA scaffold groups was significantly higher than that in the control SCI and FGF-2 injection groups.
* Indicates a p-value < 0.05. $n = 6$ animals in each group.
BBB: Basso, Beattie and Bresnahan; PLGA: Poly(lactic-*co*-glycolic acid); SCI: Spinal cord injury.

Morphologic analysis

The histological analysis at 6 weeks after injury showed incomplete degradation of the scaffold (Figure 9D) and the presence of tissue in the hemisection cavity.

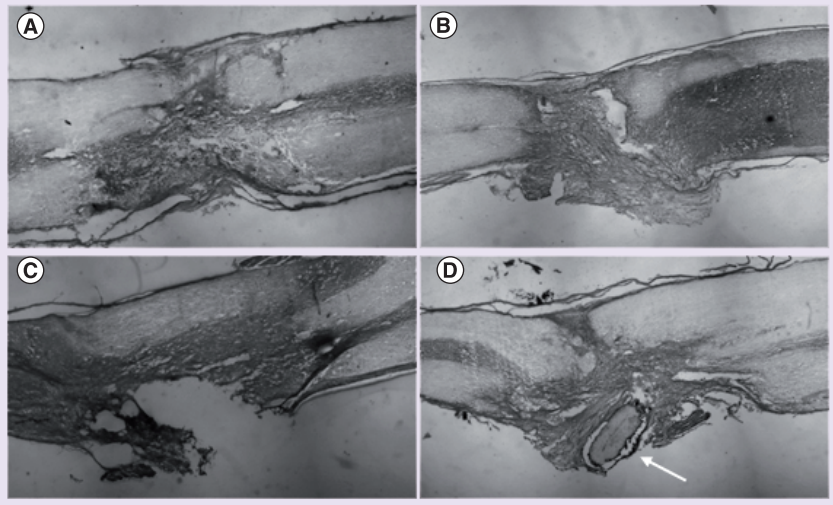

Figure 9. Representative images of hematoxylin and eosin staining for longitudinal sections of injured spinal cords at 6 weeks after spinal cord injury. (A) Control SCI, **(B)** FGF-2 injection, **(C)** PLGA scaffold and **(D)** PLGA/FGF-2 scaffold. White arrow indicates the presence of the scaffold at the local of injury.
PLGA: Poly(lactic-*co*-glycolic acid); SCI: Spinal cord injury.

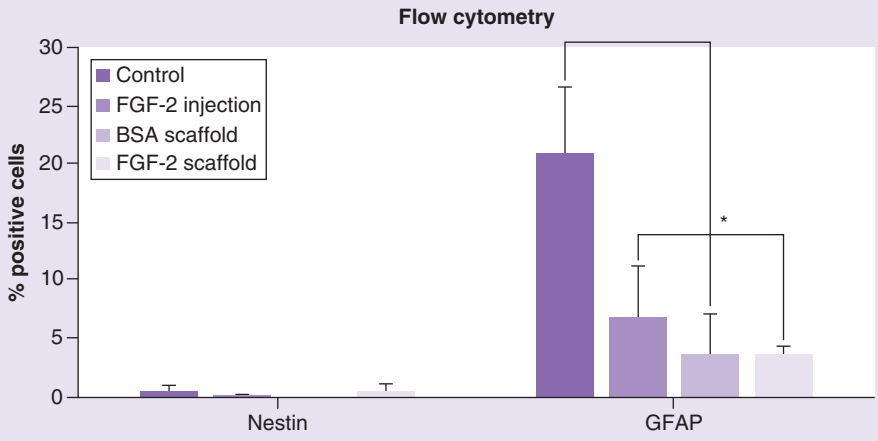

Figure 10. Analysis of expression of nestin and GFAP by flow cytometry.
* Indicates a p-value < 0.05. n = 3 animals in each group.
BSA: Bovine serum albumin; PLGA: Poly(lactic-*co*-glycolic acid).

Flow cytometry analysis

Figure 10 shows that 42 days after SCI, there is a decrease in GFAP expression on PLGA scaffold group, FGF-2/PLGA scaffold and FGF-2 injection compared with control SCI. This suggests that scaffold groups were able to prevent astrocyte hyperplasia in the parenchyma of spinal cord after contusion. Analysis of the nestin expression showed no significant difference of number of nestin-expressing cells between the groups.

Evaluation of host cells tissue infiltration into the scaffold

At 42 days after SCI, the scaffold was still present in the lesion site as a globular structure. The scaffold was infiltrated by a few astrocytes, as shown by the immunostaining with a GFAP antibody. Moreover, several neural fibers immunopositive for βIII-tubulin were shown to cross the scaffold (Figure 11).

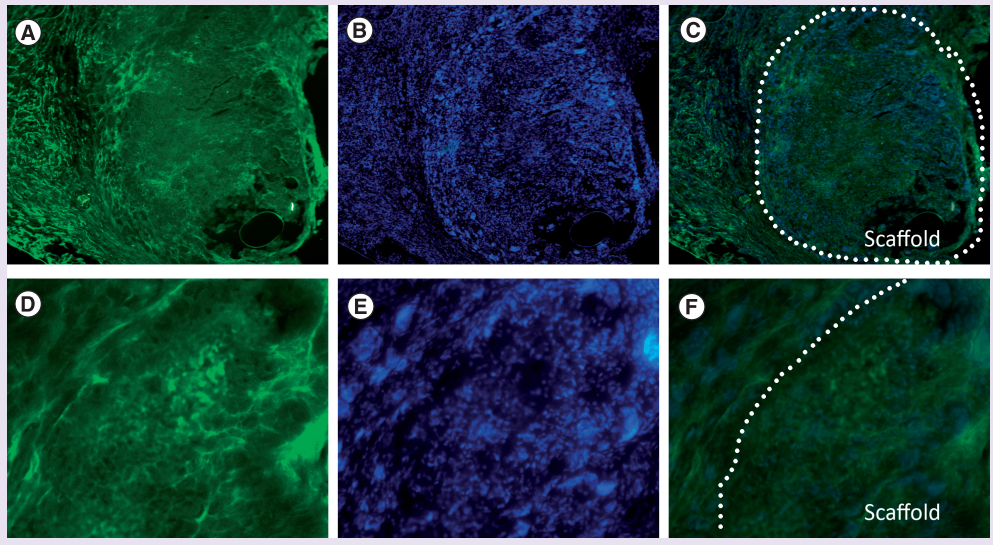

Figure 11. Immunohistochemistry analysis for βIII-tubulin and GFAP. Evaluation of the presence of tissue ingrowth within FGF2/poly(lactic-co-glycolic acid) scaffolds at 42 days after injury. The scaffolds were slightly autofluorescent and had a round, globular appearance (dotted line) that could be differentiated from the surrounding tissue. Immunofluorescence staining on 15 μm longitudinal sections revealed the presence of some regrowing axons through the implant βIII-tubulin – positive (**A & C**, green), while GFAP positive astrocytes were infiltrating the implant (**D & F**, green). The nuclei were labeled with 4′,6-diamidino-2-phenylindole (**B & E**, blue).
A,B,C: 100× magnification; **D,E,F:** 200× magnification.

Discussion

In this study, FGF2/PLGA core–shell fibers were produced and implanted in a rat model of SCI. The FGF2/PLGA scaffold effects on tissue regeneration and motor recovery were investigated. Biodegradable polymers have been widely used to construct scaffolds for neural regeneration in SCI models or as drug-delivery systems at the lesion site [36–38]. PLGA was used as the shell polymer because it is a well-known biocompatible and biodegradable copolymer [39–41], which protects drugs from degradation, has sustained release possibility and by degrading, produces no toxic molecules [42–45]. FGF2, a GF with notable effects on neuronal cells such as neurotrophic activity, improvement of neuronal survival and stimulation of neurogenesis [16,46,47]. A combination of a biodegradable scaffold with a fibrous structure that continuously releases a GF may represent a successful strategy in the treatment of SCI.

In the present study, FGF-2 was incorporated into PLGA microfibers, showing a sustained release and these functionalized fibers supported the PC-12 cell proliferation and migration. The scaffold of electrospun fibers containing FGF-2 was implanted at the site of the hemisected spinal cord. The use of scaffolds in the treatment of SCI is gaining attention in the last year, mainly due to the fact that the scaffold will bridge the spinal cord [25].

In order to find the appropriate parameters for the electrospinning process, initial tests were performed. The parameters chosen offered greater and more frequently stability. PEG was added to the aqueous protein solution of the core to improve its viscosity, stabilize the processing parameters and also to enhance stability of the GF [48–50]. Coaxial electrospinning resulted in fibers with a uniform morphology and without beads, similar to the fibers generated by traditional electrospinning. No significant increase of the fiber diameter was observed when compared with the fibers of the traditional electrospun scaffolds. The reason behind this phenomenon may be the fact that for coaxial electrospinning, the voltage was increased in order to maintain the stability of the process. The value of the contact angle for the core–shell microfiber scaffold is very similar to the value of the uniaxial PLGA fibers. This demonstrates that the hydrophobic nature of PLGA was maintained and there was no extravasation of the aqueous internal content of the fibers. These values were similar to those found in the previous studies [51–53].

The two structural components of the fibers could not clearly be detected separately in the LCSM images due to the fiber diameter and the resolution of the confocal microscopy. This correlates with previous studies [50,54,55].

However, the TEM confirmed the core–shell structure of the microfibers (Figure 2A). Desirable mechanical properties for the scaffolds are especially important because of the forces they must endure in applications of *in vivo* tissue engineering [56]. The average value of Young's modulus of the coaxial PLGA-FGF2 microfibers is approximately 2 MPa, a value similar to that reported for spinal cord tissue [57].

In this study, a burst release of FGF-2 occurred within the first 8 h. This burst effect may be related to the migration of FGF-2 during the drying and storage steps, which resulted in a higher number of FGF-2 molecules located near the fiber surface [54,58,59]. This conclusion was also in accordance with the results obtained from other similar core–shell fibers [49,59]. In this work, coaxial electrospinning demonstrated superior release time of FGF-2 compared with previous studies [60,61]. The GF was detected for at least 30 days. The prolonged liberation of the FGF-2 may be due to the hydrophobic surface of the biomaterial, which was able to effectively retard the penetration of the medium into the core layer, thereby sustaining the drug release [62]. The initial burst effect, caused by the presence of drug molecules on fiber surface, is functional to the treatment of primary SCI, contributing to the reduction of even the cascade of secondary events. The subsequent prolonged drug release, guaranteed by the drug loaded in the fiber core, is useful in slowing down SCI progression, particularly in the chronic phase; drug release is controlled by drug diffusion across the polymer matrix and system slow biodegradation [2].

The PC12 cell lineage was used in order to evaluate cell behavior on microfibers and the potential neural application of the core–shell scaffolds. The MTT assay demonstrated that the microfibers consistently sustained cell growth and allowed for cell spreading, as seen at 3 and 7 days in culture. The cells presented similar viability at day 3, indicating that there were no differences in the cell ability for attaching themselves to the biomaterials with different morphology or molecular composition. However, on day 7, the PC12 cell viability on the scaffolds was significantly lower than the thin PLGA film. This could have been the result of differences on the surface topography between the microfibers and the PLGA film. An increase of the contact area between the cell surface and the material can be seen in the SEM images (Figure 5). This difference in material topography is confirmed by the reduction of the contact angle measurement [63]. It has already been shown that the roughness of the scaffold surface influences cell proliferation [51].

FGF-2 is expected to promote PC12 cell differentiation into neuronal phenotypes [31,32], thereby increasing neuronal markers, such as β-III tubulin [31]. In this study, an increase in β-III tubulin expression was observed, but with a culture-to-culture variability (Figure 7), which is typical in such cellular assays [64]. Nonetheless, this experiment did indicate that the FGF-2 released from the PLGA/FGF-2 microfibers retained at least some degree of bioactivity. Besides this, in the presence of FGF-2, PC12 cells stop division [65]. This correlates with the present study where a decrease in cell viability after 7 days with treatment with PLGA/FGF-2 conditioned medium was observed (Figure 8). Taking together, the results of the β-III tubulin expression, this indicates that the FGF-2 remained bioactive.

In order to evaluate the effect of PLGA/FGF-2 scaffold implantation on SCI, a SCI animal model of hemisection was used. For this, the scaffolds were implanted at the site of the hemisected spinal cord. As revealed by hematoxylin and eosin staining, the scaffold was present and integrated in the local injury at 6 weeks after SCI without obvious toxicity, which would have been reflected in tissue loss or cavity formation. The presence of scaffold at the injury site is important to support the tissue regeneration in SCI animal models, considering that a period of 3–6 months is required to achieve a functional regeneration [66]. In other words, the scaffold degradation should occur in a timely fashion, allowing for the regenerated nerve tissue to become mature enough to be self-supporting [67] and not so fast as to avoid invasion of connective tissue cells, which could diminish the regeneration outcome [68]. However, the optimal timing of scaffold degradation in the context of spinal cord tissue repair processes has not yet been studied in detail [28]. The immunofluorescence staining revealed the presence of some regrowing axons through the implant, while GFAP-positive astrocytes were infiltrating the implant. These findings are similar to the results of Teng *et al.*, where a porous PLGA scaffold was implanted in a rat SCI hemisection model. The authors demonstrated the presence of immunopositive staining for neurofilament and a small population of GFAP-positive astrocytes in the implanted scaffold [36].

According to open-field BBB analyses at day 7 postsurgery, a tendency of better locomotor improvement in the FGF-2 injection group could be observed. However, this tendency diminished until finally reduced at 35 and 42 days. This was probably because one single FGF2 injection will not lead to a sustained delivery of FGF-2 into the injured spinal cord. Besides this, our results demonstrate that PLGA/FGF-2 scaffolds were effective in promoting functional recovery at 28 days after SCI. However, this result was very similar to the PLGA scaffold group. The addition of FGF-2 into microfibers seemed not to have a better effect than the PLGA scaffold only on

10.2217/rme-2018-0060

the locomotor parameters after SCI. This result suggests a lower amount of FGF-2 delivered from the microfibers. These findings are consistent with published data that demonstrate that the use of a fibrous scaffold into a rat hemisection model of SCI was sufficient to promote functional recovery [36,69].

Astrocytes usually promote the formation of scar in SCI, which hinders regeneration of axons [23]. The expression of the astrocyte-specific marker, GFAP, was significantly reduced in the PLGA, PLGA/FGF-2 scaffolds and FGF-2 injection group when compared with control lesion group at 6 weeks after lesion. This result indicates a reduction in glial scaring at the local lesion at those indicated groups. In fact, our hypothesis was that a scaffold can help prevent the formation of scar tissue [70] and subsequent cyst formation [36]. The mechanism for this phenomenon is not yet known but may be correlated with inhibition of cellular ingrowth by the scaffold [36]. Therefore, these results suggested a possible decrease in astroglial scar formation in the presence of the microfiber scaffold.

Conclusion

In this study, core–shell microfiber scaffolds with encapsulated FGF-2 were successfully produced by coaxial electrospinning technology. TEM of FGF-2 microfiber indicated that the GF was distributed in the core of the microfibers. The FGF-2 released from the microfibers was in a sustained manner for about 30 days with a burst release in the first 8 h. The scaffold showed biocompatibility as seen by the *in vitro* tests with PC12 cells that were able to attach and proliferate onto the scaffolds. Besides, implanted scaffolds promoted locomotor recovery at 28 days after injury and reduced GFAP expression into the lesion. This study could be considered a basis for further development of functionalized FGF-2/PLGA scaffolds.

Translational perspective

Because of the scarce treatment options for spinal cord injury (SCI) patients, there is increased necessity for new strategies and combinatorial therapies. Combinations of fibrous materials with growth factors that stimulate axonal regeneration present an interesting treatment option. This preclinical study, using PC12 cells *in vitro* and SCI model in rats as the *in vivo* model showed that FGF-2/PLGA microfibers could be a promising alternative to improve recuperation after SCI. However, these scaffolds should be optimized prior to the initiation of clinical trials. Successful future therapies will require these and other synergistic approaches, such as cell transplantation, to address the problem of persistent barriers in SCI regeneration. More studies will be crucial for the development of an effective clinically relevant therapy for SCI.

Summary points

- FGF-2 was encapsulated into core–shell microfibers by coaxial electrospinning.
- The coaxial electrospinning resulted in a uniform microfiber morphology with a core–shell structure.
- FGF-2/poly(lactic-*co*-glycolic acid) microfibers showed a sustained release of FGF-2 from the fibers for 30 days.
- Scaffolds was implanted in a model of hemisection spinal cord injury in rats.
- The scaffold was present and integrated in the local injury at 6 weeks after spinal cord injury (SCI).
- Implanted scaffolds into SCI promoted locomotor recovery at 28 days after injury.
- Implanted scaffolds into SCI reduced GFAP expression 6 weeks after injury.

Acknowledgements

KP Reis thanks IME Technologies and the laboratory group of Greiner and Agarwal from the University of Bayreuth for the electrospinning training. The authors thank Daniel Weibel's laboratory for the contact angle measurements, Creusa Ferreira and Raquel Santos Mauler for the Young's module measurements and Centro de Microscopia e Microanálise (CMM) UFRGS, in particular, Tao Hasse for assistance for the scanning electron microscopy.

Financial & competing interests disclosure

Financial support received from FINEP, CNPq, CAPES and IPCT. LE Sperling is the recipient of a CNPq grant number 465656/2014-5. The authors have no other relevant affiliations or financial involvement with any organization or entity with a financial interest in or financial conflict with the subject matter or materials discussed in the manuscript apart from those disclosed.

No writing assistance was utilized in the production of this manuscript.

Ethical conduct of research

The authors state that they have obtained approval from the Research Ethics Committee of the Universidade Federal do Rio Grande do Sul (#28079) for animal experimental investigations.

References

1. Santhosh KT, Alizadeh A, Karimi-Abdolrezaee S. Design and optimization of PLGA microparticles for controlled and local delivery of neuregulin-1 in traumatic spinal cord injury. *J. Control. Rel.* 261, 147–162 (2017).
2. Faccendini A, Vigani B, Rossi S *et al.* Nanofiber scaffolds as drug delivery systems to bridge spinal cord injury. *Pharmaceuticals (Basel)* 10(3), pii: E63 (2017).
3. Nagashima K, Miwa T, Soumiya H *et al.* Priming with FGF2 stimulates human dental pulp cells to promote axonal regeneration and locomotor function recovery after spinal cord injury. *Sci. Rep.* 7(1), 13500 (2017).
4. Zaviskova K, Tukmachev D, Dubisova J *et al.* Injectable hydroxyphenyl derivative of hyaluronic acid hydrogel modified with RGD as scaffold for spinal cord injury repair. *J. Biomed. Mater. Res. A* doi:10.1002/jbm.a.36311 (2017) (Epub ahead of print).
5. Anwar MA, Al Shehabi TS, Eid AH. Inflammogenesis of secondary spinal cord injury. *Front. Cell. Neurosci.* 10, 98 (2016).
6. Zhang Z, Yao S, Xie S *et al.* Effect of hierarchically aligned fibrin hydrogel in regeneration of spinal cord injury demonstrated by tractography: a pilot study. *Sci. Rep.* 7, 40017 (2017).
7. Yu S, Yao S, Wen Y, Wang Y, Wang H, Xu Q. Angiogenic microspheres promote neural regeneration and motor function recovery after spinal cord injury in rats. *Sci. Rep.* 6, 33428 (2016).
8. Ziemba AM, Gilbert RJ. Biomaterials for local, controlled drug delivery to the injured spinal cord. *Front. Pharmacol.* 8, 245 (2017).
9. Liu S, Sandner B, Schackel T *et al.* Regulated viral BDNF delivery in combination with Schwann cells promotes axonal regeneration through capillary alginate hydrogels after spinal cord injury. *Acta Biomater.* 60, 167–180 (2017).
10. Shrestha B, Coykendall K, Li Y, Moon A, Priyadarshani P, Yao L. Repair of injured spinal cord using biomaterial scaffolds and stem cells. *Stem Cell. Res. Ther.* 5(4), 91 (2014).
11. Kang MS, Kim JH, Singh RK, Jang JH, Kim HW. Therapeutic-designed electrospun bone scaffolds: mesoporous bioactive nanocarriers in hollow fiber composites to sequentially deliver dual growth factors. *Acta Biomater.* 16, 103–116 (2015).
12. Lancuški A, Abu Ammar A, Avrahami R, Vilensky R, Vasilyev G, Zussman E. Design of starch-formate compound fibers as encapsulation platform for biotherapeutics. *Carbohydr. Polym.* 158, 68–76 (2017).
13. Yun YR, Won JE, Jeon E *et al.* Fibroblast growth factors: biology, function, and application for tissue regeneration. *J. Tissue Eng.* 2010, 218142 (2010).
14. Goldshmit Y, Frisca F, Pinto AR *et al.* Fgf2 improves functional recovery-decreasing gliosis and increasing radial glia and neural progenitor cells after spinal cord injury. *Brain Behav.* 4(2), 187–200 (2014).
15. Rabchevsky AG, Fugaccia I, Turner AF, Blades DA, Mattson MP, Scheff SW. Basic fibroblast growth factor (bFGF) enhances functional recovery following severe spinal cord injury to the rat. *Exp. Neurol.* 164(2), 280–291 (2000).
16. Kasai M, Jikoh T, Fukumitsu H, Furukawa S. FGF-2-responsive and spinal cord-resident cells improve locomotor function after spinal cord injury. *J. Neurotrauma.* 31(18), 1584–1598 (2014).
17. Zhang HY, Wang ZG, Wu FZ *et al.* Regulation of autophagy and ubiquitinated protein accumulation by bFGF promotes functional recovery and neural protection in a rat model of spinal cord injury. *Mol. Neurobiol.* 48(3), 452–464 (2013).
18. Ye LB, Yu XC, Xia QH *et al.* Regulation of Caveolin-1 and junction proteins by bFGF contributes to the integrity of blood-spinal cord barrier and functional recovery. *Neurotherapeutics* 13(4), 844–858 (2016).
19. Xu HL, Tian FR, Lu CT *et al.* Thermo-sensitive hydrogels combined with decellularised matrix deliver bFGF for the functional recovery of rats after a spinal cord injury. *Sci. Rep.* 6, 38332 (2016).
20. Cuevas P, Carceller F, Ortega S, Zazo M, Nieto I, Gimenez-Gallego G. Hypotensive activity of fibroblast growth factor. *Science* 254(5035), 1208–1210 (1991).
21. Dirix LY, Vermeulen PB, Pawinski A *et al.* Elevated levels of the angiogenic cytokines basic fibroblast growth factor and vascular endothelial growth factor in sera of cancer patients. *Br. J. Cancer* 76(2), 238–243 (1997).
22. Ruotsalainen T, Joensuu H, Mattson K, Salven P. High pretreatment serum concentration of basic fibroblast growth factor is a predictor of poor prognosis in small cell lung cancer. *Cancer Epidemiol. Biomarkers Prev.* 11(11), 1492–1495 (2002).
23. Lan L, Tian FR, Zhuge DL *et al.* Implantable porous gelatin microspheres sustained release of bFGF and improved its neuroprotective effect on rats after spinal cord injury. *PLoS ONE* 12(3), e0173814 (2017).
24. Andreopoulos FM, Persaud I. Delivery of basic fibroblast growth factor (bFGF) from photoresponsive hydrogel scaffolds. *Biomaterials* 27(11), 2468–2476 (2006).
25. Chen B, He J, Yang H *et al.* Repair of spinal cord injury by implantation of bFGF-incorporated HEMA-MOETACL hydrogel in rats. *Sci. Rep.* 5, 9017 (2015).

26. Shi Q, Gao W, Han X *et al.* Collagen scaffolds modified with collagen-binding bFGF promotes the neural regeneration in a rat hemisected spinal cord injury model. *Sci. China Life Sci.* 57(2), 232–240 (2014).
27. Kang CE, Baumann MD, Tator CH, Shoichet MS. Localized and sustained delivery of fibroblast growth factor-2 from a nanoparticle-hydrogel composite for treatment of spinal cord injury. *Cells Tissues Organs* 197(1), 55–63 (2013).
28. Kubinová S, Syková E. Biomaterials combined with cell therapy for treatment of spinal cord injury. *Regen. Med.* 7(2), 207–224 (2012).
29. Liu T, Houle JD, Xu J, Chan BP, Chew SY. Nanofibrous collagen nerve conduits for spinal cord repair. *Tissue Eng. Part A* 18(9–10), 1057–1066 (2012).
30. Sperling LE, Reis KP, Pozzobon LG, Girardi CS, Pranke P. Influence of random and oriented electrospun fibrous poly(lactic-co-glycolic acid) scaffolds on neural differentiation of mouse embryonic stem cells. *J. Biomed. Mater. Res. A* doi:10.1002/jbm.a.36012 (2017) (Epub ahead of print).
31. Ohuchi T, Maruoka S, Sakudo A, Arai T. Assay-based quantitative analysis of PC12 cell differentiation. *J. Neurosci. Methods* 118(1), 1–8 (2002).
32. Nabiuni M, Rasouli J, Parivar K, Kochesfehani HM, Irian S, Miyan JA. *In vitro* effects of fetal rat cerebrospinal fluid on viability and neuronal differentiation of PC12 cells. *Fluids Barriers CNS* 9(1), 8 (2012).
33. Martini AC, Berta T, Forner S *et al.* Lipoxin A4 inhibits microglial activation and reduces neuroinflammation and neuropathic pain after spinal cord hemisection. *J. Neuroinflammation* 13(1), 75 (2016).
34. Basso DM, Beattie MS, Bresnahan JC. A sensitive and reliable locomotor rating scale for open field testing in rats. *J. Neurotrauma.* 12(1), 1–21 (1995).
35. Nicola FDC, Marques MR, Odorcyk F *et al.* Neuroprotector effect of stem cells from human exfoliated deciduous teeth transplanted after traumatic spinal cord injury involves inhibition of early neuronal apoptosis. *Brain Res.* 1663, 95–105 (2017).
36 . Teng YD, Lavik EB, Qu X *et al.* Functional recovery following traumatic spinal cord injury mediated by a unique polymer scaffold seeded with neural stem cells. *Proc. Natl Acad. Sci. USA* 99(5), 3024–3029 (2002).
37. Roman JA, Reucroft I, Martin RA, Hurtado A, Mao HQ. Local release of paclitaxel from aligned, electrospun microfibers promotes axonal extension. *Adv. Healthc. Mater.* 5(20), 2628–2635 (2016).
38. Xia T, Huang B, Ni S *et al.* The combination of db-cAMP and ChABC with poly(propylene carbonate) microfibers promote axonal regenerative sprouting and functional recovery after spinal cord hemisection injury. *Biomed. Pharmacother.* 86, 354–362 (2017).
39. Willerth SM, Sakiyama-Elbert SE. Approaches to neural tissue engineering using scaffolds for drug delivery. *Adv. Drug Deliv. Rev.* 59(4-5), 325–338 (2007).
40. Danhier F, Ansorena E, Silva JM, Coco R, Le Breton A, Préat V. PLGA-based nanoparticles: an overview of biomedical applications. *J. Control. Rel.* 161(2), 505–522 (2012).
41. Nune M, Subramanian A, Krishnan UM, Kaimal SS, Sethuraman S. Self-assembling peptide nanostructures on aligned poly(lactide-co-glycolide) nanofibers for the functional regeneration of sciatic nerve. *Nanomedicine (Lond.)* 12(3), 219–235 (2017).
42. Makadia HK, Siegel SJ. Poly lactic-co-glycolic acid (PLGA) as biodegradable controlled drug delivery carrier. *Polymers (Basel)* 3(3), 1377–1397 (2011).
43. Ranjbar-Mohammadi M, Zamani M, Prabhakaran MP, Bahrami SH, Ramakrishna S. Electrospinning of PLGA/gum tragacanth nanofibers containing tetracycline hydrochloride for periodontal regeneration. *Mater. Sci. Eng. C Mater. Biol. Appl.* 58, 521–531 (2016).
44. Li J, Zhu J, He T *et al.* Prevention of intra-abdominal adhesion using electrospun PEG/PLGA nanofibrous membranes. *Mater. Sci. Eng. C Mater. Biol. Appl.* 78, 988–997 (2017).
45. Naves L, Dhand C, Almeida L, Rajamani L, Ramakrishna S, Soares G. Poly(lactic-co-glycolic) acid drug delivery systems through transdermal pathway: an overview. *Prog. Biomater.* 6(1-2), 1–11 (2017).
46. Abe K, Saito H. Effects of basic fibroblast growth factor on central nervous system functions. *Pharmacol. Res.* 43(4), 307–312 (2001).
47. Presta M, Dell'era P, Mitola S, Moroni E, Ronca R, Rusnati M. Fibroblast growth factor/fibroblast growth factor receptor system in angiogenesis. *Cytokine Growth Factor Rev.* 16(2), 159–178 (2005).
48. Jiang H, Hu Y, Li Y, Zhao P, Zhu K, Chen W. A facile technique to prepare biodegradable coaxial electrospun nanofibers for controlled release of bioactive agents. *J. Control. Rel.* 108(2-3), 237–243 (2005).
49. Zhang YZ, Wang X, Feng Y, Li J, Lim CT, Ramakrishna S. Coaxial electrospinning of (fluorescein isothiocyanate-conjugated bovine serum albumin)-encapsulated poly(epsilon-caprolactone) nanofibers for sustained release. *Biomacromolecules* 7(4), 1049–1057 (2006).
50. Ji W, Yang F, Van Den Beucken JJ *et al.* Fibrous scaffolds loaded with protein prepared by blend or coaxial electrospinning. *Acta Biomater.* 6(11), 4199–4207 (2010).
51. Kim MS, Ahn HH, Shin YN, Cho MH, Khang G, Lee HB. An *in vivo* study of the host tissue response to subcutaneous implantation of PLGA- and/or porcine small intestinal submucosa-based scaffolds. *Biomaterials* 28(34), 5137–5143 (2007).
52. Park H, Lee JW, Park KE, Park WH, Lee KY. Stress response of fibroblasts adherent to the surface of plasma-treated poly(lactic-co-glycolic acid) nanofiber matrices. *Colloids Surf. B, Biointerfaces* 77(1), 90–95 (2010).

53. Yang J, Zhu T, Wang J, Chen S, Li W. Synthesis and characterization of fl urbiprofen axetil-loaded electrospun MgAl-LDHs/poly(lacticco-glycolic acid) composite nanofibers. *RSC Adv.* 5, 69423–69429 (2015).

54. Yang Y, Li X, Qi M, Zhou S, Weng J. Release pattern and structural integrity of lysozyme encapsulated in core-sheath structured poly(DL-lactide) ultrafine fibers prepared by emulsion electrospinning. *Eur. J. Pharm. Biopharm.* 69(1), 106–116 (2008).

55. Yin L, Wang K, Lv X *et al.* The fabrication of an ICA-SF/PLCL nanofibrous membrane by coaxial electrospinning and its effect on bone regeneration in vitro and in vivo. *Sci. Rep.* 7(1), 8616 (2017).

56. Fu W, Liu Z, Feng B *et al.* Electrospun gelatin/PCL and collagen/PLCL scaffolds for vascular tissue engineering. *Int. J. Nanomedicine* 9, 2335–2344 (2014).

57. Mckee CT, Last JA, Russell P, Murphy CJ. Indentation versus tensile measurements of Young's modulus for soft biological tissues. *Tissue Eng. Part B, Rev.* 17(3), 155–164 (2011).

58. Allison SD. Analysis of initial burst in PLGA microparticles. *Expert Opin. Drug Deliv.* 5(6), 615–628 (2008).

59. Esmaeili A, Haseli M. Optimization, synthesis, and characterization of coaxial electrospun sodium carboxymethyl cellulose-graft–methyl acrylate/poly(ethylene oxide) nanofibers for potential drug-delivery applications. *Carbohydr. Polym.* 173, 645–653 (2017).

60. Sahoo S, Ang LT, Goh JC, Toh SL. Growth factor delivery through electrospun nanofibers in scaffolds for tissue engineering applications. *J. Biomed. Mater. Res. A* 93(4), 1539–1550 (2010).

61. Rubert M, Dehli J, Li Y *et al.* Electrospun PCL/PEO coaxial fibers for basic fibroblast growth factor delivery. *J. Mater. Chem. B* 2, 8538–8546 (2014).

62. Karthikeyan K, Guhathakarta S, Rajaram R, Korrapati PS. Electrospun zein/eudragit nanofibers based dual drug delivery system for the simultaneous delivery of aceclofenac and pantoprazole. *Int. J. Pharm.* 438(1–2), 117–122 (2012).

63. Abdelsalam ME, Bartlett PN, Kelf T, Baumberg J. Wetting of regularly structured gold surfaces. *Langmuir* 21(5), 1753–1757 (2005).

64. Chew SY, Wen J, Yim EK, Leong KW. Sustained release of proteins from electrospun biodegradable fibers. *Biomacromolecules* 6(4), 2017–2024 (2005).

65. Attiah DG, Kopher RA, Desai TA. Characterization of PC12 cell proliferation and differentiation-stimulated by ECM adhesion proteins and neurotrophic factors. *J. Mater. Sci. Mater. Med.* 14(11), 1005–1009 (2003).

66. Schaub NJ, Johnson CD, Cooper B, Gilbert RJ. Electrospun fibers for spinal cord injury research and regeneration. *J. Neurotrauma.* 33(15), 1405–1415 (2016).

67. Maquet V, Martin D, Scholtes F *et al.* Poly(D,L-lactide) foams modified by poly(ethylene oxide)-block-poly(D,L-lactide) copolymers and a-FGF: in vitro and in vivo evaluation for spinal cord regeneration. *Biomaterials* 22(10), 1137–1146 (2001).

68. Oudega M, Gautier SE, Chapon P *et al.* Axonal regeneration into Schwann cell grafts within resorbable poly(alpha-hydroxyacid) guidance channels in the adult rat spinal cord. *Biomaterials* 22(10), 1125–1136 (2001).

69. Zamani F, Amani-Tehran M, Latifi M, Shokrgozar MA, Zaminy A. Promotion of spinal cord axon regeneration by 3D nanofibrous core-sheath scaffolds. *J. Biomed. Mater. Res. A* 102(2), 506–513 (2014).

70. Jiao G, Pan Y, Wang C, Li Z, Guo R. A bridging SF/Alg composite scaffold loaded NGF for spinal cord injury repair. *Mater. Sci. Eng. C Mater. Biol. Appl.* 76, 81–87 (2017).

10.2217/rme-2018-0060

Capítulo II.

VPA/PLGA microfibers produced by coaxial electrospinning for the treatment of spinal cord injury

Karina P. Reis[1,2,3]*, Laura E. Sperling[1,2], Cristian Teixeira [1,2], Luiz Sommer[1,2]

Mariana Colombo[4], Leticia Scherer Koester[4], Patricia Pranke[1,2,3,5]

[1]Hematology and Stem Cell Laboratory, Faculty of Pharmacy, [2]Stem Cell Laboratory, Fundamental Health Science Institute, [3]Post Graduate Program in Physiology, Universidade Federal do Rio Grande do Sul, [4]Post Graduate Program in Pharmaceutical Sciences, Universidade Federal do Rio Grande do Sul, [5]Stem Cell Research Institute (IPCT – Instituto de Pesquisa com Células-tronco), Porto Alegre, RS, Brazil

* Correspondence: kapire@yahoo.com.br; Tel.: +55-051-3308-3622

Artigo será submetido à revista Annals of Biomedical Engineering

Abstract

Spinal cord injury (SCI) is a devastating traumatic injury resulting in loss of sensory, motor and autonomic function distal from the level of injury. An appropriate combination of biomaterials and bioactive substances is currently thought to be a promising approach to treat this condition. Valproic acid (VPA) systemic administration has been previously shown to promote functional recovery in animal models of SCI. In this study, VPA was encapsulated in PLGA microfibers by the coaxial electrospinning technique. It was demonstrated that the fibers showed continuous and cylindrical morphology, randomly oriented fibers and compatible morphological and mechanical characteristics for application in the SCI. Drug-release tests indicated a rapid release of the VPA during the first day of the *in vitro* test. The coaxial fibers containing VPA supported adhesion, viability and proliferation of PC12 cells. In addition, the VPA/PLGA microfibers induced the reduction of PC12 cell viability, as has already been described in the literature. These results indicate the cytocompatibility of the VPA/PLGA core-shell microfibers and it may be a promising approach to treat SCI when combined with other strategies.

Keywords: coaxial electrospinning, VPA, spinal cord injury

1. Introduction

Spinal cord injury (SCI) is a major cause of paralysis (Valenzuela *et al.*, 2012). This lesion damages axonal pathways, interrupting synaptic transmission between the brain and spinal cord and subsequently altering motor, sensory and autonomic functions below the level of injury (Hassan *et al.*, 2018). The complex pathophysiology of SCI may explain the current lack of an effective therapeutic approach for the regeneration of damaged neuronal cells and the recovery of motor function (Faccendini *et al.*, 2017). There is no effective clinical treatment to date for this condition and current treatment focuses on stabilization and prevention of further damage. For this reason, many studies propose the use of biomaterials to repair the broken neuronal circuitry of the injured spinal cord. Implantable biomaterials can be mainly used to regenerate a damaged area of the spinal cord, to bridge the formed gap and act as support for axonal re-growth (Vigani *et al.*, 2017).

Valproic acid (VPA) is a well-established anticonvulsant and mood-stabilizing drug used primarily in the treatment of epilepsy and bipolar disorder (Zhu *et al.*, 2017a). Previous

studies have demonstrated that systemic administration of VPA improved locomotor function after spinal cord injury (Penas *et al.*, 2011; Lee *et al.*, 2012; Hao *et al.*, 2013; Darvishi *et al.*, 2014). In addition, VPA exerts an anti-inflammatory effect (Yu *et al.*, 2012; Chen *et al.*, 2018); reduces cell death of motor neurons (Lee *et al.*, 2014) and cellular apoptosis (Lv *et al.*, 2011; Lee *et al.*, 2012), attenuates demyelination and axonal loss, preserves the involved oligodendrocytes and neurons (Penas *et al.*, 2011), increases neurite outgrowth (Abdanipour *et al.*, 2012), reduce the cystic cavity (Yu *et al.*, 2012; Darvishi *et al.*, 2014) and increases expression of neuronal progenitor cells in the spinal cord.

The intraperitoneal injection of VPA has some disadvantages. The injection method involves repeated punctures, in general, twice a day for seven days (Lv *et al.*, 2011; Penas *et al.*, 2011; Hao *et al.*, 2013) which can result in pain and infections (Xia *et al.*, 2013). One delivery approach has circumvented these issues by delivering VPA into the injury site via an osmotic mini-pump (Lu *et al.*, 2013). However, these surgically implanted pumps can be dislodged, induce infections and have a limited loading capacity, which restricts their translational applications (Roman *et al.*, 2016). Therefore, biomaterial-based drug delivery systems such as microfibers present an additional platform to locally deliver VPA and therefore promote spinal cord tissue repair.

Electrospinning is currently one of the simplest methods to produce micro/nanofiber scaffolds. Coaxial electrospinning is a modification of this classical procedure, which promotes production of fibers with a core–shell structure and highly varied compositions (Llorens *et al.*, 2015). It is possible to encapsulate a number of agents such as cells, growth factors, small molecules and nanoparticles into the fibers (Sperling *et al.*, 2016). Electrospun fibers have been used extensively as potential scaffolds in SCI tissue engineering (Xia *et al.*, 2013; Zamani *et al.*, 2014; Colello *et al.*, 2016). A wide range of natural and synthetic polymers can be electrospun. Poly (lactic-co-glycolic acid) (PLGA) has been used in many tissue engineering applications due to its biodegradability and biocompatibility (Makadia e Siegel, 2011; Danhier *et al.*, 2012).

In this work, VPA was encapsulated in PLGA microfibers using the coaxial electrospinning technique. To our knowledge, this is the first time that VPA was encapsulated into electrospun fibers. The morphology of the microfibers was characterized by scanning electron microscope (SEM), while the distribution of VPA in the core structure was confirmed by fluorescent images. The surface hydrophilicity was evaluated by water contact angle. The

mechanical properties of the scaffold were measured with the tensile mechanical test. The *in vitro* release behavior of the VPA from the core-shell structured PLGA/VPA microfibers was also determined. The biocompatibility of the scaffold was then tested in terms of proliferation and morphology of the PC12 cells. In order to explore the potential application of the PLGA/VPA microfibers in SCI repair, the scaffold was implanted into a hemisected SCI rat to bridge the lesion site. Hind limb locomotor function of the rat was evaluated by the Basso-Beattie-Bresnahan (BBB) scale; the histological analysis was performed by hematoxylin-eosin staining and the expression of neural markers was determined by flow cytometry.

2. Materials and methods

2.1.Preparation of microfiber scaffolds

The scaffolds were produced by the coaxial electrospinning technique. The shell solution consisted of 18% poly(lactic-co-glycolic acid) (PLGA; Mw ≈ 50–75 kg/mol; 75:25 lactide/glicolide; PURAC Biochem BV) in 1,1,1,3,3,3-hexafluoro-2- propanol (Sigma Aldrich) and chloroform (Dinâmica) (3:1). The core of the fibers contained 25 μg/mL valproic acid sodium salt (VPA, Santa Cruz Biotechnology), 10% polyethylene glycol (PEG; Mw≈ 20,000; Sigma) and 2% bovine serum albumin (BSA; Sigma) diluted in water. The prepared solutions were then delivered to the outer and inner coaxial needle at 2.0 and 0.2 mL/h feeding ratios, respectively, with a programmable syringe pump. The applied voltage was in the range of 16–25 kV and the distance between the needle and the collector plate was 15 cm. The fibers were collected on an aluminum collecting plate during a 30 minutes period. The coaxial electrospinning procedure was performed at 22°C with 45% controlled air humidity within the electrospinning apparatus (IME Technologies, Netherlands). The control core-shell PLGA fibers were produced by the same procedure cited above, but without adding VPA to the core solution.

2.2.Scaffold characterization

The scaffolds were characterized for their morphology, hydrophilicity and mechanical properties tests. The average diameter of the fibers was determined using the software ImageJ 1.383 by measuring 30 fibers from each of the images obtained by SEM (n=30).

2.2.1. Morphological analysis

The morphology of the electrospun scaffolds was analyzed by scanning electron microscopy (SEM; JSM 6060). The collected fibers were dried overnight to evaporate the residual solvent and were then gold coated using a sputter coater (Bal-Tec SCD 050) prior to observation by a SEM operating at an accelerating voltage of 10kV. The fiber diameter was calculated using the ImageJ software.

2.2.2. Laser scanning confocal microscopy (LSCM)

Laser scanning confocal microscopy (LSCM, Olympus Fluoview FV1000) was used to visualize the distribution of the VPA in the microfibers, and to do so, the core solution used for electrospinning was mixed with fluorescein (Sigma).

2.2.3. Static Water Surface Contact Angle

The contact angle was measured using a Drop Shape Analyzer (Krüss). A volume of approximately 5 μL of deionized water was dropped on the surface of the electrospun scaffolds and contact angle values were calculated. To prepare samples for water contact angle measurement, the microfibers were collected during a period of 10 minutes by the coaxial electrospinning process (n=3).

2.2.4. Mechanical properties tests

Young's modulus, maximum load (tensile stress) and maximum elongation (ultimate strain %) were determined by dynamic mechanical analysis (DMA) in a Q800AT DMA instrument equipped with a tension film clamp in the DMA controlled force mode, as described in the literature (Sperling *et al.*, 2017). Scaffolds of 25×7 mm were analyzed with a ramp force of 0.5 N/min until 18 N maximum load, under 0.005 N static load at a constant temperature (37°C). The stress–strain curves were recorded and the tensile stress at maximal load was obtained from this data for each sample. The TA Universal Analysis software was used for

drawing the diagrams and analyzing the results. Young's modulus of the samples was determined as the slope of the straight-line stress-strain relationship (n=3).

2.3.*In vitro* release of VPA from VPA/PLGA microfibers

The electrospun scaffolds were placed in 7mL of phosphate buffered saline (PBS) with 1% Penicillin/Streptomycin (Sigma Aldrich). The incubation was performed at 37°C in the presence of 5% CO_2. At appropriate intervals of 1 hour, 6 hours, 24 hours, 3, 5 and 10 days, 1 mL of the supernatant was removed and replenished with an identical volume of fresh buffer. The VPA concentrations were determined by HPLC. The sample was filtered through 0.45 µm membrane filter (Millipore). The samples were acidified to pH 4 with hydrochloric acid (1M) (Chen *et al.*, 2012). The amount of VPA released was determined using high performance liquid chromatography (HPLC) (Amini *et al.*, 2006). The HPLC apparatus consisted of HPLC Proeminence device (Tokyo, Japan) equipped with FCV-10 AL system controller, LC-20 AT pump system, SIL-20A automatic injector and SPD-M20A detector. The VPA was analyzed using a Kinetex® 5µm C18 100 Å, LC Column of 150 x 4.6 mm. The mobile phase was a 55:45 (v/v) mixture of 0.05% TFA in water and acetonitrile. The injection volume was 20 µL and the HPLC system was operated at an isocratic flow of 1.0 mL/min, with detection at 210 nm. A stock solution of VPA (20 mg/mL) was prepared in methanol. The stock solution was then diluted with PBS acidified to pH 4 with hydrochloric acid (1 M) to give a series of working standard solutions for the calibration curve (10-200 µg/mL). The results are presented as mean ± standard deviation (n=3).

2.4.PC12 cell culture

PC12 cells were cultivated in DMEM high glucose (Sigma) supplemented with 15% fetal bovine serum (FBS) (Gibco), 5% horse serum (Laborclin) and 1% penicillin/streptomycin (Sigma). The cells were maintained at 37 °C in a humidified incubator with 5% CO_2, and the culture medium was changed every other day. The scaffolds were cut to fit into the wells of a 24 well plate and fixed with silicon o-rings. All the samples were sterilized for 1 hour under UV light before cell seeding. A total of 10,000 PC12 cells were seeded on each scaffold.

2.4.1. SEM analysis of cell growth on scaffolds

After 3 and 7 days in culture, the cell-scaffold constructs were rinsed twice with PBS, fixed with 4% parafolmadehyde for 20 minutes and dehydrated in graded series of alcohol (25, 40, 60, 75, 85, 100%) for 15 minutes each. After drying, the scaffolds were coated with gold (Bal-Tec SCD 050) and observed. A scanning electron microscope (Carl Zeiss EVO50) was used to observe the morphology of the cells on the microfibers at an accelerating voltage of 10 kV.

2.4.2. Analysis of the cell morphology by confocal microscopy

After 3 and 7 days in culture, all the scaffolds were rinsed with PBS, fixed in 4% paraformaldehyde for 20 minutes and permeabilized with 0.1% Triton-X100. The cells were then stained with 20 µg/ml rhodamine-phalloidin and 0.5 µg/ml (4',6-diamidino-2-phenylindole) DAPI (Life Technologies) and washed 3x with PBS. Following this, images were taken by Z-stack scanning and 3D reconstruction of an Olympus Fluoview FV1000 confocal microscope.

2.5.VPA bioactivity

The PC12 cell lineage was used to evaluate the bioactivity of the VPA. It is expected that VPA inhibits the proliferation of pheochromocytoma cells (Adler *et al.*, 2008). For this reason the scaffolds were cut to fit into the wells of a 24 well plate and fixed with silicon o-rings. The material was sterilized by UV light for 1 hour before cell seeding. PC12 cells at 10,000 cells per well were seeded on the scaffolds at 37 °C with 5% CO2. The culture medium was DMEM high glucose (Sigma) supplemented with 15% fetal bovine serum (FBS) (Gibco) and 5% horse serum (Laborclin), 1% penicillin/streptomycin (Sigma) and 0.1% amphotericin (Sigma).The WST-8 assay was used to determine the impact of the VPA on the viability cells (n=3).

After 3 and 7 days, respectively, the cells were treated with WST-8 (4-[3-(2-methoxy-4-nitrophenyl)-2-(4-nitrophenyl)-2*H*-5-tetrazolio]-1,3-benzene disulfonate sodium salt) for 2 hours. This assay is based on the conversion of the tetrazolium salt WST-8 to highly water soluble formazan by viable cells (Ishiyama *et al.*, 1997). After the incubation period, the optical density (OD) of the culture media with WST-8 at 420 nm was measured using a plate reader.

The percentage of viable cells was calculated using the optical density of the control and treated cells.

Two experimental groups were used: control PLGA scaffold – cells cultivated on electrospun PLGA core-shell fibers without VPA, and PLGA/VPA scaffold – cells cultivated on electrospun PLGA core-shell fibers with VPA in the core of the fibers. A control group, which consisted of cells directly cultivated on the well, was also evaluated by WST-8 assay.

2.6. *In vivo* tests

A total of 18 male Wistar rats aged 2 months (250–300 g body weight) were obtained from the Animal House of the Instituto de Ciências Básicas da Saúde da Universidade Federal do Rio Grande do Sul. They were maintained in a temperature-controlled room (21 ± 2 °C) on a 12/12 hour light/dark cycle, with food and water available ad libitum. All the procedures were in accordance with the Guide for the Care and Use of Laboratory Animals adopted by the National Institute of Health (USA) and with the Federation of Brazilian Societies for Experimental Biology. The study was approved by the Research Ethics Committee of the University (#28079). The animals were randomly divided into three experimental groups: SCI (laminectomy followed by SCI); PLGA scaffold (SCI with implanted PLGA scaffold) and PLGA/VPA scaffold (SCI with implanted PLGA/VPA scaffold).

2.6.1. Spinal cord injury and scaffold implantation in rats

Spinal cord injury by right-side hemisection was performed, as described previously (Martini *et al.*, 2016), with some modifications. All the animals were anaesthetized by an intraperitoneal (IP) injection with a mixture of xylasine (5-10 mg/kg) and ketamine (75–100 mg/kg); a longitudinal incision was made and a laminectomy was performed at two vertebral segments, T9–T10. The spinal cord was then hemisected at T10 on the right side by placing a 28-gauge needle dorsiventrally at the midline of the cord and pulling it laterally to ensure the completeness of the hemisection. The scaffolds, with a diameter of 2mm and a thickness of approximately 300μm, were carefully placed into the hemisected gap immediately after the SCI. Subsequently, the fascia, musculature and skin were sutured. Antibiotic (Enrofloxacino, Bayer, Brazil; 10 mg/kg) was administered IP for 5 days after the procedure to prevent infection

and analgesic (Tramal, Pfizer; 10 mg/kg) was administered to prevent pain, followed by two drops of baby Tylenol twice a day for 5 days.

2.6.2. Locomotor activity assessment

Hind limb locomotor function was assessed with the Basso, Beatie and Bresnahan (BBB) scale. Each score represents a distinct motor functional state from 0 (complete paralysis) to 21 (normal mobility) through joint movements, stepping ability, coordination and trunk stability (Basso *et al.*, 1995). Evaluation began 2 days after injury and was repeated weekly until the sixth week after SCI.

2.6.3. Tissue processing and histological analyses

The histological evaluation was performed at six weeks post injury. The animals were anesthetized with a lethal dose of chloral hydrate followed by transcardiac perfusion with 0.9% saline and then 4% paraformaldehyde (Reagen, Brazil) in 0.1 M phosphate buffer (PBS, pH 7.4). The spinal cord was removed from C5 to L5 in the thoracic region, post-fixed in the same fixative solution and cryoprotected with 30% sucrose diluted in phosphate buffer saline (PBS). After cryoprotection, the samples were maintained at -80°C until cryosectioning. For histological analysis, the thoracic region of the spinal cord was longitudinal cut into 30 μm sections in cryostat (Leica, Germany). The sections were stained with hematoxylin and eosin and the images were captured using a Nikon Eclipse E-600 microscope (Japan) coupled with a digital camera.

2.6.4. Flow cytometry analysis

After blocking for 20 minutes with 3% BSA in PBS with 0.1% Triton X-100, the cells were incubated with primary antibodies, including anti-GFAP (DAKO; 14.5 μg/mL), anti-βIII tubulin (Millipore, 05559), anti-nestin (Santa Cruz, SC-33677, 1μg/mL), , and anti-CD68 (Millipore, MAB 1435). The cells were washed twice with PBS1X and incubated for 1 hour with the secondary antibody Alexa-fluor 488 anti-mouse or anti-rabbit (Thermo, 10μg/mL) at

37°C. Negative controls (samples incubated only with the secondary antibody) were included for setting up the machine voltages and to determine the negative region of dot plot.

2.7.Statistical analysis

The experiments were repeated three times and all the data presented were expressed as mean±standard deviation of the three replicates. Statistical analysis was performed using t-test and two-way Anova, followed by the Bonferroni poshoc test. A p value of less than 0.05 was considered statistically significant. Statistical analysis was performed using GraphPad Prism 5 for Windows.

3. Results

3.1.Characterization of the electrospun scaffolds

The fiber morphology, as seen by scanning electron microscopy and the distribution of PLGA or VPA/PLGA fiber diameter, is shown in Fig. 1. Both groups of electrospun microfibers showed a smooth and bead-free surface with uniform diameters. It was concluded that VPA was incorporated into the electrospun PLGA microfibers without modifying the fiber shape. Image analysis showed that the average fiber diameters for PLGA and PLGA/VPA were 2.18μm ± 0.74 and 2.00μm ± 0.61, respectively, with no significant difference between the two groups.

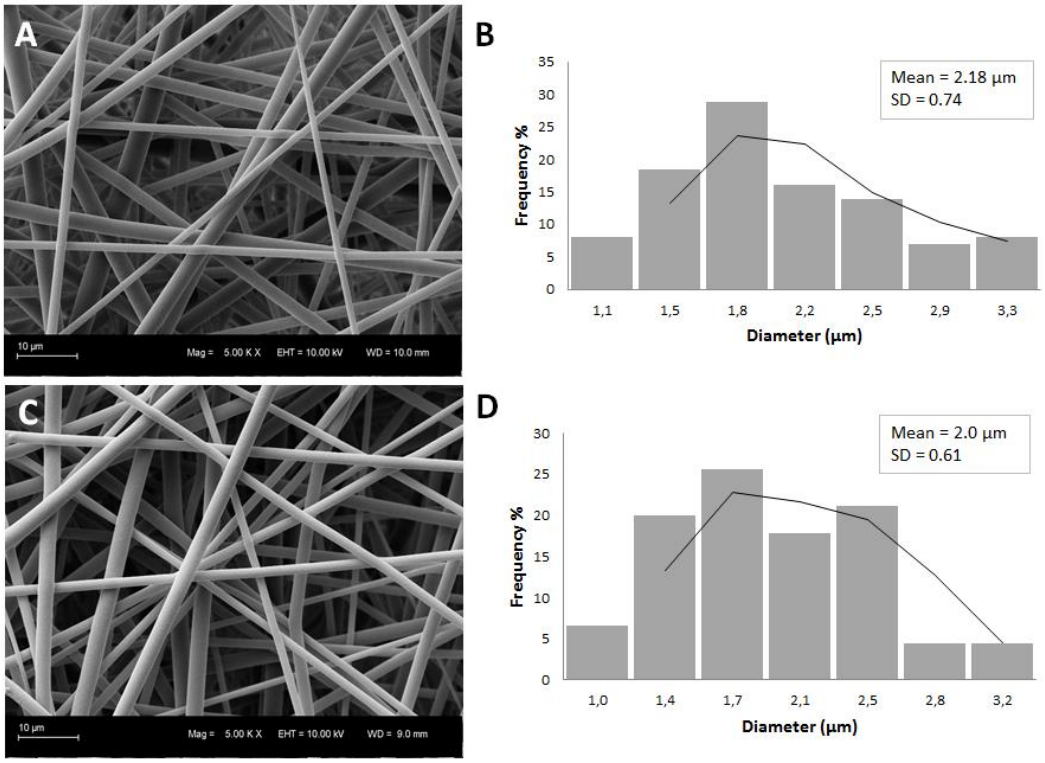

Figure 1. SEM images showing the morphology of the microfibers. (A) PLGA coaxial electrospun fibers of an average diameter of 2.18 µm and (C) PLGA/VPA coaxial microfibers of an average diameter of 2.0 µm. (B) and (D) show the corresponding histograms of the fiber diameter distribution.

Laser scanning confocal microscopy (LSCM) analysis showed the presence of green fluorescence (Fig. 2A) in the fibers, suggesting the incorporation of the fluorescein in the core.

Hydrophilicity of the electrospun microfiber scaffolds was measured by water contact angle. For the PLGA microfibers, the contact angle was 129.7° ± 0.01, which is similar to the value of 127.0° ± 1.80 obtained from the VPA/PLGA core-shell microfibers (Figure 2B and C).

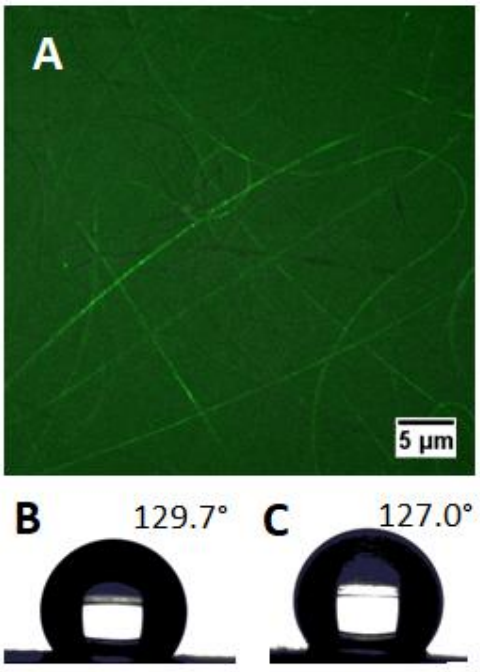

Figure 2. (A) Confocal microscopy image of the coaxial electrospun microfibers using fluorescein in the core. (B) and (C) correspond to images from contact angle measurement 129.7° ± 0.01 and 127.0° ± 1.80 PLGA and VPA/PLGA scaffolds, respectively. N=3

3.2.Mechanical properties

The mechanical properties of the coaxial microfibers were measured and evaluated according to the following categories: Young's modulus (MPa), tensile stress at yield (MPa) and tensile strain at maximum (%) (Table 1). The spinal cord presents specific viscoelastic characteristics with specific mechanical properties and therefore the mechanical properties of the microfibers should be similar to the neural tissue. The scaffolds should provide sufficient mechanical support for neural regeneration.

Table 1. Values for Young's Modulus (MPa), the maximal elongation (%) under the applied force and the maximal load (MPa).

Sample	Young's Modulus (MPa)	Max Elongation (%)	Max Load (MPa)
PLGA	1.437 ± 1.11	177.83 ± 13.97	0.538 ± 0.06
PLGA/VPA	1.758 ± 0.94	204.03 ± 8.15	0.693 ± 0.12

All results are show as mean ± standard deviation of the mean. N=3

3.3.*In vitro* release of VPA and bioactivity

The VPA cumulative release from the scaffolds incubated in phosphate buffer solution (PBS), pH 7.4 at 37°C was measured by HPLC, as shown in Figure 3. An initial burst release was observed during the first day of the test.

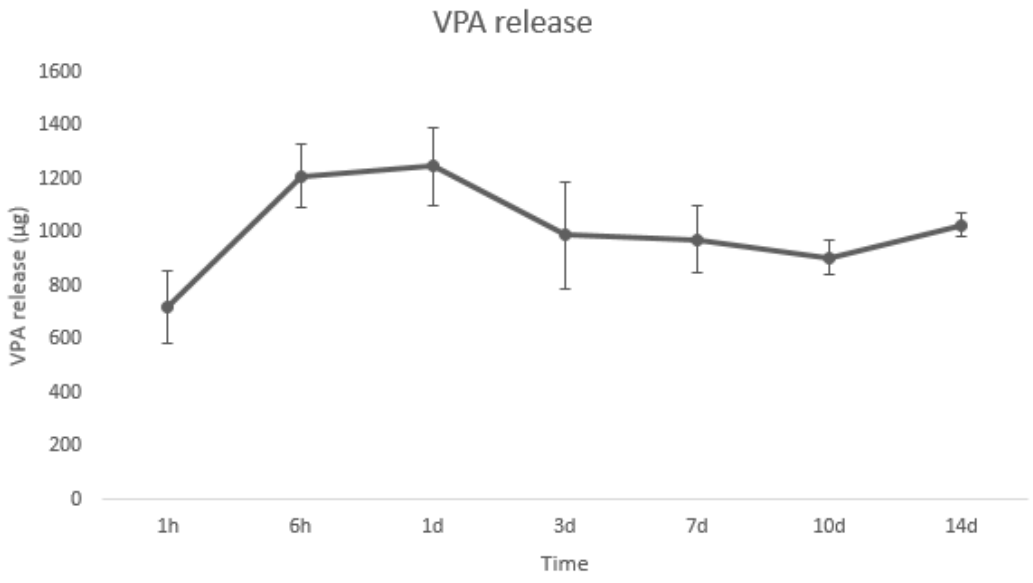

Figure 3. Cumulative release profile of VPA from core-shell fibers determined by HPLC. Results are shown as average and SD. N=3

3.4.Cell viability on the scaffolds

Rat pheochromocytoma 12 (PC12) cells were cultivated on the microfibers to evaluate the potential application of the scaffolds for nerve tissue engineering. As shown in figure 4, the scaffolds had good biocompatibility and favored PC12 cell attachment, spreading, and proliferation, 3 and 7 days after seeding. No morphological differences were observed between the cells cultivated on the PLGA fibers and VPA/PLGA fibers (see Figure 4). Cell proliferation on all the scaffolds was found to increase with the culture time, as seen by the WST-8 assay. When compared to the control cells cultivated directly on the culture plate, a reduction in the cell viability was observed in the cells cultivated on the microfiber scaffolds. Moreover, after 7 days in culture, the VPA/PLGA significantly inhibited the growth of the PC12 cells (Figure 5).

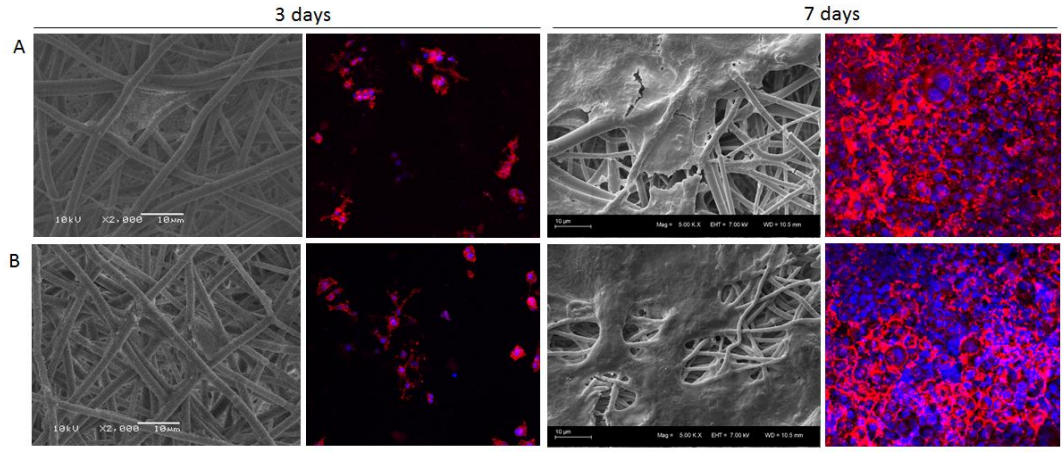

Figure 4. Scanning electron microscopy and fluorescence microscopy images of PC12 cells cultivated on the PLGA scaffold (A) and VPA/PLGA scaffold (B) after 3 and 7 days in culture. Red –actin filament, phalloidin staining; blue – cell nuclei, DAPI staining. The cells attached and spread on the biomaterials. Scale bar 10 μm, N=2

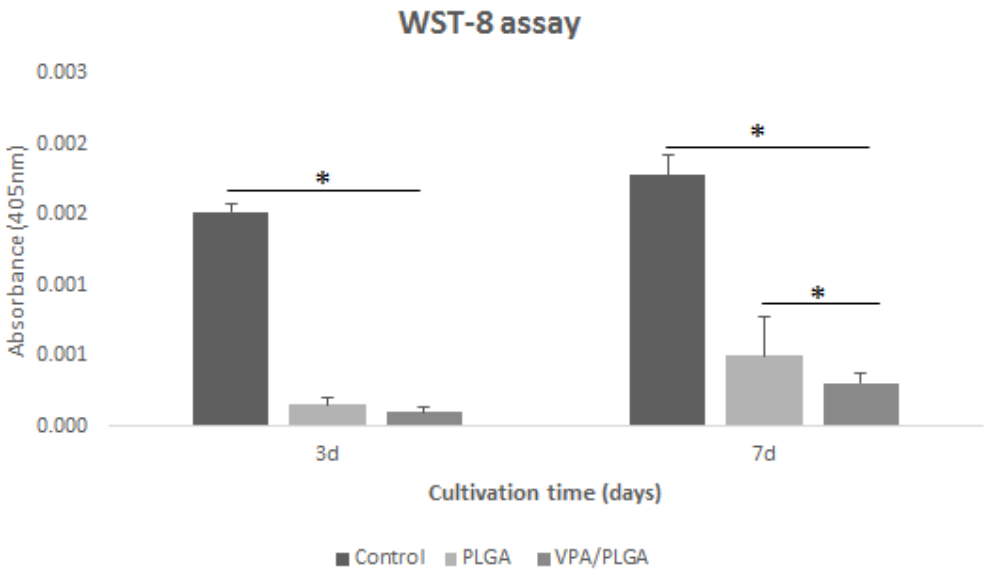

Figure 5. Analysis of cell viability on the scaffolds by WST-8 assay. The optical density value (405 nm) was measured at 3 and 7 days in culture. * indicates a p value < 0.05.

3.5.*In vivo* results

3.5.1. BBB score

The Basso, Beattie, and Bresnahan (BBB) scoring is a common method to assess the locomotor function of rats after SCI. Two trained investigators who were blind to the experimental conditions scored the locomotion recovery in an open field according to the BBB scale. The BBB scores, which are shown in figure 6, demonstrated that there were no significant differences at any of the weekly time points between the control and scaffold groups.

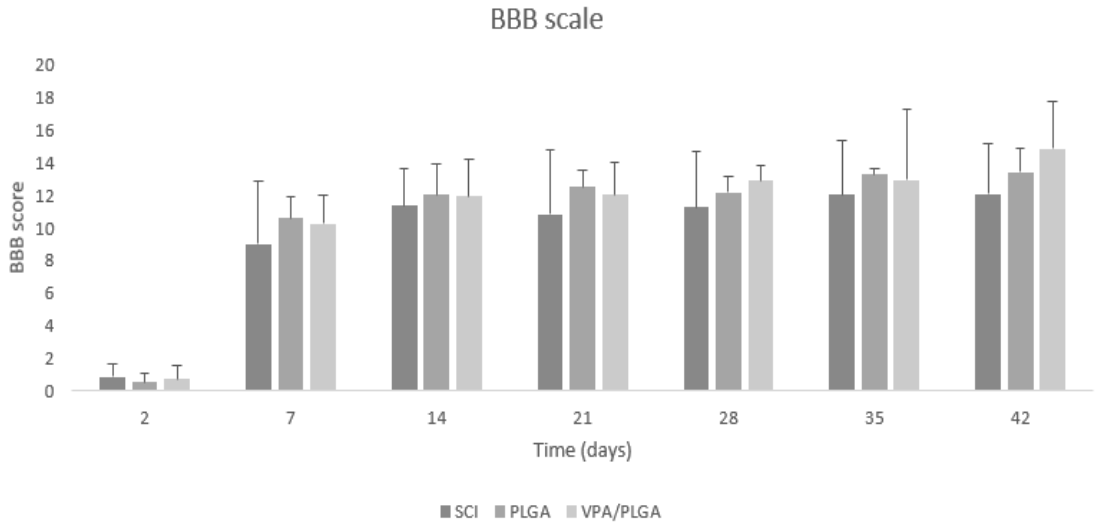

Figure 6. BBB open-field walking scores for the four groups on the ipsilateral, lesioned side. N=6 animals in each group.

3.5.2. Histological analysis of the spinal cord after lesion

Figure 7. Representative images of H&E staining for longitudinal sections of injured spinal cords at six weeks after SCI. (A) control SCI, (B) PLGA scaffold, and (C) VPA/PLGA scaffold. It was not possible to visualize the scaffold at the local lesion. 4x magnification

3.5.3. Flow cytometry analyses

Figure 8 showsthe analysis of the βIII-tubulin, nestin, GFAP, and CD68 expression showed no significant difference in the number of the expressing cells between the groups.

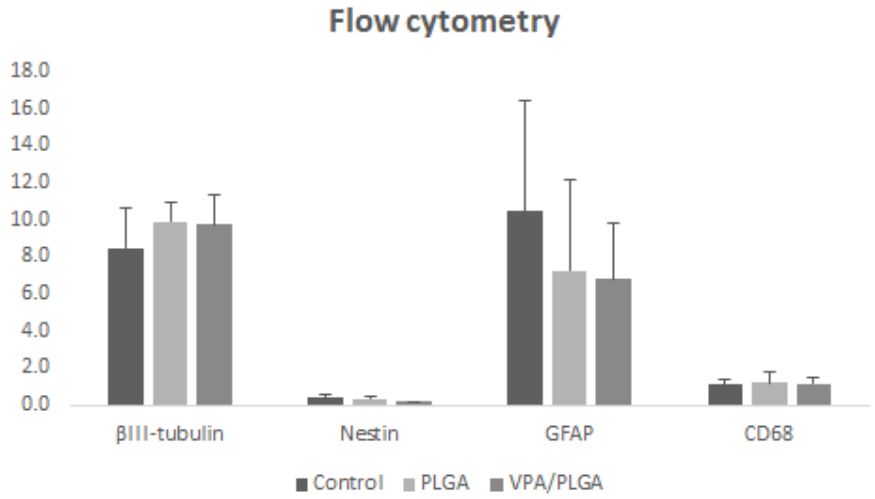

Figure 8. Analysis of expression of βIII-tubulin, Nestin, GFAP, and CD68 by flow cytometry. Results represent percentage of positive cells. N=4 animals in each group.

4. Discussion

Spinal cord injury (SCI) can cause clinically irreversible disability and result in a high level of comorbidity. In adult mammals, the central nervous system exhibits insufficient regeneration capacity; therefore, various therapeutic strategies have been applied to improve the regeneration of injured spinal cord. Biomaterial-based scaffolds have been designed to provide mechanical support and deliver biochemical signals to modulate specific cells responses (Yao *et al.*, 2018). Thus, in the present study, core-shell microfibers of PLGA encapsulating VPA were produced. The scaffold of randomized coaxial fibers was implanted at the site of the hemisected spinal cord to create a bridge that could span over the spinal cord injury site as well as provide neuroprotection through the local release of VPA. The SCI animals that received the scaffold implant displayed modest gains in functional recovery. This is the first study to demonstrate the potential of encapsulating VPA in electrospun microfibers and its application for SCI repair.

Coaxial electrospinning resulted in samples with continuous and smooth cylindrical morphology, randomly oriented fibers with fairly uniform diameter and without any beads (figure 1), which indicates the stability of the electrospinning process (Zuo *et al.*, 2005). Analysis of the contact angle showed that there was no significant difference in the values measured of the coaxial microfibers compared with the uniaxial PLGA fibers. Moreover, the

contact angle value was similar to that reported by previous studies (Kim, M. S. *et al.*, 2007). This result indicates that there was no extravasation of the core content of the fibers (Nguyen *et al.*, 2012). Bilston et al. reported that the average Young's modulus (MPa) of spinal cord tissue was 1.37 MPa ± 0.39 (Bilston e Thibault, 1996). Comparing the value of the tissue with the value obtained for the PLGA/VPA fibrous scaffold, it can be concluded that the produced microfibers had sufficient tensile stress to be utilized as a biomaterial for the treatment of SCI.

Scaffolds can be fabricated by using various substrates derived from either natural or synthetic materials (Vigani *et al.*, 2017). Among these materials, PLGA is one of the most used biocompatible and biodegradable polymers and is approved by the US FDA and European Medicine Agency in various drug delivery systems in humans (Danhier *et al.*, 2012). Previous studies have demonstrated the use of PLGA as a polymer for studies of SCI repair (Kang *et al.*, 2013; Zamani *et al.*, 2014; Santhosh *et al.*, 2017). In hemisected and transected rat SCI models, implantation of PLGA scaffolds into the injured site resulted in functional improvement (Teng *et al.*, 2002; Zamani *et al.*, 2014; Liu *et al.*, 2015). These findings provided a biological basis for the use of PLGA in this work.

VPA was incorporated into the PLGA microfibers without modifying the morphology and fiber shape (figure 1). A burst release of the VPA in the first six hours was observed, which comprised around 80% of the encapsulated substance (figure 3). The burst effect is functional for the treatment of primary SCI, contributing to the reduction of the cascade of secondary events and attenuation of a specific cellular response (Johnson *et al.*, 2016; Faccendini *et al.*, 2017). For example, VPA is known to act in reducing oxidative stress (Lee *et al.*, 2014), cell apoptosis (Lv *et al.*, 2011) and inflammation (Chen *et al.*, 2018). This conclusion is also in agreement with results obtained from other similar core-shell-type configurations (Jiang *et al.*, 2012). Moreover, the core-shell fibers present a thinner sheath layer and the porous structure of the fiber surface may allow for higher water adsorption and for more drug molecules to diffuse out of the core into the surrounding media (Nguyen *et al.*, 2012).

In order to test the biocompatibility of the PLGA and PLGA/VPA core-shell fibers, the PC12 cell line was used and their proliferation and adhesion onto the scaffold was analyzed. The PC12 cells were derived from a tumor (pheochromocytoma) of the rat adrenal medulla. Given the neural origin of the adrenal medulla, these cells are widely used as a model in neurophysiological and neuropharmacological studies (Hou *et al.*, 2014; Wang *et al.*, 2018). All the experimental groups were able to support cell attachment and growth (figure 4). The

control group presented greater absorbance when compared with the other groups, representing a larger number of cells in the wells of the plastic plates (cell culture control). Such a result was expected because cultivating cells in plastic wells is the conventional procedure and a higher viability on plastic has already been observed in previous studies (Steffens *et al.*, 2015; Galuppo *et al.*, 2017). Besides this, the cells presented similar viability at day 3, indicating that there were no differences in the cell ability in terms of the cells attaching themselves to the biomaterials. However, on day 7, the PC12 cell viability on the VPA/PLGA microfibers group was significantly lower than that of the PLGA group. Adler and collaborators (2008), who studied the effect of VPA on the growth of PC12 cells, demonstrated that the treatment of PC12 cells with VPA inhibited the growth of this cell type by activation of cellular apoptosis (Adler *et al.*, 2008), thereby making VPA a drug candidate for the treatment of pheochromocytomas. The present results are therefore indicative of the maintenance of VPA bioactivity after its encapsulation in microfibers.

In order to test the effect of VPA/PLGA core-shell fibers on neural regeneration, a lateral hemisection SCI rat model was used. The hemisection approach causes light injury and reduces animal mortality (Wang *et al.*, 2013).It is a model of choice when studying bridging approaches because the model involves the sectioning of the spinal cord. After lesioning, the motor behavior of the animals was analyzed by the open field BBB scoring. According to BBB analyses, the function of hind limb ipsilateral to the injury was severely impaired after the operation; meanwhile the contra-lateral hind limb was inevitably affected. There were no significant differences in functional recovery between the experimental scaffolds and control groups (figure 6). It is possible, that the number of animals used in each group (n=6) was insufficient to demonstrate statistical significance.

Histological analysis of the spinal cord tissue six weeks after the surgery showed the presence of the scaffolds at the injury site. However, the scaffold adhered strongly to the meninges and conjunctive tissue and when the spinal cord was removed, it became detached from the nervous tissue. The presence of the biomaterial at six weeks after injury is significant because regeneration of nerve tissue can require weeks to months; it is important that the physical structure of a guidance scaffold remains stable over this time period (Stokols e Tuszynski, 2004).

Flow cytometry analyses revealed that βIII-tubulin expression was not altered by the presence of the VPA/PLGA scaffold. The scaffold, therefore had no adverse effect on the neural

cell populations in the injured spinal cord, indicating that it is safe for use in the treatment of SCI. Besides this, there is no difference between the groups for CD68 expression. This is indicative that the scaffolds did not induce inflammatory responses at the lesion site. The expression of the astrocyte specific marker, GFAP, was reduced in the PLGA and VPA/PLGA scaffolds when compared with the control lesion group at 6 weeks after lesion (figure 8). This result indicates a reduction in glial scaring at the local lesion in these indicated groups. It is in accordance with the study of Darvish and colaborators (2014), which demonstrated that treatment with VPA reduces GFAP expression in SCI rats (Darvishi *et al.*, 2014). Besides this, the presence of a scaffold can help prevent the formation of scar tissue (Jiao *et al.*, 2017).

In this study, core-shell microfiber scaffolds with encapsulated VPA were successfully produced by coaxial electrospinning. The scaffolds showed good biocompatibility, as seen by the *in vitro* tests. The PC12 cells were able to attach and proliferate onto the scaffolds. In addition to this, when the scaffolds were implanted into the hemisected spinal cord of rats, they did not demonstrate negative effects on the neural cell populations and did not cause inflammatory responses at the lesion site.This study could also be considered a basis for further development of VPA/PLGA scaffolds as a suitable substrate to be combined with other strategies.

5. Acknowledgements

KPR thanks IME Technologies and the laboratory group of professor Greiner and professor Agarwal from the University of Bayreuth for the electrospinning training. We thank professor Daniel Weibel's laboratory for the contact angle measurements, Creusa Ferreira and Raquel Santos Mauler for the Young's module measurements and Centro de Microscopia e Microanálise (CMM) UFRGS, in particular, Tao Hasse for assistance in the scanning electron microscopy.

6. Financial support

Financial support from FINEP, CNPq, CAPES and IPCT. LES is the recipient of a CNPq grant number 465656/2014-5.

Abdanipour A., H. J. Schluesener and T. Tiraihi. Effects of valproic acid, a histone deacetylase inhibitor, on improvement of locomotor function in rat spinal cord injury based on epigenetic science. *Iran Biomed J* 16: 90-100, 2012.

Adler J. T., D. G. Hottinger, M. Kunnimalaiyaan and H. Chen. Histone deacetylase inhibitors upregulate Notch-1 and inhibit growth in pheochromocytoma cells. *Surgery* 144: 956-961; discussion 961-952, 2008.

Amini H., M. Javan and A. Ahmadiani. Development and validation of a sensitive assay of valproic acid in human plasma by high-performance liquid chromatography without prior derivatization. *Journal of Chromatography B* 830: 368-371, 2006.

Basso D. M., M. S. Beattie and J. C. Bresnahan. A sensitive and reliable locomotor rating scale for open field testing in rats. *J Neurotrauma* 12: 1-21, 1995.

Bilston L. E. and L. E. Thibault. The mechanical properties of the human cervical spinal cord in vitro. *Ann Biomed Eng* 24: 67-74, 1996.

Chen S., J. Ye, X. Chen, J. Shi, W. Wu, W. Lin, Y. Li, H. Fu and S. Li. Valproic acid attenuates traumatic spinal cord injury-induced inflammation via STAT1 and NF-κB pathway dependent of HDAC3. *J Neuroinflammation* 15: 150, 2018.

Chen Z.-j., X.-d. Wang, H.-s. Wang, S.-d. Chen, L.-m. Zhou, J.-l. Li, W.-y. Shu, J.-q. Zhou, Z.-y. Fang, Y. Zhang and M. Huang. Simultaneous determination of valproic acid and 2-propyl-4-pentenoic acid for the prediction of clinical adverse effects in Chinese patients with epilepsy. *Seizure* 21: 110-117, 2012.

Colello R. J., W. N. Chow, J. W. Bigbee, C. Lin, D. Dalton, D. Brown, B. S. Jha, B. E. Mathern, K. D. Lee and D. G. Simpson. The incorporation of growth factor and chondroitinase ABC into an electrospun scaffold to promote axon regrowth following spinal cord injury. *J Tissue Eng Regen Med* 10: 656-668, 2016.

Danhier F., E. Ansorena, J. M. Silva, R. Coco, A. Le Breton and V. Préat. PLGA-based nanoparticles: an overview of biomedical applications. *J Control Release* 161: 505-522, 2012.

Darvishi M., T. Tiraihi, S. A. Mesbah-Namin, A. Delshad and T. Taheri. Decreased GFAP expression and improved functional recovery in contused spinal cord of rats following valproic acid therapy. *Neurochem Res* 39: 2319-2333, 2014.

Faccendini A., B. Vigani, S. Rossi, G. Sandri, M. C. Bonferoni, C. M. Caramella and F. Ferrari. Nanofiber Scaffolds as Drug Delivery Systems to Bridge Spinal Cord Injury. *Pharmaceuticals (Basel)* 10: 2017.

Galuppo A. G., P. C. Chagastelles, D. Gamba, D. B. Iglesias, L. E. Sperling, J. Machado, J. F. Petry, J. Wendorff, C. L. Petzhold and P. Pranke. Effect of feeder free poly(lactide-co-glycolide) scaffolds on morphology, proliferation, and pluripotency of mouse embryonic stem cells. *J Biomed Mater Res A* 105: 424-432, 2017.

Hao H. H., L. Wang, Z. J. Guo, L. Bai, R. P. Zhang, W. B. Shuang, Y. J. Jia, J. Wang, X. Y. Li and Q. Liu. Valproic acid reduces autophagy and promotes functional recovery after spinal cord injury in rats. *Neurosci Bull* 29: 484-492, 2013.

Hassan A., B. M. Arnold, S. Caine, B. M. Toosi, V. M. K. Verge and G. D. Muir. Acute intermittent hypoxia and rehabilitative training following cervical spinal injury alters neuronal hypoxia- and plasticity-associated protein expression. *PLoS One* 13: e0197486, 2018.

Hou X. Q., R. Yan, C. Yang, L. Zhang, R. Y. Su, S. J. Liu, S. J. Zhang, W. Q. He, S. H. Fang, S. Y. Cheng, Z. R. Su, Y. B. Chen and Q. Wang. A novel assay for high-throughput screening of anti-Alzheimer's disease drugs to determine their efficacy by real-time monitoring of changes in PC12 cell proliferation. *Int J Mol Med* 33: 543-549, 2014.

Ishiyama M., Y. Miyazono, K. Sasamoto, Y. Ohkura and K. Ueno. A highly water-soluble disulfonated tetrazolium salt as a chromogenic indicator for NADH as well as cell viability. *Talanta* 44: 1299-1305, 1997.

Jiang Y. N., H. Y. Mo and D. G. Yu. Electrospun drug-loaded core-sheath PVP/zein nanofibers for biphasic drug release. *Int J Pharm* 438: 232-239, 2012.

Jiao G., Y. Pan, C. Wang, Z. Li and R. Guo. A bridging SF/Alg composite scaffold loaded NGF for spinal cord injury repair. *Mater Sci Eng C Mater Biol Appl* 76: 81-87, 2017.

Johnson C. D., A. R. D'Amato and R. J. Gilbert. Electrospun Fibers for Drug Delivery after Spinal Cord Injury and the Effects of Drug Incorporation on Fiber Properties. *Cells Tissues Organs* 202: 116-135, 2016.

Kang C. E., M. D. Baumann, C. H. Tator and M. S. Shoichet. Localized and sustained delivery of fibroblast growth factor-2 from a nanoparticle-hydrogel composite for treatment of spinal cord injury. *Cells Tissues Organs* 197: 55-63, 2013.

Kim M. S., H. H. Ahn, Y. N. Shin, M. H. Cho, G. Khang and H. B. Lee. An in vivo study of the host tissue response to subcutaneous implantation of PLGA- and/or porcine small intestinal submucosa-based scaffolds. *Biomaterials* 28: 5137-5143, 2007.

Lee J. Y., H. S. Kim, H. Y. Choi, T. H. Oh, B. G. Ju and T. Y. Yune. Valproic acid attenuates blood-spinal cord barrier disruption by inhibiting matrix metalloprotease-9 activity and improves functional recovery after spinal cord injury. *J Neurochem* 121: 818-829, 2012.

Lee J. Y., S. Maeng, S. R. Kang, H. Y. Choi, T. H. Oh, B. G. Ju and T. Y. Yune. Valproic acid protects motor neuron death by inhibiting oxidative stress and endoplasmic reticulum stress-mediated cytochrome C release after spinal cord injury. *J Neurotrauma* 31: 582-594, 2014.

Liu C., Y. Huang, M. Pang, Y. Yang, S. Li, L. Liu, T. Shu, W. Zhou, X. Wang, L. Rong and B. Liu. Tissue-engineered regeneration of completely transected spinal cord using induced neural stem cells and gelatin-electrospun poly (lactide-co-glycolide)/polyethylene glycol scaffolds. *PLoS One* 10: e0117709, 2015.

Llorens E., H. Ibañez, L. J. Del Valle and J. Puiggalí. Biocompatibility and drug release behavior of scaffolds prepared by coaxial electrospinning of poly(butylene succinate) and polyethylene glycol. *Mater Sci Eng C Mater Biol Appl* 49: 472-484, 2015.

Lu W. H., C. Y. Wang, P. S. Chen, J. W. Wang, D. M. Chuang, C. S. Yang and S. F. Tzeng. Valproic acid attenuates microgliosis in injured spinal cord and purinergic P2X4 receptor expression in activated microglia. *J Neurosci Res* 91: 694-705, 2013.

Lv L., Y. Sun, X. Han, C. C. Xu, Y. P. Tang and Q. Dong. Valproic acid improves outcome after rodent spinal cord injury: potential roles of histone deacetylase inhibition. *Brain Res* 1396: 60-68, 2011.

Makadia H. K. and S. J. Siegel. Poly Lactic-co-Glycolic Acid (PLGA) as Biodegradable Controlled Drug Delivery Carrier. *Polymers (Basel)* 3: 1377-1397, 2011.

Martini A. C., S. Forner, J. Koepp and G. A. Rae. Inhibition of spinal c-Jun-NH2-terminal kinase (JNK) improves locomotor activity of spinal cord injured rats. *Neurosci Lett* 621: 54-61, 2016.

Nguyen T. T., C. Ghosh, S. G. Hwang, N. Chanunpanich and J. S. Park. Porous core/sheath composite nanofibers fabricated by coaxial electrospinning as a potential mat for drug release system. *Int J Pharm* 439: 296-306, 2012.

Penas C., E. Verdú, E. Asensio-Pinilla, M. S. Guzmán-Lenis, M. Herrando-Grabulosa, X. Navarro and C. Casas. Valproate reduces CHOP levels and preserves oligodendrocytes and axons after spinal cord injury. *Neuroscience* 178: 33-44, 2011.

Roman J. A., I. Reucroft, R. A. Martin, A. Hurtado and H. Q. Mao. Local Release of Paclitaxel from Aligned, Electrospun Microfibers Promotes Axonal Extension. *Adv Healthc Mater* 5: 2628-2635, 2016.

Santhosh K. T., A. Alizadeh and S. Karimi-Abdolrezaee. Design and optimization of PLGA microparticles for controlled and local delivery of Neuregulin-1 in traumatic spinal cord injury. *J Control Release* 261: 147-162, 2017.

Sperling L. E., K. P. Reis, L. G. Pozzobon, C. S. Girardi and P. Pranke. Influence of random and oriented electrospun fibrous poly(lactic-co-glycolic acid) scaffolds on neural differentiation of mouse embryonic stem cells. *J Biomed Mater Res A* 2017.

Sperling L. E., K. P. Reis, P. Pranke and J. H. Wendorff. Advantages and challenges offered by biofunctional core-shell fiber systems for tissue engineering and drug delivery. *Drug Discov Today* 21: 1243-1256, 2016.

Steffens D., M. B. Mathor, B. T. Santi, D. P. Luco and P. Pranke. Development of a biomaterial associated with mesenchymal stem cells and keratinocytes for use as a skin substitute. *Regen Med* 10: 975-987, 2015.
Stokols S. and M. H. Tuszynski. The fabrication and characterization of linearly oriented nerve guidance scaffolds for spinal cord injury. *Biomaterials* 25: 5839-5846, 2004.

Teng Y. D., E. B. Lavik, X. Qu, K. I. Park, J. Ourednik, D. Zurakowski, R. Langer and E. Y. Snyder. Functional recovery following traumatic spinal cord injury mediated by a unique polymer scaffold seeded with neural stem cells. *Proc Natl Acad Sci U S A* 99: 3024-3029, 2002.

Valenzuela V., E. Collyer, D. Armentano, G. B. Parsons, F. A. Court and C. Hetz. Activation of the unfolded protein response enhances motor recovery after spinal cord injury. *Cell Death Dis* 3: e272, 2012.

Vigani B., S. Rossi, G. Sandri, M. C. Bonferoni and F. Ferrari. Design and criteria of electrospun fibrous scaffolds for the treatment of spinal cord injury. *Neural Regen Res* 12: 1786-1790, 2017.

Wang D., Y. Fan and J. Zhang. Transplantation of Nogo-66 receptor gene-silenced cells in a poly(D,L-lactic-co-glycolic acid) scaffold for the treatment of spinal cord injury. *Neural Regen Res* 8: 677-685, 2013.

Wang J., L. Tian, L. He, N. Chen, S. Ramakrishna, K. F. So and X. Mo. Lycium barbarum polysaccharide encapsulated Poly lactic-co-glycolic acid Nanofibers: cost effective herbal medicine for potential application in peripheral nerve tissue engineering. *Sci Rep* 8: 8669, 2018.

Xia T., S. Ni, X. Li, J. Yao, H. Qi, X. Fan and J. Wang. Sustained delivery of dbcAMP by poly(propylene carbonate) micron fibers promotes axonal regenerative sprouting and functional recovery after spinal cord hemisection. *Brain Res* 1538: 41-50, 2013.

Yao S., S. Yu, Z. Cao, Y. Yang, X. Yu, H. Q. Mao, L. N. Wang, X. Sun, L. Zhao and X. Wang. Hierarchically aligned fibrin nanofiber hydrogel accelerated axonal regrowth and locomotor function recovery in rat spinal cord injury. *Int J Nanomedicine* 13: 2883-2895, 2018.

Yu S. H., D. C. Cho, K. T. Kim, K. H. Nam, H. J. Cho and J. K. Sung. The neuroprotective effect of treatment of valproic Acid in acute spinal cord injury. *J Korean Neurosurg Soc* 51: 191-198, 2012.

Zamani F., M. Amani-Tehran, M. Latifi, M. A. Shokrgozar and A. Zaminy. Promotion of spinal cord axon regeneration by 3D nanofibrous core-sheath scaffolds. *J Biomed Mater Res A* 102: 506-513, 2014.

Zhu M. M., H. L. Li, L. H. Shi, X. P. Chen, J. Luo and Z. L. Zhang. The pharmacogenomics of valproic acid. *J Hum Genet* 62: 1009-1014, 2017.

Zuo W., M. Zhu, W. Yang, H. Yu, Y. Chen and Z. Yu. Experimental Study on Relationship Between Jet Instability and Formation of Beaded Fibers During Electrospinning. *POLYMER ENGINEERING AND SCIENCE* 704-709, 2005.

6. Discussão

O presente trabalho teve como objetivo o desenvolvimento de biomateriais para utilização no tratamento da lesão da medula espinal (LME). A LME é um grave problema de saúde pública e significa, para o paciente, o confinamento a uma cadeira de rodas e uma vida inteira de cuidados médicos constantes. A LME é uma importante causa de morbidade e mortalidade e envolve altos custos relacionados ao tratamento e à reabilitação dessa condição. Além disso, o fato de afetar principalmente indivíduos na faixa etária economicamente ativa (e destes, em sua maioria do sexo masculino), gera um outro conjunto de questões, pois é necessário conviver com disfunções motoras, sensoriais e autonômicas limitantes, com consequências econômicas e psicossociais (Castro *et al.*, 2015).

Atualmente, não há tratamento efetivo para essa condição. Tratamentos utilizados atualmente incluem a cirurgia de descompressão e a administração de metilprednisolona (Ahuja *et al.*, 2017; Ziemba e Gilbert, 2017). Diversos ensaios clínicos têm sido realizados utilizando agentes farmacológicos, mas nenhum destes demonstrou regulação efetiva da regeneração axonal (Ziemba e Gilbert, 2017). Portanto, é urgente a busca de novos tratamentos e fármacos com maior efetividade para o tratamento da LME. O uso de estratégias da medicina regenerativa são promissoras na busca pelo reparo no local da lesão (Kim *et al.*, 2014).

Neste estudo, dois tipos de *scaffolds* foram desenvolvidos pela técnica de eletrofiação coaxial para uso no tratamento da LME. No artigo do capítulo I foi descrito o estudo realizado com a utilização de microfibras de poli(ácido lático-co-ácido glicólico) (PLGA) contendo o fator de crescimento de fibroblastos 2 (FGF-2). Já no artigo do capítulo II, um estudo similar foi realizado com microfibras contendo outra substância bioativa, o ácido valpróico (VPA).

Padronização do biomaterial

A fim de encontrar os parâmetros adequados para a realização da eletrofiação coaxial, diversos testes foram realizados, incluindo a escolha do solvente adequado, concentração do polímero, temperatura, umidade e distância da agulha à placa coletora. A escolha do solvente iniciou por testes utilizando diclorometano e etanol, tetraidrofurano/dimetilformamida, 2,2,3,3-tetrafluoro-1-propanol. Por fim, o solvente que ofereceu maior estabilidade ao procedimento, com fibras uniformes e reprodutíveis foi o 1,1,1,3,3,3-Hexafluoro-2-propanol. A concentração do polímero influencia a viscosidade da solução, bem como o diâmetro das fibras. Duas

concentrações de PLGA foram testadas: 12% e 18%. Nas duas concentrações, foi possível obter fibras uniformes, porém na concentração de 12% de PLGA não foi possível obter reprodutibilidade das fibras. A escolha da temperatura e umidade só foi possível devido a uma das principais vantagens do aparelho de eletrofiação utilizado nesse estudo (IME Technologies, Holanda), que é o controle dessas duas variáveis. Em geral, os equipamentos utilizados nesse processo não possuem uma cabine fechada, portanto, o desenvolvimento da técnica é extremamente influenciada por variáveis ambientais. Por fim, os parâmetros escolhidos, que ofereceram maior estabilidade ao processo de eletrofiação coaxial, bem como fibras contínuas e uniformes foram: 18% de concentração de PLGA em hexafluoro-2-propanol e clorofórmio (3:1), 22°C, 45% de umidade, tensão de 16 à 25 kV e 15 centímetros de distância da agulha até a placa coletora.

O polímero escolhido para produção da parte externa das fibras foi o PLGA, devido a sua biodegradabilidade e biocompatibilidade (Jaworek e Sobczyk, 2008; Danhier *et al.*, 2012), uma vez que durante a sua degradação não há a formação de moléculas tóxicas (Makadia e Siegel, 2011; Ranjbar-Mohammadi *et al.*, 2016; Li *et al.*, 2017; Naves *et al.*, 2017). O PLGA sofre hidrólise *in vivo* que leva à formação de monômeros biodegradáveis, o ácido lático e o ácido glicólico (Kumari *et al.*, 2010). Esses metabólitos entram para o ciclo de Krebs e são eliminados como dióxido de carbono e água (Paul *et al.*, 2013). Já o polietilenogliocol (PEG) foi o polímero de escolha para ser adicionado à solução do núcleo das fibras, pois aumenta a viscosidade da solução aquosa, estabiliza os parâmetros do processo e também aumenta a estabilidade do fator de crescimento (Jiang *et al.*, 2005; Zhang *et al.*, 2006; Ji *et al.*, 2010).

As fibras produzidas nesse estudo apresentaram morfologia uniforme e sem a formação de *beads* (figura 1, capítulo I e figura 1, capítulo II). A presença de *beads*, ou seja, fibras com formato semelhante a um colar de pérolas, é considerada uma característica indesejada na formação das fibras, pois são associadas à presença de instabilidades no processo de eletrofiação (Zuo *et al.*, 2005). Não houve aumento significativo no diâmetro das microfibras após a incorporação de substâncias no core, pois houve aumento da voltagem afim de manter a estabilidade do processo. Estudos *in vitro* que investigaram o efeito do diâmetro das fibras, em escala nano a micro, mostraram que um crescimento de neuritos mais robusto foi induzido em fibras com diâmetros na faixa de poucos micrometros (1-2 μm), se comparado a *scaffolds* nanofibrosos (Johnson *et al.*, 2016; Kennedy *et al.*, 2017). Além disso, micro e nanofibras exibem uma grande área de superfície em relação ao volume que fazem dela eficientes sistemas de entrega para moléculas neuroprotetoras. Essas propriedades morfológicas garantem que

quaisquer compostos bioquímicos (como fármacos e/ou fatores de crescimento) incorporados na matriz dessas fibras possam ser eficientemente liberados no local da lesão e otimizar o contato entre as fibras e as células danificadas, favorecendo a absorção química (Cao *et al.*, 2009).

O valor do ângulo de contato dos *scaffolds* produzidos por eletrofiação coaxial foi similar ao valor encontrado nas fibras produzidas apenas com PLGA por eletrofiação tradicional (figura 2, capítulo II). Os valores encontrados demonstram a natureza hidrofóbica do PLGA e são similares aos reportados em estudos prévios (Kim, M. S. *et al.*, 2007; Park *et al.*, 2010; Yang *et al.*, 2015). Esse resultado demonstra que não houve extravasamento do conteúdo aquoso interno das fibras e indica a adequada formação da estrutura núcleo-casca das microfibras (Nguyen *et al.*, 2012).

A microscopia confocal foi utilizada para visualizar e verificar a distribuição do conteúdo interno (*core*) das microfibras (figura 2, capítulo I e figura 2, capítulo II). Porém, com essa metodologia, não é possível detectar claramente os dois componentes estruturais das microfibras (casca/núcleo), devido ao diâmetro das fibras e a resolução do microscópio confocal (Willerth e Sakiyama-Elbert, 2007; Danhier *et al.*, 2012; Santhosh *et al.*, 2017). Para isso, foi utilizada a microscopia eletrônica de transmissão, com a qual foi possível confirmar a estrutura núcleo/casca das microfibras (figura 2, capítulo I).

As propriedades mecânicas dos *scaffolds* são importantes devido as forças que esse biomaterial deve suportar, quando aplicados na engenharia de tecidos *in vivo* (Fu *et al.*, 2014). Além disso, os biomateriais devem exibir propriedades mecânicas similares ao tecido nativo (Vigani *et al.*, 2017). A média do valor encontrado para o módulo de Young, tanto para as microfibras PLGA/FGF-2 e PLGA/VPA, foi ao redor de ~2MPa. Esse valor é similar ao reportado por Bilston e Thibault, em 1996, em que foram obtidas medulas da autópsia de cadáveres humanos e o tecido apresentou um valor do Modulo de Young ao redor de 1,37 MPa (Bilston e Thibault, 1996). A resistência mecânica do biomaterial é crítica para a integração bem sucedida do *scaffold* no tecido circundante, bem como para afetar a função celular. No caso de materiais que são muito rígidos, a diferença nas propriedades mecânicas entre o implante e o tecido da medula espinal pode causar compressão dos axônios em regeneração, e cistos entre o implante e o tecido da medula espinal circundante podem ser formados após o implante, assim como um *scaffold* excessivamente rígido não se ajusta adequadamente à forma

da cavidade da lesão (Kubinová e Syková, 2012). Isso demonstra o potencial das microfibras produzidas nesse estudo para uso na regeneração da LME.

Fator de crescimento de fibroblastos 2 (FGF-2)

O FGF-2 foi incorporado em microfibras de PLGA através da técnica de eletrofiação coaxial. Houve uma rápida liberação inicial dessa substância, em 8 horas de incubação (figura 3, capítulo I). Essa rápida liberação é denominada "efeito *burst*", cujo achado está de acordo com os resultados obtidos em outros estudos, onde fibras com estrutura núcleo-casca foram produzidas (Jiang *et al.*, 2012). Em alguns sistemas de liberação de drogas, esse efeito é indesejado. No entanto, é uma boa estratégia no tratamento da fase aguda da LME, contribuindo para atenuar os eventos secundários e respostas celulares específicas, como a inflamação (Johnson *et al.*, 2016; Faccendini *et al.*, 2017), principalmente pela presença da droga próximo à superfície da fibra. Nguyen e colaboradores, em 2006, observaram que o aumento no fluxo da parte interna da fibra durante o processo de eletrofiação levava à redução da espessura da camada polimérica externa (casca - *shell*) das fibras e, assim, contribuía para a ocorrência do efeito *burst*.

A linhagem de células PC12 foi utilizada para avaliar o comportamento das células sobre as microfibras e o potencial de aplicação desses *scaffolds* de microfibras como implantes biocompatíveis. Essa é uma das linhagens celulares de escolha para estudo de biomateriais que visam a regeneração de tecidos do SNC (Genchi *et al.*, 2015; Zhang *et al.*, 2016; Heidari *et al.*, 2017). Através do ensaio MTT demonstrou-se que as células PC12 aderiram, proliferaram e se espalharam sobre as microfibras após 3 e 7 dias de cultura. Todos os grupos de células estudados apresentaram viabilidade similar no terceiro dia de cultivo, indicando que não houve diferença na habilidade das células em aderirem ao biomaterial. No entanto, no sétimo dia de cultivo, a viabilidade das células cultivadas sobre os *scaffolds* foi menor quando comparada ao filme de PLGA. Esse resultado provavelmente está relacionado a diferenças na topografia da superfície entre as microfibras e o filme de PLGA. O aumento na área de contato entre as células e a superfície do material pode ser observada pelas imagens de MEV (figura 5, capítulo I). Essa diferença na topografia do material é confirmada pela redução na medida do ângulo de contato no filme (figura 3, capítulo I) (Abdelsalam *et al.*, 2005).

Já foi demonstrado que o FGF-2 promove a diferenciação das células PC12 em fenótipo neuronal (Ohuchi *et al.*, 2002; Nabiuni *et al.*, 2012) provocando, portanto, o aumento de marcadores neuronais, como a β–III tubulina (Ohuchi *et al.*, 2002). Nesse trabalho, foi observado o aumento da expressão, mas com uma variabilidade entre as culturas celulares (figura 7, capítulo I), o que é típico nesse tipo de ensaio celular (Chew *et al.*, 2005). Não obstante, esse experimento indicou que o FGF2 liberado das fibras retiveram algum grau de bioatividade do FGF-2. Além disso, na presença de FGF-2 as células param a sua divisão celular (Attiah *et al.*, 2003). Isso é correlacionado com o presente estudo, onde houve redução da viabilidade celular aos 7 dias com tratamento com meio condicionado PLGA/FGF-2 (figura 8, capítulo I). Portanto, os resultados da expressão de β–III tubulina e da redução da viabilidade celular indicam que o FGF-2 manteve sua bioatividade.

Para avaliação do efeito das microfibras no tratamento da LME, os *scaffolds* foram implantados em um modelo animal de lesão medular por hemisecção. Através da marcação com hematoxilina e eosina foi possível observar a presença do *scaffold* no local da lesão 6 semanas após a LME. Os *scaffolds* integraram-se ao local da lesão sem apresentar sinais óbvios de citotoxicidade que pudessem refletir em perda de tecido e formação de cavidades (figura 9, capítulo I). A presença do biomaterial no local da lesão é importante para fornecer suporte à regeneração tecidual em modelo animal de LME, considerando que o período de três à seis meses é necessário para conquistar a regeneração funcional (Schaub *et al.*, 2016). Ou seja, a degradação do *scaffold* deve ocorrer concomitante ao período em que o tecido nervoso torne-se maduro o suficiente para se auto sustentar (Maquet *et al.*, 2001) e também não deve ter uma degradação muito rápida, para evitar a invasão de tecido conetivos, o que pode reduzir a regeneração (Oudega *et al.*, 2001). No entanto, o tempo ótimo para a degradação do *scaffold* no contexto do reparo da LME, ainda não foi estudado em detalhes.

A atividade locomotora dos animais foi avaliada durante seis semanas, com a utilização da escala BBB (Basso *et al.*, 1995). No segundo dia após a lesão, a locomoção dos animais foi aferida em vista de avaliar os déficits locomotores e, assim, verificar se o modelo de hemisecção foi bem-sucedido. A função da pata posterior ipsilateral foi prejudicada gravemente após a LME; enquanto o membro posterior contralateral também foi inevitavelmente afetado (figura 8 capítulo I e figura 6, capítulo II). Os animais que não apresentaram sinais consistentes de LME foram excluídos do estudo. Em todos os grupos observou-se melhora locomotora espontânea ao longo das seis semanas de avaliação. Esses resultados são similares aos de estudos realizados com esse mesmo modelo de LME por hemisecção (Pertici *et al.*, 2014; Shi

et al., 2014). Alguma recuperação da função locomotora após lesão pode ser observada em pacientes e modelos animais (Ballermann e Fouad, 2006) e está relacionada principalmente com a neuroplasticidade da medula espinal e ao recrutamento lateral (Ballermann e Fouad, 2006).

Em relação aos achados do teste BBB no primeiro estudo (capítulo I), no sétimo dia após a lesão houve uma tendência a melhora locomotora no grupo que recebeu a injeção de FGF-2 diretamente no local da lesão. No entanto, essa tendência diminuiu aos 35 dias e, finalmente, reduziu aos 42 dias. Isso ocorreu provavelmente porque uma única injeção de FGF-2 deve ter atuado em eventos iniciais da lesão, como por exemplo, provando a redução da permeabilidade da BHE, inibindo rotas que levam à apoptose neuronal e minimizando a inflamação (Zhou *et al.*, 2018). Porém, devido a vulnerabilidade desse fator de crescimento à degradação, seu efeito não foi sustentado ao longo das semanas após a LME.

Além disso, os resultados demonstram que os *scaffolds* de PLGA/FGF-2 foram efetivos em promover melhora locomotora 28 dias após a LME. No entanto, esse resultado foi similar ao grupo que recebeu o implante de microfibras de PLGA sem o fator de crescimento. A adição de FGF-2 nas microfibras não teve efeito melhor que apenas o *scaffold* de PLGA na melhora locomotora dos animais com LME. Esses resultados sugerem que uma pequena quantidade de FGF-2 foi liberada das microfibras. Esses resultados são consistentes com os dados já publicados, os quais demonstraram que o uso de *scaffolds* de fibras, em modelo de rato com lesão medular por hemisecção, foi suficiente para promover melhora locomotora dos animais (Teng *et al.*, 2002; Zamani *et al.*, 2014).

A análise por imunohistoquímica, através da marcação com DAPI, foi possível observar a infiltração de células no *scaffolds* utilizados no estudo. Também, foi possível observar que os *scaffolds* foram infiltrados por alguns astrócitos, através da marcação com anticorpo anti-GFAP. Além disso, diversas fibras neurais imunopositivas para βIII tubulina foram observadas atravessando o *scaffold* (figura 11, capítulo I).

A redução da cicatriz glial é crucial para a regeneração axonal e para a melhora locomotora (Xia *et al.*, 2017). A expressão de GFAP foi significativamente reduzida nos grupos que receberam o implante dos *scaffold*s nos grupos onde utilizou-se PLGA e FGF-2/PLGA, comparado ao grupo controle lesão, seis semanas após a LME (figura 10, capítulo I). Esse resultado é um indicativo da redução da cicatriz glial nesses grupos. Teng e colaboradores, em 2002, hipotetizaram que a presença do *scaffold* pode prevenir a formação da cicatriz glial

possivelmente pela inibição do crescimento celular (Teng *et al.*, 2002). Esse resultado sugere que a presença dos *scaffolds* de microfibras reduziu a formação da cicatriz glial.

Ácido valpróico (VPA)

Pela primeira vez, o VPA foi encapsulado em microfibras de PLGA através da eletrofiação coaxial. Houve uma rápida liberação do VPA, efeito *burst* entre uma hora e seis horas do teste de liberação em que cerca de 80% da substância encapsulada nos *scaffolds* foi liberada no meio (figura 3, capítulo II). Além disso, em 24 horas houve liberação de cerca de 91% do total de VPA encapsulado nas microfibras. Como citado no estudo do capítulo 1, essa liberação inicial é uma boa estratégia no tratamento da fase aguda da LME, contribuindo para atenuar os eventos secundários e respostas celulares específicas, como a inflamação (Johnson *et al.*, 2016; Faccendini *et al.*, 2017).

Uma das limitações do teste MTT é a adsorção dos cristais de formazan no interior dos poros das fibras de PLGA (Qi *et al.*, 2011). Além disso, esse é um método destrutivo de determinação da viabilidade celular e, por provocar a ruptura das membranas celulares, não permite que essas mesmas células sejam sujeitas a novas análises. Por isso, nos estudos da atividade metabólica celular do capítulo II, foi escolhido o ensaio WST-8. Com esse ensaio é possível determinar a viabilidade celular de forma não-destrutiva, permitindo que as células analisadas sejam utilizadas para investigações adicionais, como, por exemplo, para a visualização das células por microscopia (Stoddart, 2011).

No teste de viabilidade celular, como grupo controle, foram utilizadas células cultivadas diretamente no poço placa. O grupo controle apresentou maior absorbância quando comparado com os outros grupos, indicando um número maior de células nos poços das placas de cultura. Esse resultado era esperado e de acordo com resultados prévios (Steffens *et al.*, 2015; Galuppo *et al.*, 2017), já que o poço das placas tem um formato 2D e é a forma convencional de cultivar células. Já nos grupos *scaffolds*, houve redução da viabilidade celular nas células cultivadas sobre as microfibras contendo VPA (figura 5, capítulo II). As células PC12 são células neoplásicas neuroendócrinas (Adler *et al.*, 2008). Adler e colaboradores, em 2008, estudaram o efeito do VPA na inibição do crescimento das células PC12 para a utilização desse fármaco no tratamento de feocromocitomas (neoplasias formadas por esse tipo celular). Dessa forma, os autores demonstraram que o tratamento das células PC12 com VPA realmente provocou a

inibição do crescimento desse tipo celular por ativação da apoptose celular. Da mesma maneira, no presente estudo, as células cultivadas sobre os as microfibras contendo VPA apresentaram menor viabilidade celular comparadas às células cultivadas sobre o *scaffold* controle, sendo esse um indicativo da manutenção da bioatividade dessa substância após ser encapsulada nas microfibras.

Os *scaffolds* produzidos foram implantados em um modelo animal de lesão medular por hemisecção para avaliação do efeito das microfibras no tratamento da LME. Após seis semanas da LME, os animais foram eutanasiados e, durante a remoção da medula espinal, foi possível observar a presença do *scaffold* no local implantado. Em alguns animais o biomaterial estava aderido no tecido cicatricial anterior e não foi possível removê-los em conjunto com o tecido da medula espinal. Por essa razão, nas imagens por HE, não se observa a presença do biomaterial no local da lesão (figura 6, capítulo II).

Da mesma forma como no capítulo I desse estudo, a atividade locomotora dos animais foi avaliada durante seis semanas com a utilização da escala BBB (Basso *et al.*, 1995). A locomoção dos animais no segundo dia após a LME demonstrou que o modelo de hemisecção foi bem-sucedido. A função da pata posterior ipsilateral foi prejudicada gravemente após a LME; enquanto o membro posterior contralateral também foi inevitavelmente afetado. Também, foi possível observar melhora locomotora espontânea em todos os grupos estudados, ao longo das seis semanas. Assim como nos resultados demonstrados no capítulo I, as médias dos valores da escala BBB encontrado no grupo PLGA *scaffold* foram similares. No entanto, nesse estudo do capítulo II, não houve diferença estatística significativa entre os grupos estudados. Isso se deve ao maior desvio padrão observado dentro desse experimento. Porém, foi possível observar tendência à melhora no grupo que recebeu o implante dos *scaffolds* especialmente a partir dos 28 dias após a lesão (figura 6, capítulo II).

Os resultados experimentais obtidos nesse estudo fornecem base para futuras estratégias destinadas ao tratamento da LME. A utilização de terapias combinadas oferece vantagens sinérgicas suplementares em uma abordagem multidisciplinar no tratamento da LME. Várias combinações de estratégias incluindo *scaffolds*, substâncias bioativas e células ainda devem ser realizadas para encontrar-se qual a combinação mais efetiva para o tratamento dessa condição. Portanto, esse trabalho representa uma parcela dos diversos estudos que visam encontrar a terapia ideal para a LME.

A interação entre os *scaffolds* e células podem ser aperfeiçoadas por modificações na estrutura da superfície das fibras, por exemplo, com a inclusão de proteínas de reconhecimento celular como colágeno, laminina, fibronectina que podem aumentar a bioatividade dos biomateriais (Sperling *et al.*, 2016). Métodos químicos também podem ser utilizados para modificar a superfície dos *scaffolds* e aumentar sua hidrofilicidade, como o tratamento utilizando hidróxido de sódio (Sperling *et al.*, 2017).

Além da utilização de biomateriais funcionalizados e contendo substâncias bioativas, podem-se incluir células cultivadas sobre os *scaffolds*. A terapia celular é uma das estratégias promissoras para o tratamento da LME. Estudo pré-clínicos demonstraram que o uso de transplante de células pode amenizar alguns eventos secundários através da neuroproteção e também da regeneração do tecido lesado. Diversos tipos celulares têm sido estudados no tratamento da lesão da medula espinal, como células-tronco derivadas de dentes decíduos (Nicola *et al.*, 2017; Nicola *et al.*, 2018), células olfativas (Tabakow *et al.*, 2013) e células de Schwann (Pearse *et al.*, 2018). O principal desafio do terapia celular é a busca da fonte de células ideal, porém o progresso contínuo na tecnologia de células-tronco permitirá a produção de linhagens celulares específicas ou células-tronco autólogas que podem vir a ser usadas com segurança em pacientes (Kubinová e Syková, 2012).

Além do desenvolvimento de tratamento mais efetivos, a utilização de avaliações mais específicas para determinar a recuperação do tecido podem elucidar outros mecanismos relacionados à progressão da lesão e levar ao desenvolvimento de novas estratégias de tratamento. Por exemplo, pela utilização da ressonância magnética nuclear é possível visualizar mudanças estruturais durante o período de recuperação *in vivo*. Também a ressonância magnética por tensor de difusão, um avanço da ressonância magnética, permite caracterizar e avaliar os danos à substância branca após a LME em humanos e em animais a qual permite avaliar a regeneração e a remielinização (Sakiyama-Elbert *et al.*, 2012). Essas técnicas também permitem verificar a reprodutibilidade das novas terapias abrindo caminho para aplicações clínicas mais seguras e eficientes aos pacientes (Dalamagkas *et al.*, 2018). Além disso, no futuro, com o uso de ferramentas da bioengenharia será possível prever e antecipar os resultados de tratamentos e mudar o caminho translação dos resultados, acelerando o processo de aprovação de medicamentos e a implementação de novos tratamentos na clínica.

Por fim, um dos desafios no estudo do tratamento da LME é determinar a terapia mais efetiva em diferentes estágios, após a ocorrência da lesão. A maioria dos estudos foca no

tratamento da fase aguda da LME. Poucos trabalhos comparam a efetividade de um tratamento em diferentes períodos e qual seria a fase mais adequada para a utilização de uma determinada terapia. Portanto, o tempo entre a lesão e início do tratamento é um importante fator a ser estudado e otimizado para maximizar a recuperação dos pacientes com lesão medular (Wang *et al.*, 2011).

Assim como já foi demonstrado no tratamento de outras patologias, o futuro da terapia da LME está na combinação e interação entre substâncias bioativas, biomateriais e células para que, na soma de seus efeitos, levem a melhora e recuperação após a lesão medular do paciente.

7. Conclusões

- As substâncias bioativas, fator de crescimento de fibroblastos 2 (FGF-2) e ácido valpróico (VPA), foram encapsuladas com sucesso em *scaffolds* de microfibras através da técnica de eletrofiação coaxial;

- Os *scaffolds* apresentaram características morfológicas e propriedades mecânicas adequadas à aplicação na regeneração da lesão da medula espinal (LME);

- As substâncias foram liberadas das microfibras apresentando um efeito *burst* nas primeiras horas dos testes *in vitro*. O FGF-2 estava presente no meio de liberação pelo período analisado de 30 dias. Enquanto 80% do VPA foi liberado nas primeiras seis horas do teste de liberação e a substância ainda foi encontrada no meio pelo período do teste, 14 dias.

- Os *scaffolds* permitiram a adesão e proliferação das células PC12 em ensaios *in vitro*. Foi observada uma tendência ao aumento na expressão de β-III tubulina das células. Já as células cultivadas sobre os *scaffolds* contendo o VPA apresentaram redução na viabilidade celular, sendo um indicativo da bioatividade dessa substância.

- Os animais que receberam o implante dos *scaffolds* de microfibras não apresentaram melhora locomotora na análise do teste BBB, mas uma melhora pontual foi observada 28 dias após a lesão;

- A análise morfológica, 6 semanas após a lesão medular, demonstrou que os *scaffolds* implantados integraram-se ao local da lesão. Não houve diferença na expressão dos marcadores neurais: nestina, GFAP, CD68 e β-III tubulina.

8. Perspectivas

Como perspectivas futuras na continuação desse trabalho, pretende-se aumentar a eficiência de encapsulamento e o período de liberação das substâncias bioativas estudadas. Também realizar tratamentos químicos na superfície dos *scaffolds* para aumentar o caráter hidrofílico do biomaterial. Além disso, cultivar células-tronco mesenquimais nos *scaffolds* para serem implantados no modelo de lesão *in vivo*. Por fim, analisar a expressão de diferentes marcadores de tecido neural para verificar a neuroregeneração e a redução da gliose no local da lesão.

9. Referências bibliográficas

ABDANIPOUR, A.; SCHLUESENER, H. J.; TIRAIHI, T. Effects of valproic acid, a histone deacetylase inhibitor, on improvement of locomotor function in rat spinal cord injury based on epigenetic science. **Iran Biomed J,** v. 16, n. 2, p. 90-100, 2012. ISSN 2008-823X. Disponível em: < https://www.ncbi.nlm.nih.gov/pubmed/22801282 >.

ABDELSALAM, M. E. et al. Wetting of regularly structured gold surfaces. **Langmuir,** v. 21, n. 5, p. 1753-7, Mar 2005. ISSN 0743-7463. Disponível em: < https://www.ncbi.nlm.nih.gov/pubmed/15723469 >.

ADLER, J. T. et al. Histone deacetylase inhibitors upregulate Notch-1 and inhibit growth in pheochromocytoma cells. **Surgery,** v. 144, n. 6, p. 956-61; discussion 961-2, Dec 2008. ISSN 1532-7361. Disponível em: < https://www.ncbi.nlm.nih.gov/pubmed/19041003 >.

Advancing regenerative medicine. **Nat Med,** v. 20, n. 8, p. 795, Aug 2014. ISSN 1546-170X. Disponível em: < https://www.ncbi.nlm.nih.gov/pubmed/25100512 >.

AHUJA, C. S. et al. Traumatic spinal cord injury. **Nat Rev Dis Primers,** v. 3, p. 17018, Apr 2017. ISSN 2056-676X. Disponível em: < https://www.ncbi.nlm.nih.gov/pubmed/28447605 >.

ATTIAH, D. G.; KOPHER, R. A.; DESAI, T. A. Characterization of PC12 cell proliferation and differentiation-stimulated by ECM adhesion proteins and neurotrophic factors. **J Mater Sci Mater Med,** v. 14, n. 11, p. 1005-9, Nov 2003. ISSN 0957-4530. Disponível em: < https://www.ncbi.nlm.nih.gov/pubmed/15348515 >.

BALLERMANN, M.; FOUAD, K. Spontaneous locomotor recovery in spinal cord injured rats is accompanied by anatomical plasticity of reticulospinal fibers. **Eur J Neurosci,** v. 23, n. 8, p. 1988-96, Apr 2006. ISSN 0953-816X. Disponível em: < https://www.ncbi.nlm.nih.gov/pubmed/16630047 >.

BANG, W. S. et al. Valproic Acid increases expression of neuronal stem/progenitor cell in spinal cord injury. **J Korean Neurosurg Soc,** v. 54, n. 1, p. 8-13, Jul 2013. ISSN 2005-3711. Disponível em: < https://www.ncbi.nlm.nih.gov/pubmed/24044073 >.

BASSO, D. M.; BEATTIE, M. S.; BRESNAHAN, J. C. A sensitive and reliable locomotor rating scale for open field testing in rats. **J Neurotrauma,** v. 12, n. 1, p. 1-21, Feb 1995. ISSN 0897-7151 (Print)

0897-7151 (Linking). Disponível em: < http://www.ncbi.nlm.nih.gov/pubmed/7783230 >.

BEATTIE, M. S. Inflammation and apoptosis: linked therapeutic targets in spinal cord injury. **Trends Mol Med,** v. 10, n. 12, p. 580-3, Dec 2004. ISSN 1471-4914. Disponível em: < https://www.ncbi.nlm.nih.gov/pubmed/15567326 >.

BILSTON, L. E.; THIBAULT, L. E. The mechanical properties of the human cervical spinal cord in vitro. **Ann Biomed Eng,** v. 24, n. 1, p. 67-74, 1996 Jan-Feb 1996. ISSN 0090-6964. Disponível em: < https://www.ncbi.nlm.nih.gov/pubmed/8669719 >.

BLAHETA, R. A.; CINATL, J. Anti-tumor mechanisms of valproate: a novel role for an old drug. **Med Res Rev,** v. 22, n. 5, p. 492-511, Sep 2002. ISSN 0198-6325. Disponível em: < https://www.ncbi.nlm.nih.gov/pubmed/12210556 >.

BYDON, M. et al. The current role of steroids in acute spinal cord injury. **World Neurosurg,** v. 82, n. 5, p. 848-54, Nov 2014. ISSN 1878-8769. Disponível em: < https://www.ncbi.nlm.nih.gov/pubmed/23454689 >.

CAO, H.; LIU, T.; CHEW, S. Y. The application of nanofibrous scaffolds in neural tissue engineering. **Adv Drug Deliv Rev,** v. 61, n. 12, p. 1055-64, Oct 2009. ISSN 1872-8294. Disponível em: < https://www.ncbi.nlm.nih.gov/pubmed/19643156 >.

CASTRO, D. et al. Spinal cord trauma patients treated in a tertiary

hospital in Palmas, BRAZIL. **Coluna/Columna,** v. 14, 2015.

CHAN, W. S. et al. Differential regulation of proliferation and neuronal differentiation in adult rat spinal cord neural stem/progenitors by ERK1/2, Akt, and PLCγ. **Front Mol Neurosci,** v. 6, p. 23, 2013. ISSN 1662-5099. Disponível em: < https://www.ncbi.nlm.nih.gov/pubmed/23986655 >.

CHASE, G. G.; VARABHAS, J. S.; RENEKER, D. H. New Methods to Electrospin Nanofibers. **Journal of Engineered Fibers and Fabrics,** v. 6, n. 3, p. 32 - 38, 2011.

CHEN, B. et al. Repair of spinal cord injury by implantation of bFGF-incorporated HEMA-MOETACL hydrogel in rats. **Sci Rep,** v. 5, p. 9017, Mar 2015. ISSN 2045-2322. Disponível em: < https://www.ncbi.nlm.nih.gov/pubmed/25761585 >.

CHEN, S. et al. Valproic acid attenuates traumatic spinal cord injury-induced inflammation via STAT1 and NF-κB pathway dependent of HDAC3. **J Neuroinflammation,** v. 15, n. 1, p. 150, May 2018. ISSN 1742-2094. Disponível em: < https://www.ncbi.nlm.nih.gov/pubmed/29776446 >.

CHERIYAN, T. et al. Spinal cord injury models: a review. **Spinal Cord,** v. 52, n. 8, p. 588-95, Aug 2014. ISSN 1476-5624. Disponível em: < https://www.ncbi.nlm.nih.gov/pubmed/24912546 >.

CHEW, S. Y. et al. Sustained release of proteins from electrospun biodegradable fibers. **Biomacromolecules,** v. 6, n. 4, p. 2017-24, 2005 Jul-Aug 2005. ISSN 1525-7797. Disponível em: < https://www.ncbi.nlm.nih.gov/pubmed/16004440 >.

CHOO, A. M. et al. Contusion, dislocation, and distraction: primary hemorrhage and membrane permeability in distinct mechanisms of spinal cord injury. **J Neurosurg Spine,** v. 6, n. 3, p. 255-66, Mar 2007. ISSN 1547-5654. Disponível em: < https://www.ncbi.nlm.nih.gov/pubmed/17355025 >.

CHUANG, D. M. et al. Multiple roles of HDAC inhibition in neurodegenerative conditions. **Trends Neurosci,** v. 32, n. 11, p. 591-601, Nov 2009. ISSN 1878-108X. Disponível em: < https://www.ncbi.nlm.nih.gov/pubmed/19775759 >.

COLELLO, R. J. et al. The incorporation of growth factor and chondroitinase ABC into an electrospun scaffold to promote axon regrowth following spinal cord injury. **J Tissue Eng Regen Med,** v. 10, n. 8, p. 656-68, 08 2016. ISSN 1932-7005. Disponível em: < https://www.ncbi.nlm.nih.gov/pubmed/23950083 >.

CORONA, B. T. et al. Regenerative medicine: basic concepts, current status, and future applications. **J Investig Med,** v. 58, n. 7, p. 849-58, Oct 2010. ISSN 1708-8267. Disponível em: < https://www.ncbi.nlm.nih.gov/pubmed/20683344 >.

DALAMAGKAS, K. et al. Translational Regenerative Therapies for Chronic Spinal Cord Injury. **Int J Mol Sci,** v. 19, n. 6, Jun 2018. ISSN 1422-0067. Disponível em: < https://www.ncbi.nlm.nih.gov/pubmed/29914060 >.

DANHIER, F. et al. PLGA-based nanoparticles: an overview of biomedical applications. **J Control Release,** v. 161, n. 2, p. 505-22, Jul 2012. ISSN 1873-4995. Disponível em: < https://www.ncbi.nlm.nih.gov/pubmed/22353619 >.

DARVISHI, M. et al. Decreased GFAP expression and improved functional recovery in contused spinal cord of rats following valproic acid therapy. **Neurochem Res,** v. 39, n. 12, p. 2319-33, Dec 2014. ISSN 1573-6903. Disponível em: < https://www.ncbi.nlm.nih.gov/pubmed/25205382 >.

DAVOODI, P. et al. Coaxial electrohydrodynamic atomization: microparticles for drug delivery applications. **J Control Release,** v. 205, p. 70-82, May 2015. ISSN 1873-4995. Disponível em: < https://www.ncbi.nlm.nih.gov/pubmed/25483422 >.

FACCENDINI, A. et al. Nanofiber Scaffolds as Drug Delivery Systems to Bridge Spinal Cord Injury. **Pharmaceuticals (Basel),** v. 10, n. 3, Jul 5 2017. ISSN 1424-8247 (Print)

1424-8247 (Linking). Disponível em: < http://www.ncbi.nlm.nih.gov/pubmed/28678209 >.

FEHLINGS, M. G. Editorial: recommendations regarding the use of methylprednisolone in acute spinal cord injury: making sense out of the controversy. **Spine (Phila Pa 1976),** v. 26, n. 24 Suppl, p. S56-7, Dec 2001. ISSN 0362-2436. Disponível em: < https://www.ncbi.nlm.nih.gov/pubmed/11805611 >.

FU, W. et al. Electrospun gelatin/PCL and collagen/PLCL scaffolds for vascular tissue engineering. **Int J Nanomedicine,** v. 9, p. 2335-44, 2014. ISSN 1178-2013. Disponível em: < https://www.ncbi.nlm.nih.gov/pubmed/24872696 >.

FURUYA, T. et al. Treatment with basic fibroblast growth factor-incorporated gelatin hydrogel does not exacerbate mechanical allodynia after spinal cord contusion injury in rats. **J Spinal Cord Med,** v. 36, n. 2, p. 134-9, Mar 2013. ISSN 1079-0268. Disponível em: < https://www.ncbi.nlm.nih.gov/pubmed/23809528 >.

GALUPPO, A. G. et al. Effect of feeder free poly(lactide-co-glycolide) scaffolds on morphology, proliferation, and pluripotency of mouse embryonic stem cells. **J Biomed Mater Res A,** v. 105, n. 2, p. 424-432, 02 2017. ISSN 1552-4965. Disponível em: < https://www.ncbi.nlm.nih.gov/pubmed/27684050 >.

GANAI, S. A.; RAMADOSS, M.; MAHADEVAN, V. Histone Deacetylase (HDAC) Inhibitors - emerging roles in neuronal memory, learning, synaptic plasticity and neural regeneration. **Curr Neuropharmacol,** v. 14, n. 1, p. 55-71, 2016. ISSN 1875-6190. Disponível em: < https://www.ncbi.nlm.nih.gov/pubmed/26487502 >.

GELAIN, F. Novel opportunities and challenges offered by nanobiomaterials in tissue engineering. **Int J Nanomedicine,** v. 3, n. 4, p. 415-24, 2008. ISSN 1178-2013. Disponível em: < https://www.ncbi.nlm.nih.gov/pubmed/19337410 >.

GENCHI, G. G. et al. PC12 neuron-like cell response to electrospun poly(3-hydroxybutyrate) substrates. **J Tissue Eng Regen Med,** v. 9, n. 2, p. 151-61, Feb 2015. ISSN 1932-7005. Disponível em: < https://www.ncbi.nlm.nih.gov/pubmed/23086861 >.

GERSTNER, T.; BELL, N.; KÖNIG, S. Oral valproic acid for epilepsy--long-term experience in therapy and side effects. **Expert Opin Pharmacother,** v. 9, n. 2, p. 285-92, Feb 2008. ISSN 1744-7666. Disponível em: < https://www.ncbi.nlm.nih.gov/pubmed/18201150 >.

GOEY, A. K. et al. Pharmacogenomics and histone deacetylase inhibitors. **Pharmacogenomics,** v. 17, n. 16, p. 1807-1815, Nov 2016. ISSN 1744-8042. Disponível em: < https://www.ncbi.nlm.nih.gov/pubmed/27767376 >.

GOLDSHMIT, Y. et al. Fgf2 improves functional recovery-decreasing gliosis and increasing radial glia and neural progenitor cells after spinal cord injury. **Brain Behav,** v. 4, n. 2, p. 187-200, Mar 2014. ISSN 2162-3279. Disponível em: < https://www.ncbi.nlm.nih.gov/pubmed/24683512 >.

HAO, H. H. et al. Valproic acid reduces autophagy and promotes functional recovery after spinal cord injury in rats. **Neurosci Bull,** v. 29, n. 4, p. 484-92, Aug 2013. ISSN 1995-8218. Disponível em: < https://www.ncbi.nlm.nih.gov/pubmed/23852559 >.

HEIDARI, M.; BAHRAMI, H.; RANJBAR-MOHAMMADI, M. Fabrication, optimization and characterization of electrospun poly(caprolactone)/gelatin/graphene nanofibrous mats. **Mater Sci Eng C Mater Biol Appl,** v. 78, p. 218-229, Sep 2017. ISSN 1873-0191. Disponível em: < https://www.ncbi.nlm.nih.gov/pubmed/28575978 >.

HROMADKA, M. et al. Nanofiber applications for burn care. **J Burn Care Res,** v. 29, n. 5, p. 695-703, 2008 Sep-Oct 2008. ISSN 1559-047X. Disponível em: < https://www.ncbi.nlm.nih.gov/pubmed/18779672 >.

HSU, C. Y.; DIMITRIJEVIC, M. R. Methylprednisolone in spinal cord injury: the possible mechanism of action. **J Neurotrauma,** v. 7, n. 3, p. 115-9, 1990. ISSN 0897-7151. Disponível em: < https://www.ncbi.nlm.nih.gov/pubmed/2258942 >.

ITOH, N. The Fgf families in humans, mice, and zebrafish: their evolutional processes and roles in development, metabolism, and disease. **Biol Pharm Bull,** v. 30, n. 10, p. 1819-25, Oct 2007. ISSN 0918-6158. Disponível em: < https://www.ncbi.nlm.nih.gov/pubmed/17917244 >.

ITOH, N.; ORNITZ, D. M. Fibroblast growth factors: from molecular evolution to roles in development, metabolism and disease. **J Biochem,** v. 149, n. 2, p. 121-30, Feb 2011. ISSN 1756-2651. Disponível em: < https://www.ncbi.nlm.nih.gov/pubmed/20940169 >.

JAWOREK, A.; SOBCZYK, A. T. Electrospraying route to nanotechnology: An overview. **Journal of Electrostatics,** v. 66, p. 197 - 219, 2008.

JI, W. et al. Fibrous scaffolds loaded with protein prepared by blend or coaxial electrospinning. **Acta Biomater,** v. 6, n. 11, p. 4199-207, Nov 2010. ISSN 1878-7568. Disponível em: < https://www.ncbi.nlm.nih.gov/pubmed/20594971 >.

JIA, Z. Q. et al. Ebselen protects mitochondrial function and oxidative stress while inhibiting the mitochondrial apoptosis pathway after acute spinal cord injury. **Neurosci Lett,** v. 678, p. 110-117, Jun 2018. ISSN 1872-7972. Disponível em: < https://www.ncbi.nlm.nih.gov/pubmed/29733976 >.

JIANG, H. et al. A facile technique to prepare biodegradable coaxial electrospun nanofibers for controlled release of bioactive agents. **J Control Release,** v. 108, n. 2-3, p. 237-43, Nov 2005. ISSN 0168-3659. Disponível em: < https://www.ncbi.nlm.nih.gov/pubmed/16153737 >.

JIANG, H.; WANG, L.; ZHU, K. Coaxial electrospinning for encapsulation and controlled release of fragile water-soluble bioactive agents. **J Control Release,** v. 193, p. 296-303, Nov 2014. ISSN 1873-4995. Disponível em: < https://www.ncbi.nlm.nih.gov/pubmed/24780265 >.

JIANG, Y. N.; MO, H. Y.; YU, D. G. Electrospun drug-loaded core-sheath PVP/zein nanofibers for biphasic drug release. **Int J Pharm,** v. 438, n. 1-2, p. 232-9, Nov 2012. ISSN 1873-3476. Disponível em: < https://www.ncbi.nlm.nih.gov/pubmed/22981688 >.

JOHNSON, C. D.; D'AMATO, A. R.; GILBERT, R. J. Electrospun Fibers for Drug Delivery after Spinal Cord Injury and the Effects of Drug Incorporation on Fiber Properties. **Cells Tissues Organs,** v. 202, n. 1-2, p. 116-135, 2016. ISSN 1422-6421. Disponível em: < https://www.ncbi.nlm.nih.gov/pubmed/27701153 >.

JONES, L. L.; TUSZYNSKI, M. H. Chronic intrathecal infusions after spinal cord injury cause scarring and compression. **Microsc Res Tech,** v. 54, n. 5, p. 317-24, Sep 2001. ISSN 1059-910X. Disponível em: < https://www.ncbi.nlm.nih.gov/pubmed/11514988 >.

KANG, C. E. et al. Localized and sustained delivery of fibroblast growth factor-2 from a nanoparticle-hydrogel composite for treatment of spinal cord injury. **Cells Tissues Organs,** v. 197, n. 1, p. 55-63, 2013. ISSN 1422-6421 (Electronic)

1422-6405 (Linking). Disponível em: < http://www.ncbi.nlm.nih.gov/pubmed/22796886 >.

KASAI, M. et al. FGF-2-responsive and spinal cord-resident cells improve locomotor function after spinal cord injury. **J Neurotrauma,** v. 31, n. 18, p. 1584-98, Sep 2014. ISSN 1557-9042. Disponível em: < https://www.ncbi.nlm.nih.gov/pubmed/20199141 >.

KENNEDY, K. M.; BHAW-LUXIMON, A.; JHURRY, D. Cell-matrix mechanical interaction in electrospun polymeric scaffolds for tissue engineering: Implications for scaffold design and performance. **Acta Biomater,** v. 50, p. 41-55, 03 2017. ISSN 1878-7568. Disponível em: < https://www.ncbi.nlm.nih.gov/pubmed/28011142 >.

KIM, H. J. et al. Histone deacetylase inhibitors exhibit anti-inflammatory and neuroprotective effects in a rat permanent ischemic model of stroke: multiple mechanisms of action. **J Pharmacol Exp Ther,** v. 321, n. 3, p. 892-901, Jun 2007. ISSN 0022-3565. Disponível em: < https://www.ncbi.nlm.nih.gov/pubmed/17371805 >.

KIM, M.; PARK, S. R.; CHOI, B. H. Biomaterial scaffolds used for the regeneration of spinal cord injury (SCI). **Histol Histopathol,** v. 29, n. 11, p. 1395-408, Nov 2014. ISSN 1699-5848. Disponível em: < https://www.ncbi.nlm.nih.gov/pubmed/24831814 >.

KIM, M. S. et al. An in vivo study of the host tissue response to subcutaneous implantation of PLGA-and/or porcine small intestinal submucosa-based scaffolds. **Biomaterials,** v. 28, n. 34, p. 5137-43, Dec 2007. ISSN 0142-9612. Disponível em: < https://www.ncbi.nlm.nih.gov/pubmed/17764737 >.

KIM, W. R. et al. Functional Test Scales for Evaluating Cell-Based Therapies in Animal Models of Spinal Cord Injury. **Stem Cells Int,** v. 2017, p. 5160261, 2017. ISSN 1687-966X. Disponível em: < https://www.ncbi.nlm.nih.gov/pubmed/29109741 >.

KUBINOVÁ, Š. et al. SIKVAV-modified highly superporous PHEMA scaffolds with oriented pores for spinal cord injury repair. **J Tissue Eng Regen Med,** v. 9, n. 11, p. 1298-309, Nov 2015. ISSN 1932-7005. Disponível em: < https://www.ncbi.nlm.nih.gov/pubmed/23401421 >.

KUBINOVÁ, S. et al. Highly superporous cholesterol-modified poly(2-hydroxyethyl methacrylate) scaffolds for spinal cord injury repair. **J Biomed Mater Res A,** v. 99, n. 4, p. 618-29, Dec 2011. ISSN 1552-4965. Disponível em: < https://www.ncbi.nlm.nih.gov/pubmed/21953978 >.

KUBINOVÁ, S.; SYKOVÁ, E. Biomaterials combined with cell therapy for treatment of spinal cord injury. **Regen Med,** v. 7, n. 2, p. 207-24, Mar 2012. ISSN 1746-076X. Disponível em: < https://www.ncbi.nlm.nih.gov/pubmed/22397610 >.

KUMAR, R. et al. Traumatic Spinal Injury: Global Epidemiology and Worldwide Volume. **World Neurosurg,** v. 113, p. e345-e363, May 2018. ISSN 1878-8769. Disponível em: < https://www.ncbi.nlm.nih.gov/pubmed/29454115 >.

KUMARI, A.; YADAV, S. K.; YADAV, S. C. Biodegradable polymeric nanoparticles based drug delivery systems. **Colloids Surf B Biointerfaces,** v. 75, n. 1, p. 1-18, Jan 2010. ISSN 1873-4367. Disponível em: < https://www.ncbi.nlm.nih.gov/pubmed/19782542 >.

KWON, B. K. et al. Pathophysiology and pharmacologic treatment of acute spinal cord injury. **Spine J,** v. 4, n. 4, p. 451-64, 2004 Jul-Aug 2004. ISSN 1529-9430. Disponível em: < https://www.ncbi.nlm.nih.gov/pubmed/15246307 >.

LAN, L. et al. Implantable porous gelatin microspheres sustained release of bFGF and improved its neuroprotective effect on rats after spinal cord injury. **PLoS One,** v. 12, n. 3, p. e0173814, 2017. ISSN 1932-6203. Disponível em: < https://www.ncbi.nlm.nih.gov/pubmed/28291798 >.

LAPLACA, M. C. et al. CNS injury biomechanics and experimental models. **Prog Brain Res,** v. 161, p. 13-26, 2007. ISSN 0079-6123. Disponível em: < https://www.ncbi.nlm.nih.gov/pubmed/17618967 >.

LEE, J. Y. et al. Valproic acid attenuates blood-spinal cord barrier disruption by inhibiting matrix metalloprotease-9 activity and improves functional recovery after spinal cord injury. **J Neurochem,** v. 121, n. 5, p. 818-29, Jun 2012. ISSN 1471-4159. Disponível em: < https://www.ncbi.nlm.nih.gov/pubmed/22409448 >.

LEE, J. Y. et al. Valproic acid protects motor neuron death by inhibiting oxidative stress and endoplasmic reticulum stress-mediated cytochrome C release after spinal cord injury. **J Neurotrauma,** v. 31, n. 6, p. 582-94, Mar 2014. ISSN 1557-9042. Disponível em: < https://www.ncbi.nlm.nih.gov/pubmed/24294888 >.

LI, D.; XIA, Y. N. Electrospinning of nanofibers: Reinventing the wheel? **Advanced Materials,** v. 16, n. 14, p. 1151-1170, Jul 19 2004. ISSN 0935-9648. Disponível em: < <Go to ISI>://WOS:000223289600001 >.

LI, J. et al. Prevention of intra-abdominal adhesion using electrospun PEG/PLGA nanofibrous membranes. **Mater Sci Eng C Mater Biol Appl,** v. 78, p. 988-997, Sep 2017. ISSN 1873-0191. Disponível em: < https://www.ncbi.nlm.nih.gov/pubmed/28576076 >.

LI, S.; BOCK, E.; BEREZIN, V. Neuritogenic and neuroprotective properties of peptide agonists of the fibroblast growth factor receptor. **Int J Mol Sci,** v. 11, n. 6, p. 2291-305, May 2010. ISSN 1422-0067. Disponível em: < https://www.ncbi.nlm.nih.gov/pubmed/20640153 >.

LIU, S. et al. Biomaterial-Supported Cell Transplantation Treatments for Spinal Cord Injury: Challenges and Perspectives. **Front Cell Neurosci,** v. 11, p. 430, 2017. ISSN 1662-5102. Disponível em: < https://www.ncbi.nlm.nih.gov/pubmed/29375316 >.

LIU, T. et al. Nanofibrous collagen nerve conduits for spinal cord repair. **Tissue Eng Part A,** v. 18, n. 9-10, p. 1057-66, May 2012. ISSN 1937-335X. Disponível em: < https://www.ncbi.nlm.nih.gov/pubmed/22220714 >.

LOSCERTALES, I. G. et al. Micro/nano encapsulation via electrified coaxial liquid jets. **Science,** v. 295, n. 5560, p. 1695-8, Mar 2002. ISSN 1095-9203. Disponível em: < https://www.ncbi.nlm.nih.gov/pubmed/11872835 >.

LU, W. H. et al. Valproic acid attenuates microgliosis in injured spinal cord and purinergic P2X4 receptor expression in activated microglia. **J Neurosci Res,** v. 91, n. 5, p. 694-705, May 2013. ISSN 1097-4547. Disponível em: < https://www.ncbi.nlm.nih.gov/pubmed/23404572 >.

LU, Y. et al. Mild immobilization of diverse macromolecular bioactive agents onto multifunctional fibrous membranes prepared by coaxial electrospinning. **Acta Biomater,** v. 5, n. 5, p. 1562-74, Jun 2009. ISSN 1878-7568. Disponível em: < https://www.ncbi.nlm.nih.gov/pubmed/19251494 >.

LV, L. et al. Valproic acid improves locomotion in vivo after SCI and axonal growth of neurons in vitro. **Exp Neurol,** v. 233, n. 2, p. 783-90, Feb 2012. ISSN 1090-2430. Disponível em: < https://www.ncbi.nlm.nih.gov/pubmed/22178331 >.

LV, L. et al. Valproic acid improves outcome after rodent spinal cord injury: potential roles of histone deacetylase inhibition. **Brain Res,** v. 1396, p. 60-8, Jun 2011. ISSN 1872-6240. Disponível em: < https://www.ncbi.nlm.nih.gov/pubmed/21439269 >.

MAKADIA, H. K.; SIEGEL, S. J. Poly Lactic-co-Glycolic Acid (PLGA) as Biodegradable Controlled Drug Delivery Carrier. **Polymers (Basel),** v. 3, n. 3, p. 1377-1397, Sep 2011. ISSN 2073-4360. Disponível em: < https://www.ncbi.nlm.nih.gov/pubmed/22577513 >.

MAQUET, V. et al. Poly(D,L-lactide) foams modified by poly(ethylene oxide)-block-poly(D,L-lactide) copolymers and a-FGF: in vitro and in vivo evaluation for spinal cord regeneration. **Biomaterials,** v. 22, n. 10, p. 1137-46, May 2001. ISSN 0142-9612 (Print)

0142-9612 (Linking). Disponível em: < http://www.ncbi.nlm.nih.gov/pubmed/11352093 >.

METZ, G. A. et al. Validation of the weight-drop contusion model in rats: a comparative study of human spinal cord injury. **J Neurotrauma,** v. 17, n. 1, p. 1-17, Jan 2000. ISSN 0897-7151. Disponível em: < https://www.ncbi.nlm.nih.gov/pubmed/10674754 >.

MOCCHETTI, I. et al. Increased basic fibroblast growth factor expression following contusive spinal cord injury. **Exp Neurol,** v. 141, n. 1, p. 154-64, Sep 1996. ISSN 0014-4886. Disponível em: < https://www.ncbi.nlm.nih.gov/pubmed/8797678 >.

MOGHE, A. K.; GUPTA, B. S. Co-axial Electrospinning for Nanofiber Structures: Preparation and Applications. **Polymer Reviews,** v. 48, n. 2, p. 353 - 377, 2008.

MORRISON, R. S.; KEATING, R. F.; MOSKAL, J. R. Basic fibroblast growth factor and epidermal growth factor exert differential trophic effects on CNS neurons. **J Neurosci Res,** v. 21, n. 1, p. 71-9, Sep 1988. ISSN 0360-4012. Disponível em: < https://www.ncbi.nlm.nih.gov/pubmed/3265159 >.

NABIUNI, M. et al. In vitro effects of fetal rat cerebrospinal fluid on viability and neuronal differentiation of PC12 cells. **Fluids Barriers CNS,** v. 9, n. 1, p. 8, Jun 2012. ISSN 2045-8118. Disponível em: < https://www.ncbi.nlm.nih.gov/pubmed/22494846 >.

NAVES, L. et al. Poly(lactic-co-glycolic) acid drug delivery systems through transdermal pathway: an overview. **Prog Biomater,** v. 6, n. 1-2, p. 1-11, May 2017. ISSN 2194-0509. Disponível em: < https://www.ncbi.nlm.nih.gov/pubmed/28168430 >.

NEO, Y. P. et al. Influence of solution and processing parameters towards the fabrication of electrospun zein fibers with sub-micron diameter. **Journal of Food Engineering,** v. 109, p. 645 - 651, 2012.

NGUYEN, T. T. et al. Porous core/sheath composite nanofibers fabricated by coaxial electrospinning as a potential mat for drug release system. **Int J Pharm,** v. 439, n. 1-2, p. 296-306, Dec 2012. ISSN 1873-3476. Disponível em: < https://www.ncbi.nlm.nih.gov/pubmed/22989981 >.

NICOLA, F. et al. Stem Cells from Human Exfoliated Deciduous Teeth Modulate Early Astrocyte Response after Spinal Cord Contusion. **Mol Neurobiol**, May 2018. ISSN 1559-1182. Disponível em: < https://www.ncbi.nlm.nih.gov/pubmed/29796991 >.

NICOLA, F. D. C. et al. Neuroprotector effect of stem cells from human exfoliated deciduous teeth transplanted after traumatic spinal cord injury involves inhibition of early neuronal apoptosis. **Brain Res,** v. 1663, p. 95-105, 05 2017. ISSN 1872-6240. Disponível em: < https://www.ncbi.nlm.nih.gov/pubmed/28322752 >.

NODA, M. et al. FGF-2 released from degenerating neurons exerts microglial-induced neuroprotection via FGFR3-ERK signaling pathway. **J Neuroinflammation,** v. 11, p. 76, Apr 2014. ISSN 1742-2094. Disponível em: < https://www.ncbi.nlm.nih.gov/pubmed/24735639 >.

NORENBERG, M. D.; SMITH, J.; MARCILLO, A. The pathology of human spinal cord injury: defining the problems. **J Neurotrauma,** v. 21, n. 4, p. 429-40, Apr 2004. ISSN 0897-7151. Disponível em: < https://www.ncbi.nlm.nih.gov/pubmed/15115592 >.

OHUCHI, T. et al. Assay-based quantitative analysis of PC12 cell differentiation. **J Neurosci Methods,** v. 118, n. 1, p. 1-8, Jul 2002. ISSN 0165-0270. Disponível em: < https://www.ncbi.nlm.nih.gov/pubmed/12191752 >.

OKUTAN, N.; TERZI, P.; ALTAY, F. Affecting parameters on electrospinning process and characterization of electrospun gelatin nanofibers. **Food Hydrocolloids,** v. 39, p. 19 - 26, 2014.

ORNOY, A. Valproic acid in pregnancy: how much are we endangering the embryo and fetus? **Reprod Toxicol,** v. 28, n. 1, p. 1-10, Jul 2009. ISSN 1873-1708. Disponível em: < https://www.ncbi.nlm.nih.gov/pubmed/19490988 >.

OUDEGA, M. et al. Axonal regeneration into Schwann cell grafts within resorbable poly(alpha-hydroxyacid) guidance channels in the adult rat spinal cord. **Biomaterials,** v. 22, n. 10, p. 1125-36, May 2001. ISSN 0142-9612. Disponível em: < https://www.ncbi.nlm.nih.gov/pubmed/11352092 >.

PARK, H. et al. Stress response of fibroblasts adherent to the surface of plasma-treated poly(lactic-co-glycolic acid) nanofiber matrices. **Colloids Surf B Biointerfaces,** v. 77, n. 1, p. 90-5, May 2010. ISSN 1873-4367. Disponível em: < https://www.ncbi.nlm.nih.gov/pubmed/20138484 >.

PAUL, A. et al. Cytotoxicity and apoptotic signalling cascade induced by chelidonine-loaded PLGA nanoparticles in HepG2 cells in vitro and bioavailability of nano-chelidonine in mice in vivo. **Toxicol Lett,** v. 222, n. 1, p. 10-22, Sep 2013. ISSN 1879-3169. Disponível em: < https://www.ncbi.nlm.nih.gov/pubmed/23850776 >.

PEARSE, D. D. et al. Schwann Cell Transplantation Subdues the Pro-Inflammatory Innate Immune Cell Response after Spinal Cord Injury. **Int J Mol Sci,** v. 19, n. 9, Aug 2018. ISSN 1422-0067. Disponível em: < https://www.ncbi.nlm.nih.gov/pubmed/30154346 >.

PENAS, C. et al. Valproate reduces CHOP levels and preserves oligodendrocytes and axons after spinal cord injury. **Neuroscience,** v. 178, p. 33-44, Mar 2011. ISSN 1873-7544. Disponível em: < https://www.ncbi.nlm.nih.gov/pubmed/21241777 >.

PERTICI, V. et al. Repair of the injured spinal cord by implantation of a synthetic degradable block copolymer in rat. **Biomaterials,** v. 35, n. 24, p. 6248-58, Aug 2014. ISSN 1878-5905. Disponível em: < https://www.ncbi.nlm.nih.gov/pubmed/24814425 >.

PHIEL, C. J. et al. Histone deacetylase is a direct target of valproic acid, a potent anticonvulsant, mood stabilizer, and teratogen. **J Biol Chem,** v. 276, n. 39, p. 36734-41, Sep 2001. ISSN 0021-9258. Disponível em: < https://www.ncbi.nlm.nih.gov/pubmed/11473107 >.

QI, R. et al. Exploring the dark side of MTT viability assay of cells cultured onto electrospun PLGA-based composite nanofibrous scaffolding materials. **Analyst,** v. 136, n. 14, p. 2897-903, Jul 2011. ISSN 1364-5528. Disponível em: < https://www.ncbi.nlm.nih.gov/pubmed/21647502 >.

RABCHEVSKY, A. G. et al. Basic fibroblast growth factor (bFGF) enhances tissue sparing and functional recovery following moderate spinal cord injury. **J Neurotrauma,** v. 16, n. 9, p. 817-30, Sep 1999. ISSN 0897-7151. Disponível em: < https://www.ncbi.nlm.nih.gov/pubmed/10521141 >.

RABCHEVSKY, A. G. et al. Basic fibroblast growth factor (bFGF) enhances functional recovery following severe spinal cord injury to the rat. **Exp Neurol,** v. 164, n. 2, p. 280-91, Aug 2000. ISSN 0014-4886. Disponível em: < https://www.ncbi.nlm.nih.gov/pubmed/10915567 >.

RAMER, L. M.; RAMER, M. S.; STEEVES, J. D. Setting the stage for functional repair of spinal cord injuries: a cast of thousands. **Spinal Cord,** v. 43, n. 3, p. 134-61, Mar 2005. ISSN 1362-4393. Disponível em: < https://www.ncbi.nlm.nih.gov/pubmed/15672094 >.

RANJBAR-MOHAMMADI, M. et al. Electrospinning of PLGA/gum tragacanth nanofibers containing tetracycline hydrochloride for periodontal regeneration. **Mater Sci Eng C Mater Biol Appl,** v. 58, p. 521-31, Jan 2016. ISSN 1873-0191. Disponível em: < https://www.ncbi.nlm.nih.gov/pubmed/26478340 >.

RASPA, A. et al. Recent therapeutic approaches for spinal cord injury. **Biotechnol Bioeng,** v. 113, n. 2, p. 253-9, Feb 2016. ISSN 1097-0290. Disponível em: < https://www.ncbi.nlm.nih.gov/pubmed/26134352 >.

SAKIYAMA-ELBERT, S. et al. Scaffolds to promote spinal cord regeneration. **Handb Clin Neurol,** v. 109, p. 575-94, 2012. ISSN 0072-9752. Disponível em: < https://www.ncbi.nlm.nih.gov/pubmed/23098738 >.

SAMPOGNA, G.; GURAYA, S. Y.; FORGIONE, A. Regenerative medicine: Historical roots and potential strategies in modern medicine. **Journal of Microscopy and Ultrastructure**, p. 101-107, 2015.

SANTHOSH, K. T.; ALIZADEH, A.; KARIMI-ABDOLREZAEE, S. Design and optimization of PLGA microparticles for controlled and local delivery of Neuregulin-1 in traumatic spinal cord injury. **J Control Release,** v. 261, p. 147-162, Sep 2017. ISSN 1873-4995. Disponível em: < https://www.ncbi.nlm.nih.gov/pubmed/28668379 >.

SCHAUB, N. J. et al. Electrospun Fibers for Spinal Cord Injury Research and Regeneration. **J Neurotrauma,** v. 33, n. 15, p. 1405-15, Aug 2016. ISSN 1557-9042. Disponível em: < https://www.ncbi.nlm.nih.gov/pubmed/26650778 >.

SHI, Q. et al. Collagen scaffolds modified with collagen-binding bFGF promotes the neural regeneration in a rat hemisected spinal cord injury model. **Sci China Life Sci,** v. 57, n. 2, p. 232-40, Feb 2014. ISSN 1869-1889. Disponível em: < https://www.ncbi.nlm.nih.gov/pubmed/24445989 >.

SHIN, J. E. et al. Brain and spinal cord injury repair by implantation of human neural progenitor cells seeded onto polymer scaffolds. **Exp Mol Med,** v. 50, n. 4, p. 39, Apr 2018. ISSN 2092-6413. Disponível em: < https://www.ncbi.nlm.nih.gov/pubmed/29674624 >.

SINN, D. I. et al. Valproic acid-mediated neuroprotection in intracerebral hemorrhage via histone deacetylase inhibition and transcriptional activation. **Neurobiol Dis,** v. 26, n. 2, p. 464-72, May 2007. ISSN 0969-9961. Disponível em: < https://www.ncbi.nlm.nih.gov/pubmed/17398106 >.

SPERLING, L. E. et al. Influence of random and oriented electrospun fibrous poly(lactic-co-glycolic acid) scaffolds on neural differentiation of mouse embryonic stem cells. **J Biomed Mater Res A**, Jan 2017. ISSN 1552-4965. Disponível em: < https://www.ncbi.nlm.nih.gov/pubmed/28120428 >.

SPERLING, L. E. et al. Advantages and challenges offered by biofunctional core-shell fiber systems for tissue engineering and drug delivery. **Drug Discov Today,** v. 21, n. 8, p. 1243-56, Aug 2016. ISSN 1878-5832. Disponível em: < https://www.ncbi.nlm.nih.gov/pubmed/27155458 >.

STEFFENS, D. et al. Update on the main use of biomaterials and techniques associated with tissue engineering. **Drug Discov Today,** v. 23, n. 8, p. 1474-1488, 08 2018. ISSN 1878-5832. Disponível em: < https://www.ncbi.nlm.nih.gov/pubmed/29608960 >.

STEFFENS, D. et al. Development of a biomaterial associated with mesenchymal stem cells and keratinocytes for use as a skin substitute. **Regen Med,** v. 10, n. 8, p. 975-87, Nov 2015. ISSN 1746-076X. Disponível em: < https://www.ncbi.nlm.nih.gov/pubmed/26542841 >.

STODDART, M. J. WST-8 analysis of cell viability during osteogenesis of human mesenchymal stem cells. **Methods Mol Biol,** v. 740, p. 21-5, 2011. ISSN 1940-6029. Disponível em: < https://www.ncbi.nlm.nih.gov/pubmed/21468964 >.

TABAKOW, P. et al. Transplantation of autologous olfactory ensheathing cells in complete human spinal cord injury. **Cell Transplant,** v. 22, n. 9, p. 1591-612, 2013. ISSN 1555-3892. Disponível em: < https://www.ncbi.nlm.nih.gov/pubmed/24007776 >.

TENG, Y. D. et al. Functional recovery following traumatic spinal cord injury mediated by a unique polymer scaffold seeded with neural stem cells. **Proc Natl Acad Sci U S A,** v. 99, n. 5, p. 3024-9, Mar 5 2002. ISSN 0027-8424 (Print)

0027-8424 (Linking). Disponível em: < http://www.ncbi.nlm.nih.gov/pubmed/11867737 >.

TENG, Y. D. et al. Basic fibroblast growth factor increases long-term survival of spinal motor neurons and improves respiratory function after experimental spinal cord injury. **J Neurosci,** v. 19, n. 16, p. 7037-47, Aug 1999. ISSN 1529-2401. Disponível em: < https://www.ncbi.nlm.nih.gov/pubmed/10436058 >.

THISSE, B.; THISSE, C. Functions and regulations of fibroblast growth factor signaling during embryonic development. **Dev Biol,** v. 287, n. 2, p. 390-402, Nov 2005. ISSN 0012-1606. Disponível em: < https://www.ncbi.nlm.nih.gov/pubmed/16216232 >.

THOMATY, S. et al. Acute granulocyte macrophage-colony stimulating factor treatment modulates neuroinflammatory processes and promotes tactile recovery after spinal cord injury. **Neuroscience,** v. 349, p. 144-164, May 2017. ISSN 1873-7544. Disponível em: < https://www.ncbi.nlm.nih.gov/pubmed/28274846 >.

TUKMACHEV, D. et al. Injectable Extracellular Matrix Hydrogels as Scaffolds for Spinal Cord Injury Repair. **Tissue Eng Part A,** v. 22, n. 3-4, p. 306-17, Feb 2016. ISSN 1937-335X. Disponível em: < https://www.ncbi.nlm.nih.gov/pubmed/26729284 >.

VENUGOPAL, J. et al. Interaction of cells and nanofiber scaffolds in tissue engineering. **J Biomed Mater Res B Appl Biomater,** v. 84, n. 1, p. 34-48, Jan 2008. ISSN 1552-4973. Disponível em: < https://www.ncbi.nlm.nih.gov/pubmed/17477388 >.

VIGANI, B. et al. Design and criteria of electrospun fibrous scaffolds for the treatment of spinal cord injury. **Neural Regen Res,** v. 12, n. 11, p. 1786-1790, Nov 2017. ISSN 1673-5374. Disponível em: < https://www.ncbi.nlm.nih.gov/pubmed/29239316 >.

WANG, M. et al. Bioengineered scaffolds for spinal cord repair. **Tissue Eng Part B Rev,** v. 17, n. 3, p. 177-94, Jun 2011. ISSN 1937-3376. Disponível em: < https://www.ncbi.nlm.nih.gov/pubmed/21338266 >.

WILLERTH, S. M.; SAKIYAMA-ELBERT, S. E. Approaches to neural tissue engineering using scaffolds for drug delivery. **Adv Drug Deliv Rev,** v. 59, n. 4-5, p. 325-38, May 2007. ISSN 0169-409X. Disponível em: < https://www.ncbi.nlm.nih.gov/pubmed/17482308 >.

WOODBURY, M. E.; IKEZU, T. Fibroblast growth factor-2 signaling in neurogenesis and neurodegeneration. **J Neuroimmune Pharmacol,** v. 9, n. 2, p. 92-101, Mar 2014. ISSN 1557-1904. Disponível em: < https://www.ncbi.nlm.nih.gov/pubmed/24057103 >.

XIA, T. et al. The combination of db-cAMP and ChABC with poly(propylene carbonate) microfibers promote axonal regenerative sprouting and functional recovery after spinal cord hemisection injury. **Biomed Pharmacother,** v. 86, p. 354-362, Feb 2017. ISSN 1950-6007. Disponível em: < https://www.ncbi.nlm.nih.gov/pubmed/28011383 >.

XIAO, Z. et al. One-year clinical study of NeuroRegen scaffold implantation following scar resection in complete chronic spinal cord injury patients. **Sci China Life Sci,** v. 59, n. 7, p. 647-55, Jul 2016. ISSN 1869-1889. Disponível em: < https://www.ncbi.nlm.nih.gov/pubmed/27333785 >.

XIE, J. et al. Electrohydrodynamic atomization for biodegradable polymeric particle production. **J Colloid Interface Sci,** v. 302, n. 1, p. 103-12, Oct 2006. ISSN 0021-9797. Disponível em: < https://www.ncbi.nlm.nih.gov/pubmed/16842810 >.

XIMENES, J. C. et al. Valproic acid: an anticonvulsant drug with potent antinociceptive and anti-inflammatory properties. **Naunyn Schmiedebergs Arch Pharmacol,** v. 386, n. 7, p. 575-87, Jul 2013. ISSN 1432-1912. Disponível em: < https://www.ncbi.nlm.nih.gov/pubmed/23584602 >.

XU, H. L. et al. Sustained-release of FGF-2 from a hybrid hydrogel of heparin-poloxamer and decellular matrix promotes the neuroprotective effects of proteins after spinal injury. **Int J Nanomedicine,** v. 13, p. 681-694, 2018. ISSN 1178-2013. Disponível em: < https://www.ncbi.nlm.nih.gov/pubmed/29440894 >.

YANG, J. et al. Synthesis and characterization of fl urbiprofen axetil-loaded electrospun MgAl-LDHs/poly(lacticco-glycolic acid) composite nanofibers. **RSC Advances,** v. 5, p. 69423–69429, 2015.

YAO, S. et al. Drug-nanoencapsulated PLGA microspheres prepared by emulsion electrospray with controlled release behavior. **Regen Biomater,** v. 3, n. 5, p. 309-317, Oct 2016. ISSN 2056-3418. Disponível em: < https://www.ncbi.nlm.nih.gov/pubmed/27699061 >.

YE, L. B. et al. Regulation of Caveolin-1 and Junction Proteins by bFGF Contributes to the Integrity of Blood-Spinal Cord Barrier and Functional Recovery. **Neurotherapeutics,** v. 13, n. 4, p. 844-858, 10 2016. ISSN 1878-7479. Disponível em: < https://www.ncbi.nlm.nih.gov/pubmed/27170156 >.

YORK, E. M.; PETIT, A.; ROSKAMS, A. J. Epigenetics of neural repair following spinal cord injury. **Neurotherapeutics,** v. 10, n. 4, p. 757-70, Oct 2013. ISSN 1878-7479. Disponível em: < https://www.ncbi.nlm.nih.gov/pubmed/24081781 >.

YOUNG, T. H.; HUNG, C. H. Change in electrophoretic mobility of PC12 cells after culturing on PVA membranes modified with different diamines. **J Biomed Mater Res A,** v. 67, n. 4, p. 1238-44, Dec 2003. ISSN 1549-3296. Disponível em: < https://www.ncbi.nlm.nih.gov/pubmed/14624510 >.

YU, S. H. et al. The neuroprotective effect of treatment of valproic Acid in acute spinal cord injury. **J Korean Neurosurg Soc,** v. 51, n. 4, p. 191-8, Apr 2012. ISSN 1598-7876. Disponível em: < https://www.ncbi.nlm.nih.gov/pubmed/22737297 >.

YUN, Y. R. et al. Fibroblast growth factors: biology, function, and application for tissue regeneration. **J Tissue Eng,** v. 2010, p. 218142, Nov 2010. ISSN 2041-7314. Disponível em: < https://www.ncbi.nlm.nih.gov/pubmed/21350642 >.

ZAI, L. J.; YOO, S.; WRATHALL, J. R. Increased growth factor expression and cell proliferation after contusive spinal cord injury. **Brain Res,** v. 1052, n. 2, p. 147-55, Aug 2005. ISSN 0006-8993. Disponível em: < https://www.ncbi.nlm.nih.gov/pubmed/16005441 >.

ZAMANI, F. et al. Promotion of spinal cord axon regeneration by 3D nanofibrous core-sheath scaffolds. **J Biomed Mater Res A,** v. 102, n. 2, p. 506-13, Feb 2014. ISSN 1552-4965 (Electronic)

1549-3296 (Linking). Disponível em: < http://www.ncbi.nlm.nih.gov/pubmed/23533050 >.

ZHANG, H. Y. et al. Regulation of autophagy and ubiquitinated protein accumulation by bFGF promotes functional recovery and neural protection in a rat model of spinal cord injury. **Mol Neurobiol,** v. 48, n. 3, p. 452-64, Dec 2013. ISSN 1559-1182. Disponível em: < https://www.ncbi.nlm.nih.gov/pubmed/23516099 >.

ZHANG, H. Y. et al. Exogenous basic fibroblast growth factor inhibits ER stress-induced apoptosis and improves recovery from spinal cord injury. **CNS Neurosci Ther,** v. 19, n. 1, p. 20-9, Jan 2013. ISSN 1755-5949. Disponível em: < https://www.ncbi.nlm.nih.gov/pubmed/23082997 >.

ZHANG, K. et al. Aligned PLLA nanofibrous scaffolds coated with graphene oxide for promoting neural cell growth. **Acta Biomater,** v. 37, p. 131-42, 06 2016. ISSN 1878-7568. Disponível em: < https://www.ncbi.nlm.nih.gov/pubmed/27063493 >.

ZHANG, S. et al. Class I histone deacetylase (HDAC) inhibitor CI-994 promotes functional recovery following spinal cord injury. **Cell Death Dis,** v. 9, n. 5, p. 460, Apr 2018. ISSN 2041-4889. Disponível em: < https://www.ncbi.nlm.nih.gov/pubmed/29700327 >.

ZHANG, Y. Z. et al. Coaxial electrospinning of (fluorescein isothiocyanate-conjugated bovine serum albumin)-encapsulated poly(epsilon-caprolactone) nanofibers for sustained release. **Biomacromolecules,** v. 7, n. 4, p. 1049-57, Apr 2006. ISSN 1525-7797. Disponível em: < https://www.ncbi.nlm.nih.gov/pubmed/16602720 >.

ZHOU, Y. et al. Fibroblast growth factors in the management of spinal cord injury. **J Cell Mol Med,** v. 22, n. 1, p. 25-37, Jan 2018. ISSN 1582-4934. Disponível em: < https://www.ncbi.nlm.nih.gov/pubmed/29063730 >.

ZHU, M. M. et al. The pharmacogenomics of valproic acid. **J Hum Genet**, Sep 2017. ISSN 1435-232X. Disponível em: < https://www.ncbi.nlm.nih.gov/pubmed/28878340 >.

ZIABARI, M.; MOTTAGHITALAB, V.; HAGHI, A. K. Application of direct tracking method for measuring electrospun nanofiber diameter. **Brazilian Journal of Chemical Engineering,** v. 26, n. 1, p. 53 - 62, 2009.

ZIEMBA, A. M.; GILBERT, R. J. Biomaterials for Local, Controlled Drug Delivery to the Injured Spinal Cord. **Front Pharmacol,** v. 8, p. 245, 2017. ISSN 1663-9812. Disponível em: < https://www.ncbi.nlm.nih.gov/pubmed/28539887 >.

ZUO, W. et al. Experimental Study on Relationship Between Jet Instability and Formation of Beaded Fibers During Electrospinning. **POLYMER ENGINEERING AND SCIENCE**, p. 704-709, 2005.

10. Anexos

Anexo I. Carta de aceite da revista *Regenerative Medicine*

Regenerative Medicine

Decision Letter (FM-RME-2018-0060.R1)

From: a.price-evans@futuremedicine.com

To: kapire@yahoo.com.br

CC: laura.sperling@gmail.com, cristian-euzebio@hotmail.com, aagatapaim@gmail.com, brunojcalcantara@yahoo.com.br, gema.vizcay@kcl.ac.uk, roland.fleck@kcl.ac.uk, patriciapranke@ufrgs.br

Subject: Regenerative Medicine - Decision on Manuscript ID FM-RME-2018-0060.R1

Body: RW - CE Immediate Accept

04-Sep-2018

Dear Miss Reis,

It is a pleasure to accept your manuscript entitled "Application of PLGA/FGF-2 coaxial microfibers in spinal cord tissue engineering: an in vitro and in vivo investigation" in its current form for publication in Regenerative Medicine. Our production department will be in touch with the galley proofs soon - please do let me know if you are going to be away at any point and unable to check them.

Before we proceed to production of your article, please fill out the Copyright Assignment form (attached). Please note that the copyright form must be signed by hand or with an electronic signature.

We are also able to offer a fast-track production service, for a fee of $800, providing guaranteed online publication within 3 weeks (subject to turnaround of proofs by the author within 3 working days). Should you be interested in this service, please let me know.

Common errors to check and watch out for when approving your proofs (those that are harder for our copy editors to catch):
– Have you listed all your co-authors, and spelt their names correctly?
– Have you included correct affiliation details for yourself and your co-authors?
– Have you included all your funding information, including grant numbers, in the acknowledgement section (i.e., NIH, Wellcome Trust, etc.)?

Although corrections can be made after publication, these will only be carried out if they are deemed by the editor to be critical to the understanding of the article. So it is important to check information such as the above is correct when the article goes to print, as it cannot always be corrected at a later date.

Please note that the version uploaded to the ScholarOne system is classified as the 'Author's final version'. You are able to upload this version to your institutional repository if required. If you would like us to send you a copy of the author's final version, please let me know. For all other uses of this article version, please refer to the journal's self-archive policy.

Regenerative Medicine offers an open access option, whereby for a fee, articles can be made freely available for all to read. Pricing varies by article type; for peer-reviewed content (i.e., Original Research or Review articles), the fee is $2,500; for content not reviewed externally (i.e., Editorials or Commentaries), the fee is $850. For more information, visit our website here: https://www.future-science-group.com/services/for-researchers/open-access/. If you are interested in taking this option, please let me know.

Furthermore, Regenerative Medicine is associated with our community site, RegMedNet (https://www.regmednet.com), an online community offering medical professionals with an interest in regenerative medicine easy access to free educational webinars, expert opinion and insight, and exclusive peer-reviewed journal articles, as well as the latest news and advances. For a fee of $1400 ($700 if you have already opted for open access), your article can be featured on RegMedNet and made exclusively accessible to the ~6000 professionals registered on this site. The article abstract will be posted on RegMedNet, with a direct link to the article PDF, featured on the homepage, shared via social media and highlighted in the weekly newsletter. This further inclusion on RegMedNet will automatically ensure your article reaches its target audience, helping to increase its readership and extend its impact. Do let me know if this is of interest.

In addition, Colour Printing can enhance the impact of your article's figures with readers. Should you wish your figures to appear in colour in the print issue of the journal, there is a fee of $220 for the first figure and $135 for each subsequent figure. Please note that charges for colour

figures only apply for print issues of the journal; all figures appear online in colour at no cost. If you are interested in having one or more of your figures printed in colour, please let me know.

Finally, if your institution does not already subscribe to Regenerative Medicine, it would be great if you would be willing to email your librarian to recommend the journal to them (or alternatively, reply to this email if this is of interest, and we can contact your librarian to discuss free trial and subscription options).

Thank you for your contribution. On behalf of the Editors of Regenerative Medicine, we look forward to your continued contributions to the journal.

Sincerely,
Adam Price-Evans
Commissioning Editor, Regenerative Medicine
a.price-evans@futuremedicine.com

Date Sent: 04-Sep-2018

File 1: 1.-Publishing-Agreement-FM.docx

Close Window

Anexo II.

Outras publicações realizadas durante o período do doutorado:

SPERLING, LAURA E.; REIS, KARINA P.; POZZOBON, LAURA G.; GIRARDI, CAROLINA S.; PRANKE, PATRICIA. Influence of random and oriented electrospun fibrous poly(lactic-co -glycolic acid) scaffolds on neural differentiation of mouse embryonic stem cells. JOURNAL OF BIOMEDICAL MATERIALS RESEARCH PART A. , v.105, p.1333 - 1345, 2017.

SPERLING, LAURA E.; REIS, KARINA P.; PRANKE, PATRICIA; WENDORFF, JOACHIM H. Advantages and challenges offered by biofunctional core-shell fiber systems for tissue engineering and drug delivery. Drug Discovery Today. , v.21, p.1243 - , 2016.

Prêmios:

2018 - Primeiro lugar no pôster: "Application of FGF-2/PLGA microfibers in spinal cord tissue engineering", 1st TERMIS AM Workshop - 4° Encontro Internacional de Engenharia de Tecidos e Medicina Regenerativa

2018 - Terceiro lugar fotografia "Células na lua", 1st TERMIS AM Workshop - 4° Encontro Internacional de Engenharia de Tecidos e Medicina Regenerativa

2018 - 3º Concurso Ciência por Imagens, Centro de Microscopia e Microanálise da Universidade Federal do Rio Grande do Sul